A thesis submitted for the degree of
Doctor of Philosophy (Ph.D.)

Structure-function relationships of von Willebrand factor

by Miklós László Udvardy

Supervisor: Dr. Jolán Hársfalvi

University of Debrecen
Laki Kálmán Doctoral School

Debrecen
2009

Összefoglalás

Amint az endotélium megsérül, vérlemezkék tapadnak a felszínre kerülő szubendoteliális strukturákhoz. Kezdetben a vérlemezkék a VWF-on keresztül kötődnek a szubendoteliális kollagénhez, amelyet a VWF polymer szerkezete és a protomerenkénti GP Ib és kollagén kötőhelyei (az A1 és A3 doménekben) tesznek lehetővé. Figyelemre méltó, hogy a VWF és receptora egyidejűleg jelen vannak a keringésben, ám kölcsönhatásuk csak nagy nyíróerő hatására és/vagy a VWF kitapadása után következik be. Az ezen folyamat szabályozására vonatkozó jelenlegi feltevések különböző mértékű konformáció-változást (a kötőhely affinitása vagy hozzáférhetősége) és/vagy a multimer méret változásait (aviditás) helyeznek előtérbe .

Megvizsgáltuk a D'D3 régió jelentőségét, melyre az utalt, hogy az 1C1E7 jelzésű monoklonális antitest ide kötődik, ugyanakkor fokozza a GP Ib – VWF kölcsönhtást. Monoklonális antitestekkel végzett keresztgátlásos kísérleteink a D'D3 és az A1 domének közelségét jelezték oldat fázisban, de kitapadt VWF esetén nem. Risztocetin indukálta trombocita agglutinációs kísérletekben a D'D3 delécios VWF mutáns fokozott reaktivitását tapasztaltuk, amely arra utalt, hogy a D'D3 régió korlátozhatja az A1 domén hozzáférhetőségét. Hasonló – elképzelhetően a D'D3-hoz kötődő – szekvenciát találtunk az 1C1E7-ben és az A1 doménben is, amely alapján feltételezzük, hogy az 1C1E7 kötődése leválasztja a D'D3-at az A1-ről, és így hozzáférhetővé teszi azt.

Az aviditással kapcsolatos kérdések megválaszolásához továbbfejlesztettük a VWF elektroforézis technikáját és egy új, számítógépes eljárást dolgoztunk ki a multimer méret pontos meghatározására. Végül, kidolgoztunk egy olyan rendszert, amelyben a vérlemezkéket hasonló méretű, aktív GP Ibα-t hordozó gyöngyökkel helyettesítettük. Ezek segítségével az ármlásban a vérlemezkék által a VWF-ra kifejtett húzóerők modellezhetők lehetővé téve a nagyobb léptékű konformációváltozások tanulmányozását.

Summary

As soon as the endothelium is compromised, platelets are recruited on the exposed subendothelial structures. Initially, VWF is bridging the subendothelial collagen and the platelets, supported by its multiple subunits, each with a binding site for GP Ib and for collagen (A1 and A3 domains). Interestingly, both VWF and its receptor circulate in the bloodstream simultaneously, but they only interact if pathologically high shear forces are present and/or VWF is immobilised. Present theories about the regulation of this interaction hypothesise conformational changes at different scales (affinity or accessibility of the binding site) and/or emphasise the control of multimer size (avidity).

We have investigated the possible regulatory role of the D'D3 region, which is suggested by the fact, that the monoclonal antibody 1C1E7 binds to here, but enhances the GP Ib – VWF interaction. Cross-blocking studies with monoclonal antibodies revealed the proximity of the D'D3 and A1 domains in solution, but not when immobilised. Ristocetin induced platelet agglutination studies with VWF deletion mutants lacking the D'D3 region demonstrated increased reactivity, suggesting that D'D3 is limiting the accessibility of A1. We have found, that 1C1E7 and the A1 domain has a similar sequence — possibly binding to D'D3 — that suggests that 1C1E7 may disrupt the binding of D'D3 and A1 leaving the latter unblocked.

For avidity related questions, we have improved electrophoresis techniques of VWF multimer analysis and developed a new computerized procedure to accurately describe the size of multimers. We have compared the new and present methods, and demonstrated the accuracy and the utility of our methods. Finally, we have established a system, where platelets are substituted with similar sized corpuscules bearing functionally active GP Ibα. This aids the study of large scale conformational changes by modelling the drag forces exerted on VWF by platelets in flow.

List of abbreviations

aa	amino acid
ADAMTS13	a disintegrin and metalloproteinase with a thrombospondin type 1 motif, member 13
BSA	bovine serum albumin
C-terminal	carboxy-terminal
CUB	complement C1r/C1s, Uegf (EGFrelated sea urchin protein) and BMP-1 (bone morphogenic protein-1) domains
CV	coefficient of variation
DAB	diamino benzidine
DDAVP	desmopressin (1-desamino-8-D-arginine vasopressin)
EDAC	1-ethyl-3-(3-dimethylaminopropyl) carbodiimide also known as EDC or EDCI
EDTA	ethylenediaminetetraacetic acid
FITC	fluorescein isothiocyanate
FPLC	fast protein liquid chromatography
GP Ib	glycoprotein Ib (CD42b)
GP Ibα	glycoprotein Ibα (CD42bα)
GP Ibβ	glycoprotein Ibβ (CD42bβ/CD42c)
GP IIb/IIIa	glycoprotein IIb/IIIa (CD41/CD61, $\alpha_{IIb}\beta_3$)
GP IX	glycoprotein IX (CD42a)

GP V	glycoprotein V (CD42d)
GP VI	glycoprotein VI
HEPES	4-(2-hydroxyethyl)-1-piperazineethanesulfonic acid
HRP	horseradish peroxidase
MES	2-(N-morpholino)ethanesulfonic acid
moAb	monoclonal antibody
MW	molecular weight
N-terminal	amino terminal
PBS	phosphate buffered saline
PVDF	polyvinylidene fluoride
RD	reflective density
Rf	relative mobility (retention factor)
RIPA	ristocetin induced platelet agglutination
RPE	R-phycoerythrin
RT	room temperature
scFv	single-chain variable fragment
SDS	sodium dodecyl sulfate, also known as sodium lauryl sulfate (SLS)
TBS	Tris buffered saline
Tris	tris(hydroxymethyl)aminomethane, also known as THAM
TSP1	thrombospondin 1
TTP	thrombotic thrombocytopenic purpura

ULVWF	ultra- or unusally-large VWF
V_H	heavy chain variable region
V_L	light chain variable region
VW AgII	VWF propeptide
VWD	von Willebrand Disease
VWF	von Willebrand Factor
VWF:Ag	VWF antigen
VWF:CB	VWF collagen binding capacity
VWF:RCo	VWF Ristocetin cofactor activity

Contents

1 Introduction

Blood provides the effective means of transportation between the organs. To fullfill this task, it is distributed to the tissues in a network of blood vessels, which is closed in vertebrate. Failure to meet this requirement is incompatible with sustaining life functions, therefore it is essential to have effective counter-measures if leakage would occur. The need for intervention is obvious when blood vessels are damaged, but also the same mechanisms are utilised when the endothelial lining of blood vessels is renewed periodically. While it is important to seal the sites of injuries, it is also essential to maintain the blood in a fluid state elsewhere. The first goal is achieved by a sequence of interdependent events, involving both cellular and extracellular elements. Immediately after the injury the contraction of the vessel and the adhesion of platelets to the subendothelial structures temporary closes the wound, in the same time the coagulation cascade launches and a haemostatic plug is formed which is later degraded while the vessel wall is restored. The second goal requires these interwoven processes to be coordinated and controlled spatially and temporally; most importantly only the appropriate triggers should be able to activate this system. The interest of the tissues served by the damaged vessel also requires the size and the lifetime of the haemostatic plug to be kept within reasonable limits. The complex system realising all these functions is called haemostasis

The adhesion of platelets to the damaged vessel wall is one of the earliest steps of haemostasis. As soon as the endothelium is compromised, platelets are recruited on the exposed subendothelial structures. In veins or larger arteries where the shear forces are lower, platelets bind to the subendothelial collagen directly via their GP VI and GP IIb/IIIa receptors. However, when platelets are exposed to larger wall shear stress, especially in arterioles and stenosed vessels, these receptors are unable to support adhesion alone. This observation suggests, that under these conditions there is an additional mechanism that slows down the moving platelets and withstands the shear forces so platelets

are able to form stable bonds with the disrupted vascular surface. This process was visualised in real time microscopic systems where it has been demonstarted that platelets roll on the exposed subendothelium before they come to a stop, and that this phenomenon depends on the interaction of von Willebrand factor (VWF) and its platelet receptor glycoprotein GP Ib. The significance of this interaction is confirmed by the fact that the characteristic bleeding symptoms (e.g. mucosal bleeding) of VWD type 3 patients (lacking VWF) and patients with Bernard-Soulier syndrome (lacking GP Ib) appear in vessels where the wall shear stress is high.

VWF acts as a bridge between the subendothelial collagen and the platelets. The VWF-GP Ib interaction has some notable properties making it particularly fit for its purpose. VWF is built up from multiple subunits each one with a binding site for GP Ib and collagen, this way it provides a high local density of aligned binding places. Also the GP Ib-VWF bond has a fast on and a fast off rate and a biphasic response to forces acting upon it, that allows the platelets to roll, adhere or detach in response to shear forces. Interestingly, unlike the selectins and their receptors, which mediate leukocyte rolling, both VWF and its receptor is present in the bloodstream in the same time. However, under normal circumstances native GP Ib has an extremely low affinity towards VWF, they only interact if pathologically high shear forces are present or VWF is immobilised.

This observation implies the existence of a regulatory mechanism. Present theories about the regulation of this interaction hypothesise conformational changes at different scales (affecting the affinity or accessibility of the binding site) and/or emphasise the control of multimer size (altering avidity). This field is extensively researched, as deficient regulation can be associated with bleeding disorders and thrombotic events as well, furthermore it is a potential target of antiplatelet/antithrombotic drugs aiming on the high shear flow areas (such as stenosed arteries and stents). A definitive answer has not yet been found, perhaps a combination of several present theories will explain the gathered experimental data.

2 Review of the literature

2.1 The Synthesis and Structure of VWF

VWF is synthesised in endothelial cells and megakaryocytes[1] regulated by cell-specific elements and by the environment in which the cells are growing[2]. The gene is located to the short arm of chromosome 12, it contains 51 introns and spans approximately 178 kb[3]. A pseudogene is identified in chromosome 22 with 98% homology representing about one third of the VWF gene, which requires attention as it may interfere with molecular genetic analysis. The coding sequence was determined in 1985, the primary translation product contains 2813 amino acids (aa), including a signalpeptide (33 aa), and a large propolypeptide (741 aa), the mature VWF is built up of 2050 aminoacids. The sequence contains a high number (169 – 8,3%) of cysteine residues which are all participating in inter- and intrachain disulfide bonds[4–6]. Four types of repeating domains (A, B, C, D) have been identified based on internal homology, each subunit is composed in the follwing order: D'-D3-A1-A2-A3-D4-B1-B2-B3-C1-C2-CK. A domains found to have similar areas to complement factor B, type VI collagen, I-domain-containing integrin α-subunit, while parts of the C domains have thrombospondin and procollagen like sequence (Fig. 1).

VWF is synthesised as prepro-VWF, upon translocation into the endoplasmic reticulum the signal peptide is cleaved and intermolecular disulfide bonds are formed through the CK domains. The resulting carboxy (C) terminal-linked "tail-to-tail" pro-VWF dimer is the protomeric unit of multimerization. During the transport through the Golgi VWF is sulfated and glycosylated, 22 (10 O- and 12 N-linked) oligosaccharide chains are attached to VWF[8], which make up approximately 20% of its mass. Amino (N) terminal disulfide bonds form "head-to-head" between D3 domains in the trans-Golgi[6], the dimeric N-terminal D'D3 domains of VWF subunits align in a parallel orientation in the resulting higher order oligomers. This process is facilitated by the self-

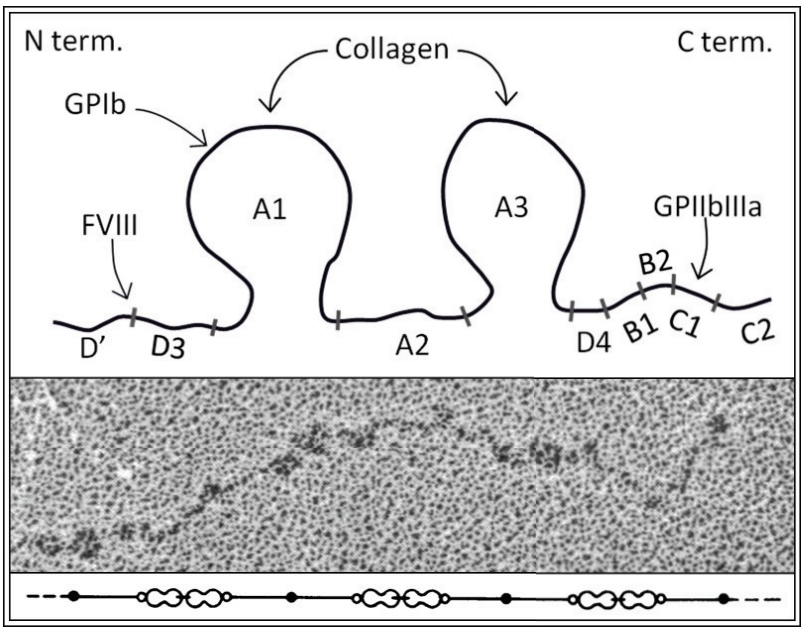

Figure 1: The structure of VWF. The upper part shows a schematic representation of the domains of mature VWF, and their important interactions. The lower part shows an electronmicrographic image (according to Fowler et al.[7]) of a VWF multimer

Region	Function
D1D2	propeptide, involved in multimerization
D'D3	FVIII, heparin binding site, cysteines in D3 are involved in multimerization
A1	GP Ib, collagen type VI, heparin, botrocetin, sulfatide binding site
A2	ADAMTS13 cleavage site
A3	collagen type I and III binding site
C1	RGDS sequence, GP IIb/IIIa binding site

Table 1: Regions of VWF important for platelet adhesion

association of the propolypeptide regions occurring in the acidic environment of this compartment[9]. The propetide (also known as VW AgII) is cleaved by furin and stored and secreted together with VWF. The secretory granules are called α-granules in case of platelets and Weibel-Palade bodies in case of endothelial cells.

VWF is released from Weibel-Palade bodies both constitutively and after stimulation while in platelets only the latter pathway exists. VWF secreted constitutively contains all multimer forms, while in response to stimulation predominantly the largest multimers are released[10]. Secretagogues include thrombin, ADP and epinephrine in case of platelets and histamine and DDAVP in case of endothelial cells. After secretion the propeptide dissociates from VWF and circulates at a concentration of about 1 µg/mL with a half-life of 2 to 3 hours, whereas VWF circulates at about 10 µg/mL with a half life of 8 to 12 hours. About 60% of the variation in the plasma concentration of VWF is due to genetic factors, bloodgroup contributes by about 30%[11]. In the normal population VWF levels are 25% – 35% lower in individuals with blood group O than in individuals with non-O blood groups[12]. It has been proposed that the survival of blood group O VWF is reduced, because of the difference in glycosilation[13,14]

Electron microscopic studies suggest that VWF has a loosely tangled non-branching coil structure in solution with a diameter of about 200 – 300nm, but extended filaments may reach up to a few micrometers in length. Protomers have a length of approximately 120 nm when fully extended, their structure is trinodular and symmetrical, consisting of two large globular end domains connected to a central node[7].

2.2 Multimer distribution of VWF

It is generally accepted, that the largest multimers have the highest haemostatic activity, presumably because of the enhanced avidity of the larger VWF multimers due to the higher number of GP Ib binding sites[15,16]. The momentary multimer distribution of VWF is determined by the collective effect of oppositely acting processes: assembly on one hand, and clearance

or degradation by ADAMTS13 (see in section 2.3) on the other[17]. Recent publications suggest additional ways, which could influence the size of VWF oligomers through thiol-disulfide exchange as well[18–20].

The deficiency of large multimers is usually seen either because of the faster clearance (von Willebrand disease [VWD] type 2B, platelet type VWD) or because of the disorders of synthesis (VWD type 2A)[21–23]. Substantial increase in the amount of large multimers is only rarely observed. It is described in VWD type Vicenza and in the recovery phase or remission of TTP, because of the deficiency of VWF's proteolytic enzyme ADAMTS13 in the latter. In otherwise healthy individuals it is currently unclear whether the increase in the total amount of VWF or in the large multimers alone is an independent risk factor for thrombosis[24,25]. There is even less information available on how the size of the largest multimers influences haemostasis.

Presently, antigen (VWF:Ag) and activity assays, such as the ristocetin cofactor assay (VWF:RCo) and the collagen binding activity (VWF:CB) are available for the evaluation of VWF. The disproportionate decrease of activity assays and the antigen level is usually treated as a sign of type 2 VWD, and according to some opinions the selective decrease of VWF:CB indicates the lack of large multimers[26]. However, direct information about the amount and the degree of multimerization of VWF is only available through non-reducing SDS agarose gel electrophoresis. Routinely these gels are qualitatively evaluated, which is a potential source of variability in the interpretation of the results. Inter-laboratory variation is further increased by the large number of running conditions for the VWF SDS agarose electrophoresis[27–33]. In addition the most commonly used Laemmli buffers do not resolve small multimers in low resolution gels[34]. There is a published approach for qualitative analyses that assesses the amount of large multimers by calculating the percentage of VWF protein in bands 11 and above. However the size of these multimers is not measured even though it is assumed to have a strong impact on VWF's haemostatic function.

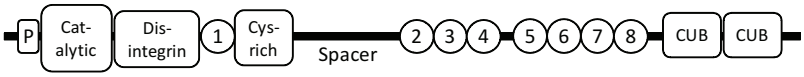

Figure 2: The structure of ADAMTS13. The catalytic domain cleaves the Tyr^{1605}–Met^{1606} bond, the Cysteine rich and spacer domains interact with an auxiliary-binding site on VWF A2 domain. P, Propeptide; TSP1 repeats are numbered 1–8.

2.3 ADAMTS13

Weibel-Palade bodies contain more ultra-large VWF (ULVWF) multimers then the normal plasma[35]. Upon release, the ULVWF is rapidly cleaved, the highly thrombogenic large multimers are converted to smaller molecules. The proteolysis is specific to a single peptide bond between Tyr^{1605} and Met^{1606} in the A2 domain (and results in a 140 and a 170 kDa proteolytic fragment in case of a single VWF molecule). A plasma metalloproteinase bearing this activity was classified as a member of the ADAMTS family and was designated as ADAMTS13. The gene of ADAMTS13 is located to chromosome 9q34 and spans 37kb coding 29 exons[36]. The translation product contains 1 427 amino acids including a signal peptide and a propeptide of 41 amino acids, the sequence predicts 10 potential N-glycosylation sites. ADAMTS13 is a multiple domain protein, that comprises a protease domain, a TSP-1 motif, a spacer, a Cys-rich domain containing an RGD sequence, seven additional TSP-1 domains, and two CUB repeats in the C-terminus (Fig. 2). This domain structure suggest that ADAMTS13 may potentially interact with TSP-1 binding proteins such as proteoglycans, integrin-associated protein (CD47), GP IV and integrins.

The regulation of the proteolytic activity of ADAMTS13 is not fully understood. ADAMTS13 and VWF circulate in the bloodstream together and it is obvious, that VWF is not fully degraded by ADAMTS13, but on the other hand ULVWF is not present either. Under static conditions (as in most *in vitro* systems), ADAMTS13 do not degrade VWF unless urea and barium ions are present. It is proposed, that probably shear forces reveal

the proteolytic site in VWF, perhaps immediately after secretion while still attached to the endothelial cells[37].

The deficiency of ADAMTS13 may result in the persistence of ULVWF, which is capable of binding GP Ib spontaneously[16]. Accordingly, the deficiency of ADAMTS13 and the presence of ULVWF has been reported at least in a fraction (33–100%) of thrombotic thrombocytopenic purpura (TTP) patients[38–40].

2.4 GP Ib-IX-V complex

The GP Ib-IX-V complex is almost exclusively expressed by the cells of megakaryocytic lineage, approximately 25 000 copies are found on resting platelets. It consists of four transmembrane subunits — GP Ibα, GP Ibβ, GP IX and GP V — each of which is a member of the leucine-rich repeat protein subfamily[41]. megakaryocytic lineage, some on endothel. GP Ibα is disulfide-linked to GP Ibβ by cystenil residues and noncovalently associated with GP IX. GP V is also non-covalently associated with the complex[42], but its copy number is half of the other chains, resulting in a stoichiometry of 2:2:2:1 (Fig. 3). VWF interacts with the GP Ibα chain which is 610 amino acids long and contains approximately 50% carbohydrate by weight. The VWF binding domain is located in the the N-terminal 282 residues which also contains binding sites for Mac-1, P-selectin, α-thrombin, clotting factors XI/XIIa, and high-molecular-weight kininogen[43]. This domain is elevated from the plasma membrane by a mucine stalk and consits of a disulfide-looped N-terminal capping sequence eight tandem leucine-rich repeats a disulfide-looped C-terminal flank and an anionic sequence containing three sulfated tyrozines[44]. The central region contains a sialumucine rich core and it is heavily O-glycosylated. According to crystallographic studies predominantly the N-terminal capping and the C-terminal flanking make contact with the top and bottom of the A1 domain[45,46].

VWF binding to GP Ib-IX-V transmits intracellular signals, triggering degranulation, elevation of cytosolic Ca^{2+}, cytoskeletal-actin rearrangements, and “inside-out” activation of GP IIb-IIIa that binds VWF or fibrinogen

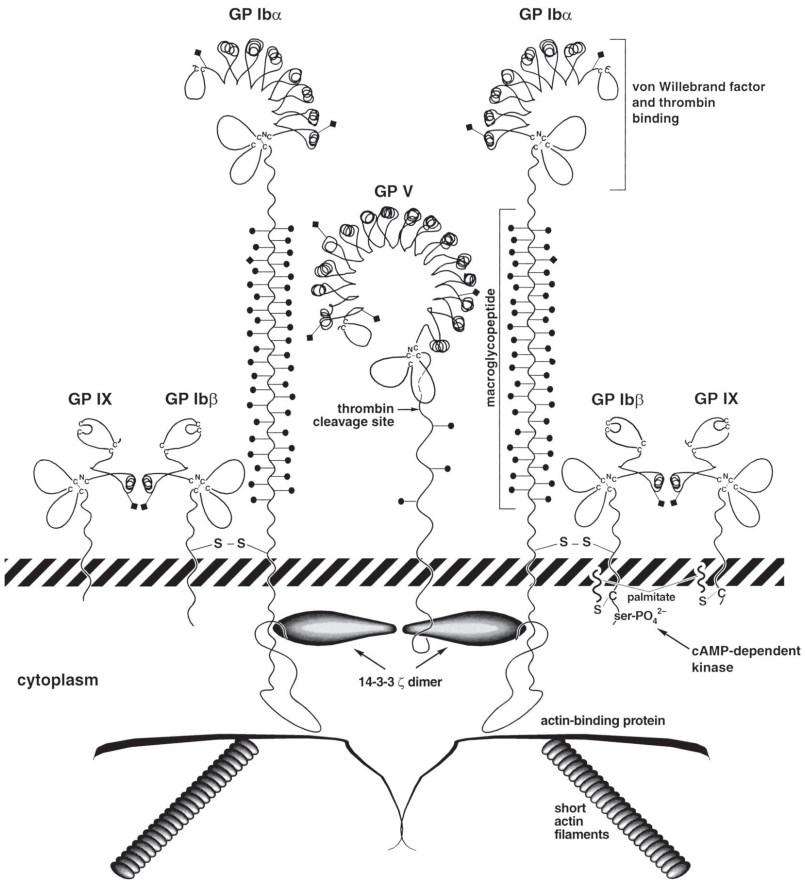

Figure 3: The structure of GP Ib-IX-V complex (according to López et al. [42]) Diamonds on stalks represent N-linked carbohydrates, circles on stalks represent O-linked carbohydrates.

and mediates platelet aggregation[42,43]. The GP Ib-IX-V complex is directly attached to actin-binding protein which functions to transmit the extracellular adhesion forces to the cytoskeleton, and also to maintaining platelet shape[47]

2.5 The VWF–GP Ib interaction

The primary roles of platelets is to stick to sites of vessel wall injuries, and to form a haemostatic plug by recruiting other platelets and by initiating and promoting blood coagulation. At high shear flow, platelets — similarly to white

blood cells — translocate on the target area, before adhering permanently[48–50]. This behaviour is dependent on the presence of VWF and GP Ib, where the role of VWF is to act as a bridge between platelets and the vessel wall. This implies that VWF must attach itself to both of these structures. In case of the vessel wall, either the activated endothelial cells secrete VWF, which stays anchored to the cell[48,51] or VWF binds to the exposed subendothelial collagen by its A1 and A3 domains. The A3 domain mainly bind to collagen type I and III[52,53], while the A1 domain binds primarily to collagen type VI[54], although there are overlaps in their specificity[55,56] and other domains might modulate the collagen binding as well[20,57]. The other end of the bridge interacts with platelet GP Ib, the involved domain is A1. The transient interactions needed for the translocation are permitted by the fast association and the fast dissociation rates of this bond[58]. Recently it has been demonstrated, that the response of this bonding to mechanical stress is biphasic: depending on the force applied, it can act like a catch bond or a slip bond[50,59]. (Catch and slip describe bonds under the influence of force: force prolongs the bond lifetimes for catch bonds and shortens it for slip bonds[60]). This explains the — rather counterintuitive — observation, that flow shear increases platelet adhesion[61,62]. The molecular details of the interaction of the GP Ibα chain and the isolated A1 domain has been described in crystallographic studies[45,46], however the regulatory mechanism that controls their interaction is not yet understood. Some kind of regulation must exist, as both VWF and platelets are present in the circulation simultaneously, but they do not interact, unless VWF is immobilised and shear forces are present. In solution only pathologically high shear flow (such as in stenosed arteries) can induce VWF mediated platelet agglutination[63]. The regulatory mechanism probably affects both VWF and GP Ib[62,64,65], as of now, several theories has been proposed on the VWF side, involving different scale conformational changes and the extent of multimerization:

1. There is evidence, that shear stress may induce conformational changes near or in the GP Ibα binding site that enhances its affinity towards GP Ibα (Fig. 4A). Forty-nine out of the fifty reported gain of function mutations (VWD type 2B phenotype) are missense mutations located

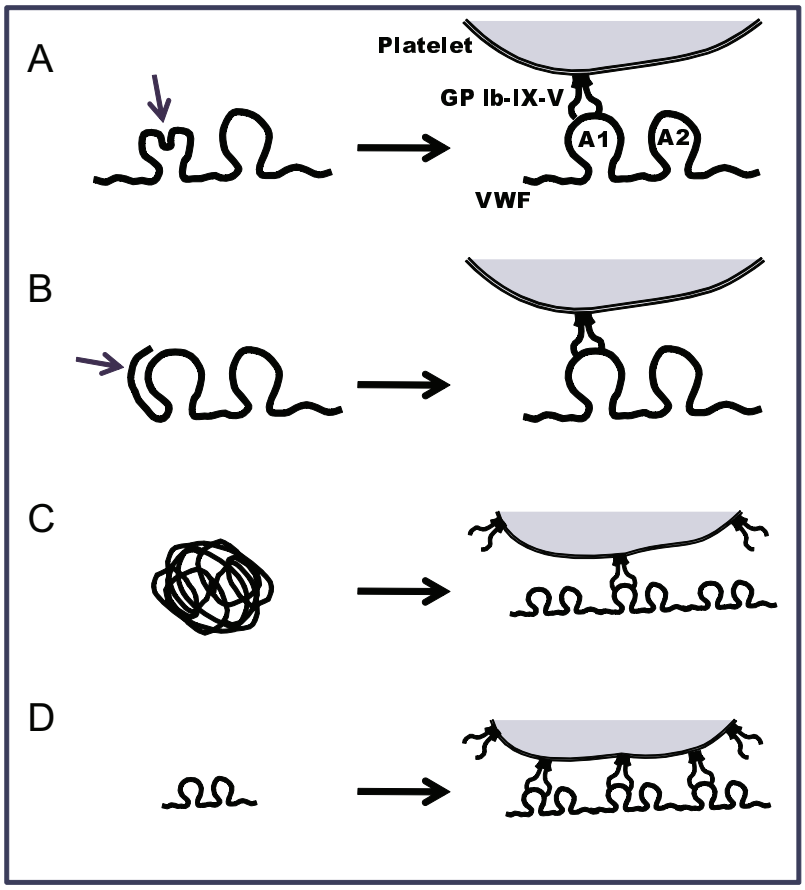

Figure 4: Putative mechanisms of the regulation of VWF GP Ibα interaction. Shear and/or immobilisation may directly alter the conformation (A) or may result in the exposition (B – shielding, C – burial) of the binding site. As ADAMTS13 cleaves large oligomers shear dependently, the avidity of VWF may change as well in response to shear forces (D).

to the A1 domain, which contains the only known GP Ibα binding site in VWF. These mutations are thought to act through the destabilisation of the base of the A1 domain and thereby mimicking the structural changes caused by shear stress[66]. It has been also demonstrated using molecule modeling that the mechanical stress changes the orientation of GP Ib and the A1 domain in a fashion that a new salt bridge forms resulting in a stronger interaction[50].

2. Shear forces also may cause larger scale conformation changes, not directly involving the conformation of the GP Ibα binding site, but affecting its accessibility. The isolated A1 domain is shown to spontaneously bind to GP Ibα[67,68], which suggest that other domains also modulate the VWF GP Ib interaction. In line with this observation the monoclonal antibody (moAb) 1C1E7 is reported to bind to the N-terminal region of VWF (D'D3 region), but it induces VWD type 2 like alterations[69,70]. Small angle neutron scattering studies also suggest local rearrangements at the domain level in response to fluid shear[71]. (Fig. 4B) and there is evidence that the A2 domain can inhibit the VWF GP Ib interaction under certain conditions[72,73].

3. VWF in solution has a coiled structure causing a large fraction of the GP Ib binding sites to be buried. It is proposed that shear forces and/or immobilisation uncoils VWF, making the binding sites accessible[71,74,75]. Not all studies were able to confirm this hypothesis[76], suggesting that the binding of platelets to VWF, and the drag forces exerted on them in flow is also needed for uncoiling(Fig. 4C).

4. The size of the VWF multimers also affects the VWF GP Ib interaction. ULVWF is more adhesive than usual plasma VWF, and can spontaneously bind to platelets. It is generally accepted that larger multimers are more effective at supporting platelet adhesion which is ascribed to the increased avidity due to the higher number of binding sites[15,16](Fig. 4D). It is not known if and how the multimer size distribution is regulated during synthesis. However, under shear conditions ADAMTS13 can

specifically cleave secreted (UL)VWF[77]. This suggests that ADAMTS13 limits platelet adhesion by decreasing multimer size at sites of high shear flow. There are several publications suggesting that the effective multimer size of VWF can also increase extracellularly[18–20,78].

In experimental and diagnostic applications VWF binding to GP Ibα can also be induced artificially by exogenous modulators, such as ristocetin and botrocetin. Ristocetin is a bacterial glycopeptide, which can induce platelet agglutination through GP Ib in the presence of VWF. This presumably involves a bridging mechanism and the binding of dimeric ristocetin to both GP Ibα and VWF[79]. Botrocetin is a snake venom isolated from *Bothrops jararaca*, acts by providing a supplemental platform suited for GP Ibα after forming a 1:1 complex with A1 domain of VWF[80]. Under these conditions binding does not necessarily resemble the mechanisms relevant for biological functions. Even so it has been demonstrated that ristocetin dependent interactions quite closely correlate with the physiological shear dependent situation[63].

3 Objectives

Our aim is to study the importance of interdomain interactions in the modulation of the affinity of VWF towards GP Ib, and to develop novel methods enabling further studies in this field.

- Analyse the role of the D'D3 region in regulating the VWF – GP Ib interaction:
  - Explore the mechanism of action of the monoclonal antibody 1C1E7. This antibody has its binding site in the D'D3 region — outside of the GP Ib binding domain (A1) — but still it enhances the VWF GP Ib interaction
  - Cross-blocking studies using monoclonal antibodies binding to different domains of VWF
  - Studies with recombinant deletion mutants of VWF
- Development of novel methods:
  - Improve and extend the methods of VWF multimer distribution analysis, including electrophoresis and data analysis techniques
  - Establish a system, where platelets are substituted with similar sized corpuscules bearing functionally active GP Ibα. This would enable the study of the effect of platelets dragging VWF under flow conditions on the conformation of VWF.

4 Materials and Methods

4.1 Interdomain interactions

4.1.1 Materials

Different moAbs against VWF were described previously. moAb 82D6A3 binds to the VWF A3 domain and inhibits VWF binding to collagen types I, III, and IV[81], and moAb 1C1E7 recognises the N-terminal part of VWF (aa 764–1035)[69]. moAbs 724, 701, and 418 were kind gifts of Dr. J. P. Girma (INSERM U143, le Kremlin-Bicêtre, Paris, France). moAbs 724 and 701 recognise the VWF A1 domain[82,83], whereas moAb 418 interacts with the first 106 aa in mature VWF[84] (Fig. 5). VWF was purchased from the Red Cross (Brussels, Belgium). moAbs or VWF were biotinylated using EZ-link Sulfo-NHS-SS-Biotin (Perbio, Helsingberg, Sweden).

Pooled plasma was prepared from the plasma of 25 healthy volunteers. The vector pSV2-dhfr[85] was obtained from American Type Cell Culture (Manassas, VA). Restriction endonucleases were from MBI Fermentas (Vilnius, Lithuania). Numbering of the aa sequence of VWF or the nucleotide sequence of the VWF gene starts with, respectively, the initiator methionine or the start codon as the +1 position. Recombinant VWF/D'A3 (aa 1–1874), VWF/D'D3 (aa 1–1247), and VWF/A1-CK (1260–2813) were expressed and purified as described before[86]. For clarity, we renamed VWF/DA3 and VWF/A1-CK as plusD'D3 and ΔD'D3, respectively (Fig. 5).

4.1.2 Construction and expression of 1C1E7 single-chain variable fragment

Total cell RNA was extracted from 1C1E7-expressing hybridoma cells using the RNeasy mini kit (Qiagen, Venlo, The Netherlands) and was reverse-transcribed using the ThermoScript reverse transcription-PCR system (Invitrogen) and

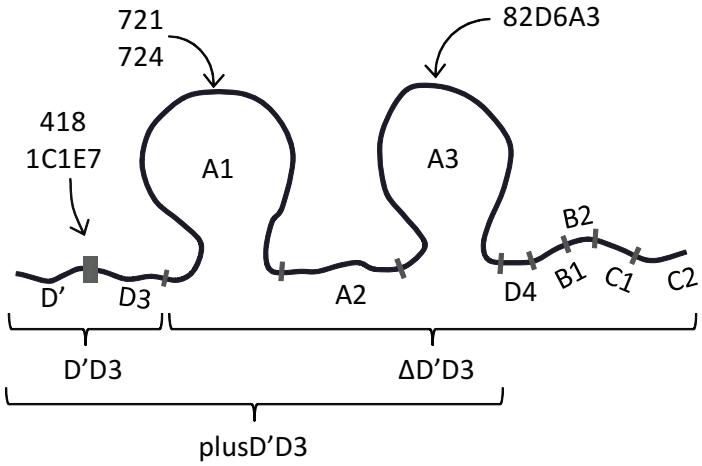

Figure 5: Schematic representation of deletion mutants used in the study. Binding regions of anti-VWF monoclonal antibodies are also indicated.

oligo$(dT)_{20}$ primers. The N-terminal sequence of the heavy and light chain of 1C1E7 was determined by Edman degradation (TopLab, Martinsried, Germany). Based on these amino acid sequences, degenerate sense primers were designed for the heavy and the light chain variable regions (V_H and V_L, respectively). These together with framework-specific antisense primers were used in the subsequent PCR reactions[87,88]. V_H was amplified using the Pfu Turbo DNA (Stratagene, La Jolla, CA) polymerase, while V_L was amplified using the Platinum® Taq DNA polymerase (Invitrogen). V_H and V_L PCR products were ligated in the pCR®-Blunt (Invitrogen) and the pCR®2.1-TOPO® vectors (Invitrogen) respectively. The single-chain variable fragment (scFv) coding sequence (V_H–$(G_4S)_3$–V_L) was constructed by splice overlapping extension PCR after extendending both V_H and V_L appropriately. This PCR product was ligated in the pSecTag/FRT/V5-His vector (Invitrogen) subsequently.

The 1C1E7 scFv was expressed in *Escherichia coli* as a His-tag fusion protein. Briefly, NcoI and XhoI restriction sites were added to the 3' and 5' ends, respectively, by PCR using sequence-specific primers. The 1C1E7 scFv DNA was cloned in the pET26+ vector (Stratagene) using the restriction sites added in the previous step. BL-21 *E. coli* were transformed with the construct

and were induced for 2 h with 0.5 M isopropyl-β-D-galactoside. The bacteria were harvested (10 000×g for 10 min), and cell proteins from the pellet were extracted with the BugBuster protein extraction reagent (Novagen, Merck). 1C1E7 scFv was found in inclusion bodies. To refold the scFv, inclusion bodies were dissolved in IB buffer (6 M guanidine-HCl, 1.5 M urea, 0.6 mM reduced glutathione, 0.3 mM oxidised glutathione in phosphate-buffered saline, PBS)[89]. The solubilised proteins were subsequently dialysed against a series of urea solutions (8, 6, 4, and 2 M, each of them overnight at 4 °C) and, finally against PBS.

4.1.3 Platelet agglutination

Agglutination studies were performed in an Elvi-840 dual channel aggregometer (Pabish, Brussels, Belgium) with constant stirring at 1000 rpm at 37 °C. For the agglutination experiments using 1C1E7 scFv, blood was drawn from healthy volunteers on trisodium citrate, pH 7.5 (0.11 M, 10:1 v/v), and centrifuged at 180×g for 10 min to obtain platelet-rich plasma. Platelet-rich plasma was incubated for 3 min with buffer and with 1C1E7 scFv or IgG, after which agglutination was induced by the addition of ristocetin. For the agglutination experiments using the VWF fragments, blood was collected on acid citrate dextrose (0.085 M trisodium citrate, 0.065 M citric acid, 0.110 M glucose, pH 4.5) (10:1.5 v/v). Platelets were washed twice and resuspended in PBS containing 1 mg/ml glucose and 1 mg/ml bovine serum albumin. A final platelet concentration of 200 000 platelets/l was used. ΔD'D3, plusD'D3, or VWF/D'D3 were added to a final concentration of 10 µg/ml, and the mixture was incubated for 3 min, after which agglutination was induced by the addition of ristocetin.

4.1.4 Cross-blocking analysis for antibody binding to immobilised VWF

96-Well microtiter plates were coated ON at 4 °C with VWF (10 µg/ml in PBS) and blocked for 2 h at RT with TBS containing 3% milk powder. Wells were

incubated for 1 h at 37 °C with one biotinylated moAb (b-418, b-701, b-724 or b-82D6A3) at its half-maximal binding concentration in the presence of one competing (non-biotynilated 418, 701, 724 or 82D6A3) moAb at saturating concentration using TBS containing 0.3% milk powder as buffer. Bound b-moAb was detected for 45 min at RT with peroxidase-labelled streptavidin (1 / 10000 in TBS containing 0.3% milk powder), and was visualised with H_2O_2 and *ortho*-phenylenediamine (Sigma), and the colouring reaction was stopped with 4 M H_2SO_4, after which the absorbance was determined at 490 nm.

4.1.5 Cross-blocking analysis for antibody binding to VWF in solution

96-Well microtiter plates were coated with moAb 418 or 82D6A3 (2 µg/mL in PBS) and blocked for 2 h at RT with TBS containing 3% milk powder. Biotinylated VWF (b-VWF, 6 µg/mL) was preincubated with one of the anti-VWF moAbs (418, 701, 724 or 82D6A3 at saturating concentration) for 1 h at 37 °C after which this solution was transferred to the coated wells. After a further incubation of 30 min at 37 °C, bound b-VWF was detected with peroxidase-labelled streptavidin as described above.

4.2 VWF multimer distribution

4.2.1 Samples

Blood samples were collected by venipuncture from the antecubital vein into tubes containing 3.2% sodium citrate (9:1, vol/vol). Platelet-poor plasma was prepared by centrifuging the samples twice at 2 000×g for 15 minutes at room temperature, after which 500 µL aliquots of the supernatants were stored at -70 °C until use. Normal control plasma was purchased from Dade-Behring (Marburg, Germany). Platelet lysate was prepared from healthy subjects' (n=20) EDTA anticoagulated whole blood. First platelet rich plasma was prepared by centrifuging the samples for 10 minutes at 150×g. Then the

platelets were pelleted at 3 000×g, and washed once with HEPES buffer supplemented with 0.05 M EDTA pH=7.4. 2×10^7 platelets were pelleted again, and suspended in 100 µL of sample buffer.

Normal samples were provided by thirty-five healthy volunteers. Twenty-five VWD type 2 patients diagnosed at the hospital of the University of Debrecen were included in the study. Written informed consent was obtained from all subjects in accordance with the Declaration of Helsinki and our Institutional Review Board approved the study.

4.2.2 SDS agarose gelelectrophoresis

VWF molecules were separated either by using the modified Laemmli buffers as described by Ruggeri and Zimmerman[27] or by a Tris-Borate discontinuous buffer system according to the agarose manufacturer's recommendation (Seakem HGT, Lonza, Basel, Switzerland). Briefly, low resolution (0.8%) agarose running gels (12.5 cm×10 cm×1.2 mm) were cast on glass plates. Not more than two hours before the runs the first 2.5 cm strip was replaced with the stacking gel. The samples were mixed with sample buffer (10 mM Tris, 1 mM EDTA, 8 M Urea, 2 % SDS, 0.05% bromophenolblue, pH=8.0) so that the final VWF concentration was 0.05 U/mL and then were denatured for 20 minutes at 60 °C. Electrophoresis was performed at constant current for either 6 hours at 20 mA/gel, or overnight at 6 mA/gel on a plate cooled to 18°C. The modified Laemmli system consists of an SDS Tris-Glycine electrophoresis buffer (0.05 M Tris, 0.384 M Glycine, 0.1% SDS), SDS Tris-HCl stacking gel buffer (0.125 M Tris, 0.1% SDS, pH=6.8 at 18 °C) and SDS Tris-Glycine running gel buffer (0.375 M Tris, pH=8.0 at 18 °C). The Tris-Borate discontinuous buffer system includes an SDS Tris-Boric acid electrophoresis buffer (0.09 M Tris, 0.09 M Boric acid, 0.1% SDS), a Tris-HCl stacking gel buffer (0.125 M Tris, pH=8.0 at 18 °C) and Tris-Boric acid running gel buffer supplemented with urea (0.5 M Tris, 0.16 M Boric acid, 1 M Urea).

4.2.3 Immunoblotting

The proteins were transferred to PVDF membranes (Immobilon-P, Millipore Corp, Bedford, MA, USA) using the tank electro-blotting method. To enhance the transfer of the largest VWF molecules, VWF multimers were degraded by treating the gels for 10 minutes with 1 mM β-mercaptoethanol (mercaptolysis) before blotting as reported recently by Bowen and Bowley[32]. VWF was visualised by immunostaining using HRP labelled polyclonal rabbit anti-human VWF antibody (DakoCytomation, Glostrup, Denmark) and DAB substrate. Some membranes were stained for IgM in a second step, using goat anti-human IgM and HRP labelled anti goat antibodies. In these cases an image was captured before and after the IgM immunostaining.

4.2.4 Quantitative multimer analysis

Digital images of the membranes were obtained by a GS-800 calibrated densitometer and processed by its QuantityOne software (Bio-Rad Laboratories, Richmond, CA, USA). First the background density of the image was subtracted coarsely, the background level was assessed as an average value from a representative, protein free area. The resulting reflective density (RD) against relative mobility (Rf) data was used for subsequent calculations. The background was further reduced in each lane based on the average RD not containing VWF. The resulting RD versus Rf curves were smoothed by the moving average method, and the VWF peaks were identified.

The quantitative analysis was performed using two methods (Fig. 6). For the first method the relative amount of large multimers (M_{10}) was calculated. Large multimers were defined as oligomers larger than the icosamer (band 10) including the area where VWF did not resolve into bands.

For the second method we assessed the degree of multimerization. The degree of multimerization was characterised by the molecular weight corresponding to the lower boundary of the largest 25% of VWF protein. First, a cumulative RD against Rf curve was constructed, and the the Rf value where the curve has reached 25% was determined. The molecular weight corresponding to this Rf (M_{MW}) was estimated based on the correlation of

the VWF peaks mobility and their molecular weight (estimated as 0.5 MDa for a homodimer unit) in each lane and was calculated using the coefficients of regression of the log Rf versus estimated Mw data. The 25% boundary was chosen after comparing the M_{MW} of groups of samples lacking large multimers, normal samples and samples containing unusually large multimers using different boundaries.

The processing of densitometric data in case of both the M_{MW} and the M_{10} calculation was computerized, no manual steps were involved. For statistical analysis, Graphpad Prism software (version 5.00 for Windows, GraphPad Software, San Diego California USA) was used.

4.2.5 VWF cleavage by ADAMTS13

VWF digestion experiments were performed according to Gerritsen et. al.[90], briefly substrate plasma was prepared by dialyzing the plasma of a healthy individual against 4.5% polyethylene glycol 5 mM Tris, pH 8.0. Before use, the substrate was mixed with 8 M Urea in 5 mM Tris pH=8.0 so that the final concentration of Urea was 1.5 M. A series of plasma dilutions between 1/5 – 1/320 in 1.5 M Urea, 5 mM Tris we re prepared and aliquots of 50 µl were preincubated with 5 µl 93 mM $BaCl_2$ for 30 min at 37 °C. 100 µl of substrate was added to the aliquots (the concentration of $BaCl_2$ was 3 mM in the reaction mixture) and further incubated for 2 hours at 37 °C. The digestion was stopped by adding 10 µl of 0.825 M Na_2SO_4, and samples were analysed by gel electrophoresis.

4.2.6 VWF antigen, collagen binding activity and ristocetin cofactor assay

VWF:Ag was measured by ELISA according to Cejka[91]. VWF:CB was measured as the antigen, but Type III collagen (Sigma, St Louis, MO, USA) was used for coating. Optical density reading was carried out using an Infinite 200M microplate reader (Tecan Trading AG, Switzerland), standard curve fitting (four-parameter Marquardt) and subsequent calculations were carried

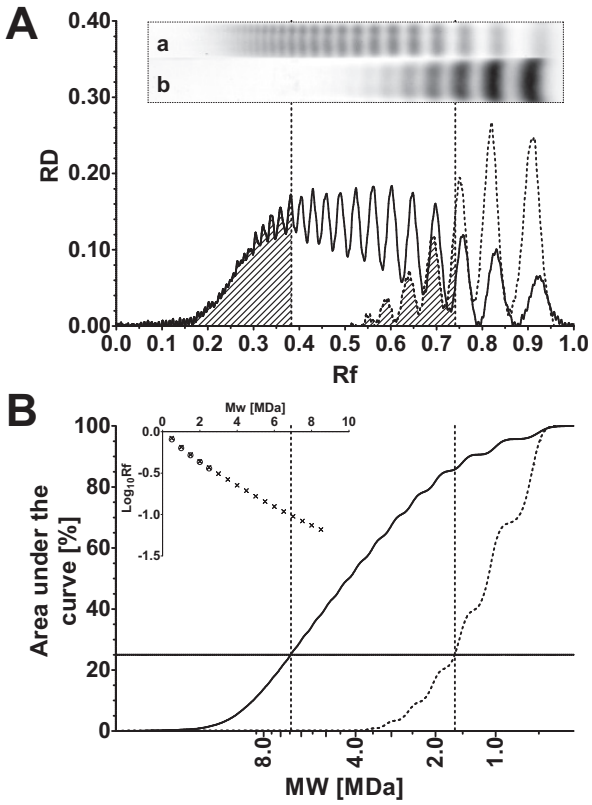

Figure 6: Calculation of the M_{MW} parameter. (A) reflective density (RD) versus relative front (Rf) curves from the normal (continuous line) and the VWD type 2 (dashed line) sample. The filled area represents the upper 25% of the total area under the curve. A picture of the normal (a) and the VWD type 2 sample (b) is shown in the inset. (B) Cumulative curve of the samples. The abscissa represents the MW calculated from the correlation between the logarithm of the VWF Rf values and their corresponding MW (correlation is shown in the inset, normal samples $\times$, VWD type 2 samples $\bigcirc$). The ordinate shows the area under the curve of Fig A between the origin and the given MW, expressed as percentage of the total area under the curve. Twenty-five percent threshold is marked with a horizontal line on the graph.

out using the Magellan software of the instrument. VWF:RCo was measured by the Helena Ristocetin Reagent (Helena BioSciences, Sunderland Enterprise Park, Sunderland, UK) and a Chrono-Log 810-CA lumiaggregometer (Chronolog, Havertown, PA, USA). The WHO Standard was used for calibration in all of these methods.

4.3 GP Ibα microspheres

4.3.1 Materials

Recently outdated platelet concentrate was obtained from the East Regional Haemophilia Centre, Regional Blood Transfusion Centre of Hungarian National Blood Transfusion Service, Debrecen. plasma was prepared from the plasma of 25 healthy volunteers. Mouse moAb 24B3 is a monoclonal antibody capable of capturing glycocalicin from plasma in a functionally active comformation[92]. (glycocalicin is a highly glycosylated, hydrophilic135 kDa proteolytic fragment of GP Ibα, circulating in plasma at a concentration of 1-3 μg/ml[93]. Polyclonal anti human VWF (A0082), phycoerythrin (RPE) conjugated anti mouse IgG (R0480) and anti human GP Ibα (clone AN51, R7014), FITC conjugated anti rabbit IgG antibodies were from Dako (Dako Cytomation, Glostrup, Denmark). 3 μm carboxylate polysterene microspheres (#09850, Polybead) and protein coupling kit (#24350-1, PolyLink Kit for COOH microparticles) were from Polysciences (Polysciences, Warrington, PA, USA). The calibrator beads of the ADIAflo Platelet GP kit (p.No. 674, American Diagnostica, Inc., Stamford, CT) were used to create calibration curves for counting purposes. Flow cytometric measurements were performed on a BD FACSCalibur flow cytometer (BD Biosciences, San Jose, CA). FPLC equipment, columns and resins (Sepharose 4FF 16/50 HR, Q Sepharose HP 16/10 HR, HiTrap Heparin HP 1ml) were purchased from Amersham Pharmacia (Amersham Pharmacia Biotech, Piscataway, NJ).

4.3.2 Preparation of 24B3 coated microbeads

24B3 antibody was covalently immobilised onto 3 µm carboxylate polysterene microspheres according to the manufacturer's protocols. Briefly, beads were activated with 20 mg/ml EDAC in coupling buffer (50 mM MES, pH 5.2, 0.05% Proclin-300), washed twice in 50 mM phosphate buffer (pH=7.4), mixed with 24B3 (final concentration 200 µg/ml) and incubated for 6 h end-over-end mixing at room temperature. Residual activated unbound groups on the bead surface were quenched using ethanolamine and the beads were resuspended in wash / storage buffer (10 mM Tris, pH 8.0, 0.05% BSA, 0.05% Proclin-300).
cytometry using the calibrator beads of the ADIAflo Platelet GP kit after incubating the beads and calibrator beads with anti mouse IgG-RPE.

4.3.3 Verification of 24B3 beads, demonstration of VWF binding

Outdated human platelets were used as the source of glycocalicin and VWF. The platelet concentrate was washed twice and then sonicated. The sonicated platelet solution was incubated at 37 °C for 30 min to allow calpain released from the platelets to cleave membrane bound GP Ibα[94]. Cell debris was removed by ultracentrifugation and the supernatant was filtered on a 300 kDa molecular weight cut off centrifugal concentrator (Vivascience AG, Hannover, Germany). The holdup was used for subsequent VWF (Mw>500kDa) purification, the filtrate was used as the source of glycocalicin (Mw~135 kDa).

24B3 coated beads were incubated with the flowthrough of the platelet lysate overnight at 4 °C and washed once with PBS (pH=7.4). Purified VWF and Botrocetin (final concentration 1 U/mL and 40 µg/mL respectively) was added to the beads, and incubated for 2 h. Samples were fixed with 1% paraformaldehyde and washed twice with PBS. Finally, the sample was incubated with rabbit anti-VWF polyclonal antibody for 45 minutes, washed once with PBS, and incubated again with swine anti rabbit IgG-FITC. An aliquot was taken after the incubation with the flowthrough, which was washed

with PBS, fixed, and incubated with anti GP Ibα-RPE. Control samples were also prepared by omitting glycocalicin or botrocetin. Bound fluorescently labelled antibodies were detected by flow cytometry.

4.3.4 VWF purification

VWF purification was adapted from previously published methods[95,96]. All purification steps were performed in 20 mM Tris / HCl buffer, pH=7.0. Where required, Tris buffer was added to the pooled fractions to lower the salt concentration between steps. First the holdup of the platelet lysate was separated on a Sepharose 4FF column equilibrated in 150 mM NaCl in Tris buffer. The VWF containing eluates were pooled, and loaded onto a column packed with Q-Sepharose HP anion exchange gel. The column was washed with 260 mM NaCl in Tris buffer, and VWF was eluted by 380 mM NaCl in Tris buffer. VWF containing fractions were filtered through a HiTrap Heparin HP column, which was subsequently washed with 90 mM NaCl in Tris buffer, and VWF was eluted with 450 mM NaCl in Tris buffer.

5 Results

5.1 Interdomain interactions

5.1.1 Platelet agglutination studies — function of D'D3 region

Previous studies has suggested, that the GP Ibα VWF-A1 interaction might also be modulated by other domains. The moAb 1C1E7 binds to the D'D3 region of VWF and it can still positively modulate the binding of GP Ibα to VWF. This suggests a functional role of D'D3, which we studied using the following dimeric recombinant VWF constructs: ΔD'D3 (lacks the D'D3 region but still contains the N-terminal flanking region of the VWF A1 domain), plusD'D3 (lacking D4-CK region, used as control possesing the D'D3 region and the A domains) and D'D3 (containing only the D'D3 domains). Dimeric constructs were used because previous studies demonstrated the necessity of at least dimeric molecules for sustaining platelet aggregation. At lower platelet concentrations, ΔD'D3 was able to sustain spontaneous platelet agglutination in contrast to plusDD3 (data not shown). The threshold dose needed for ristocetin induced platelet agglutination (RIPA) of washed platelets was lower for ΔD'D3 than for plusD'D3 (Fig. 7A), demonstrating the inhibitory effect of the D'D3 region on the interaction of VWF with GP Ibα. In line with this, D'D3 inhibited RIPA supported by ΔD'D3 while having no effect on plusD'D3 (Fig. 7B). These results show that the deletion of the D'D3 region ΔD'D3 could be reverted by external addition of these isolated D'D3 domains. These experiments demonstrate the functionality of the D'D3 region in the interaction of VWF with GP Ibα, suggesting that D'D3 is restricting the accessibility of the GP Ibα binding site in VWF-A1 possibly by a shielding mechanism.

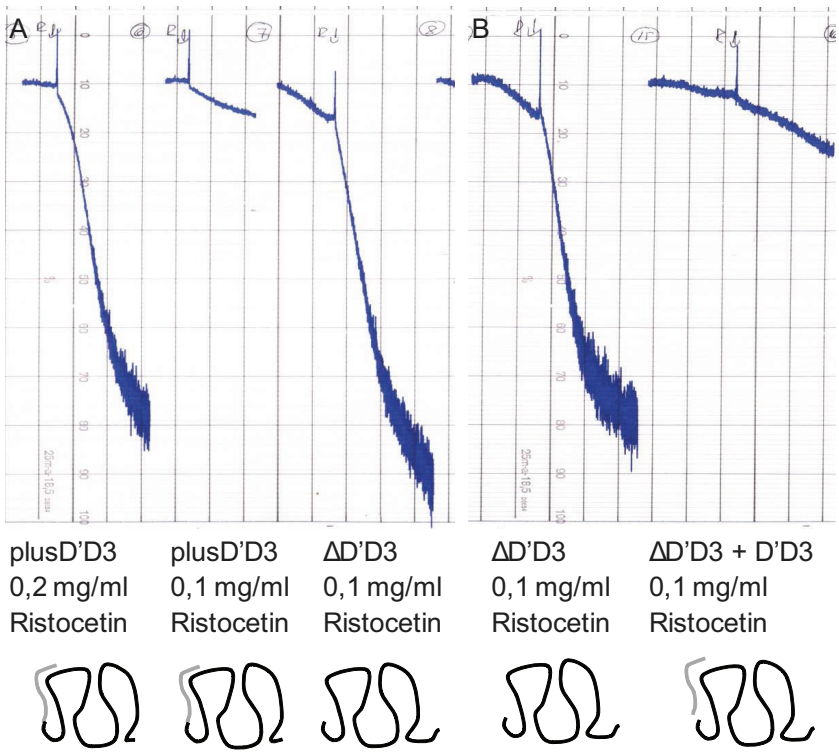

Figure 7: Ristocetin induced platelet aggregation studies with VWF deletion mutants. A, ΔD'D3 had a lower threshold in ristocetin-induced platelet agglutination. Washed platelets were incubated with 10 μg/mL ΔD'D3 or plusD'D3 after which agglutination was induced by the addition of ristocetin. B, D'D3 was able to inhibit (average inhibition 91%) ΔD'D3 mediated platelet aggregation, while it had no effect on D'A3. ΔD'D3 or plusD'D3 ± D'D3 were preincubated in a small volume for 15 min and were added to washed platelets at 10 μg/ml final concentration, agglutination was induced by threshold dose of ristocetin. Results are representative of three independent experiments.

5.1.2 Cross blocking studies

Next, we have verified the structural proximity of the D'D3 region with the A1 domain, by testing whether the binding of moAb 418 or 1C1E7 (interacting with the D'D3 region) could be blocked by moAbs 701 and 724 (both interacting with the A1 domain) both using VWF in solution and immobilised VWF. As a negative control, moAb 82D6A3 (interacting with the A3 domain) was used. Two different enzyme-linked immunosorbent assay like setups were developed, (i) cross-blocking of binding of moAbs (one biotinylated and one non-biotinylated) to immobilised VWF and (ii) the inhibition of the capture of b-VWF to immobilised 418 or 82D6A3 moAb by unlabelled moAbs. Previous data demonstrated that biotinylation of VWF had no effect on the interaction with fibrillar collagen or GP Ib, which suggests that the conformation of biotinylated VWF is intact[97]. When VWF was immobilised, no measurable inhibition of the binding of b-418 was observed by any of the moAbs except with unlabelled 418 as the positive control, although all moAbs were able to interact with immobilised VWF. In contrast, moAbs 701 and 724 did compete with moAb 418 for the binding to soluble b-VWF, whereas moAb 82D6A3 had again no effect. When 82D6A3 was coated, no inhibition was detectable by the other moAbs (Fig. 8). This would suggest that in solution the A1 domain and the D'D3 region are in close proximity since moAbs interacting with these regions cross-block each other. However, when VWF was immobilised, moAbs interacting with the A1 domain failed to block binding of moAb 418 interacting with the D'D3 region, suggesting that these regions are now more distant from each other.

5.1.3 Construction and Expression of 1C1E7 scFv

To further characterise the VWF-activating potency of the moAb 1C1E7, the scFv was expressed as a His-tagged fusion protein in E. coli. 1C1E7 scFv increased ristocetin-induced platelet aggregation, similarly to 1C1E7 IgG (Fig. 9, upper part), providing evidence that the construction was correct. Moreover, 1C1E7 scFv inhibited binding of the IgG to VWF, suggesting a same interaction site in VWF (data not shown). Comparison of the primary

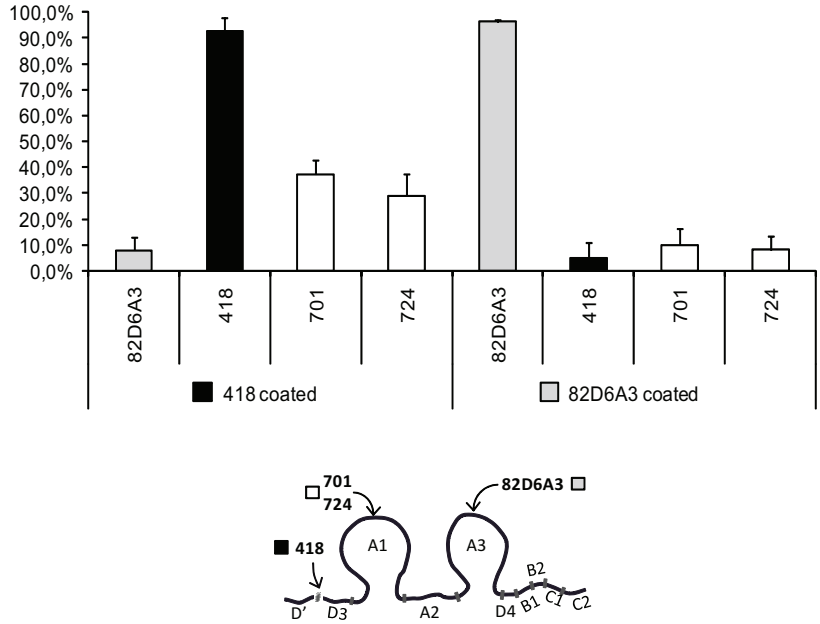

Figure 8: Cross-blocking studies of the binding b-VWF to immobilised moAb 418 or 82D6A3 by anti-VWF moAbs. Microtiter plates were coated with with moAb 418 or 82D6A3 and incubated with b-VWF in the presence of the anti-VWF moAbs 82D6A3, 418, 701, or 724. Bound b-VWF was detected. Percentage inhibition is shown (n=3). At the lower part a schematic representation of the binding areas of the moAbs (with colour coding) are shown..

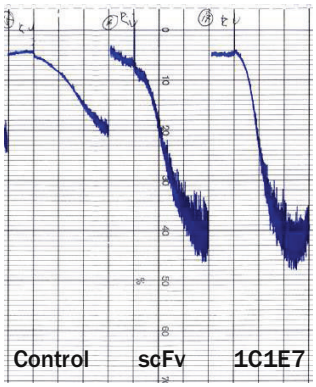

VWF A1 1261 DI**S**E**PPLH**D**F**YCSRLL**DL**VFLL
1C1E7 H3 **A**R**PPLY**G**F**TYGWYF**DV**

Figure 9: Functionality of 1C1E7 scFv. Upper part, stimulating effect of 1C1E7 scFv on platelet aggregation in platelet-rich plasma. Platelet-rich plasma was incubated with PBS buffer (Control), 1C1E7 scFv refolded from inclusion bodies (scFv) or 6 μg/ml 1C1E7 IgG (1C1E7), after which a threshold dose of ristocetin (0.2 mg/ml) was added. Results are representative of three independent experiments. Lower part, alignment of the primary sequence of the N-terminal flanking region of the human A1 domain and the complementarity determining region 3 of the 1C1E7 heavy chain.

sequence of the complementarity determining region 3 of the 1C1E7 heavy chain revealed a strong similarity with the N-terminal flanking region of the VWF A1 domain (Fig. 9, lower part). As mentioned before, there is good evidence that this N-terminal flanking region modulates the binding of VWF to GP Ib. Based on our observation, we hypothesized that 1C1E7 might be able to mimic this region of the A1 domain. Because 1C1E7 binds to the D'D3 region in VWF, the N-terminal flanking region of the A1 domain might have similar binding characteristics. This putative interaction of the A1 domain with the D'D3 region could modulate the VWF binding to GP Ib.

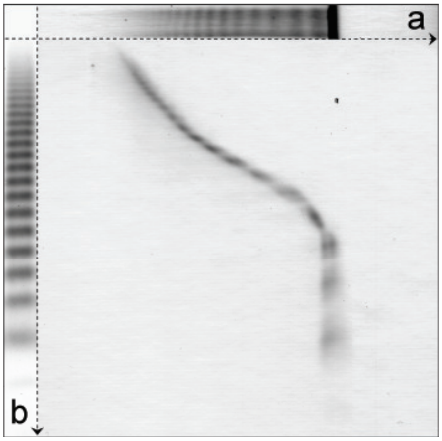

Figure 10: Comparison of VWF multimer separation in Laemmli and Tris-Borate buffers. Denatured normal plasma sample was separated by two dimensional electrophoresis, Laemmli buffers in the first dimension (a), Tris-borate gel in the second (b). For reference a representative lane from the Laemmli gel (a) and from a Tris-Borate gel is shown (b)

5.2 VWF multimer distribution

5.2.1 Comparison of buffers

We detected 18 to 22 discrete bands in normal samples when using the Tris-borate buffers. Fewer bands were resolved with the Laemmli buffers, where also a distorted band near the running front was commonly visible. To compare the resolving power of the gels, and to elucidate the contents of the distorted band, a sample was separated in a two-dimensional electrophoresis with a Laemmli gel in the first dimension and a Tris-Borate gel in the second (Fig. 10). The separation of large multimers was superior in the direction of Tris-Borate buffers, and also the distorted band in the Laemmli gel resolved into multiple bands. We excluded the possibility that the extra bands in the Tris-Borate buffers are VWF degradation products by comparing their relative mobilities to IgM (MW: ~0.8 MDa). We have found that only one VWF band — presumably the VWF dimer (MW: ~0.5 MDa) — had a smaller molecular weight than IgM.

5.2.2 Optimisation of M_{MW} calculation

After optimisation, M_{MW} was defined as the molecular weight of the lower boundary of the largest 25% of VWF protein (M_{MW}). The 25% limit was established by evaluating a subset of data (7 platelet lysate, 11 normal and 8 VWD 2B samples) using a range of limits between 1-80%. The method's ability to distinguish between the groups of samples (platelet lysate, normal and VWD type 2) was evaluated by the t-statistic. At smaller thresholds the discrimination between the platelet lysate and normal groups increased, whereas the best discrimination between the normal and VWD 2B groups was observed when calculating with larger thresholds (Fig. 11). The 25% threshold is equally spaced from the threshold where platelet lysate (10%) and where VWD type 2 samples (40%) are separated better from normal samples. At this threshold the statistical difference between groups is highly significant (mean±SD 10.42±0.78, 6.27±0.68, 2.13±1.12 MDa for platelet lysate, normal and VWD type 2 group respectively, $p<<0.01$)

5.2.3 Method Characteristics

Reproducibility, expressed as the coefficient of variation of M_{MW} and M_{10} measurements of the same normal control sample on different days (n=20) was 7.8% and 15.9% respectively. The M_{MW} and M_{10} of 35 healthy individuals was 6.1±0.72 and 33.5±7.9 (mean±SD). The methods' tolerance towards the variations in the intensity of immunostaining was studied by evaluating a series of dilutions of one sample between 0.25 – 2.5 times the standard dilution. The different dilutions yielded an average RD between 0.061 and 0.319 for the VWF containing part of the lanes, M_{MW} or M_{10} results were not affected in this range. The coefficient of variation (CV) of the different dilutions was 4.4% and 7.7% for M_{MW} and M_{10} respectively.

5.2.4 Correlation of M_{MW} and M_{10}

We evaluated M_{MW} and M_{10} of platelet lysate, control samples, VWF degraded by ADAMTS13 and samples from VWD type 2 patients. The VWF in platelet

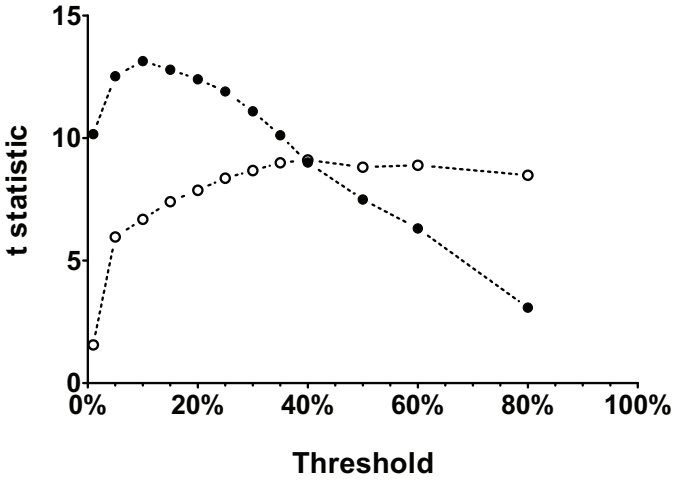

Figure 11: t-statistic is calculated at different thresholds for platelet lysate versus normal samples (●) and normal samples versus VWD type 2 samples (○). The highest t-statistic is observed at 10% in the first case and at 40% in the second. 25% threshold is equally spaced from the two peaks of the two curves, at this threshold the t-statistic is high in both relations, which shows that the null hypothesis is highly unlikely ($p << 0.0001$, group means±SD for platelet lysate, normal, and VWD type 2 samples are 10.42±0.78, 6.27±0.68 and 2.13±1.12 MDa respectively).

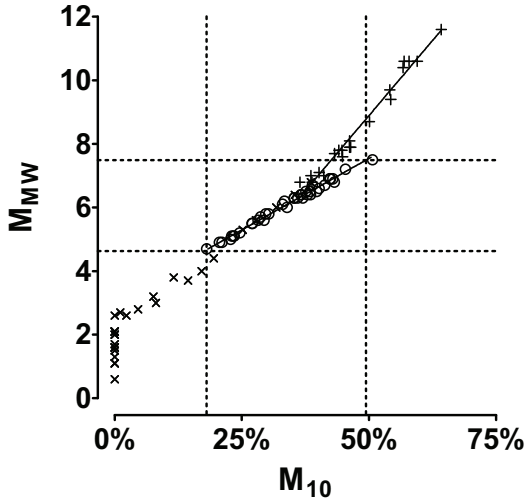

Figure 12: Correlation between M_{MW} and M_{10}. M_{MW} and M_{10} was calculated for VWD type 2 (×), healthy (○) and platelet lysate samples (+), mean ± 2SD is shown for the normal group (dotted lines). In cases of normal samples there is a good agreement between methods (r^2=0.98), in the case of platelet lysate the M_{MW} seems to increase more than M_{10}. For most VWD type 2 samples only M_{MW} was able to provide results other than 0.

lysate is protected from plasma proteases and consequently it contains larger multimers, whereas VWD type 2 patients typically have less or no large multimers. We found good correlation between the degree of multimerization and the amount of large multimers in normal samples (r^2=0.98) and platelet lysate, however the slope of the regression lines were different ($p<0.001$). Characteristically VWF in platelet lysate contained larger multimers than healthy samples with the same amount of large multimers. The M_{10} was 0 in about 50% of VWD type 2 samples (Fig. 12) as these patients do not have icosamers or larger oligomers. The rest of the VWD type 2 samples tend to have smaller multimers (lower M_{MW}) than ADAMTS-13 degraded VWF with the same amount of large multimers (M_{10}).

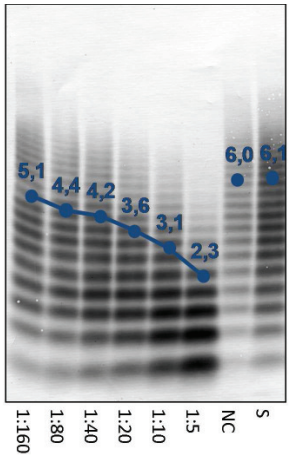

Figure 13: VWF substrate was degraded by different amounts of plasma ADAMTS-13 activated with $BaCl_2$ for 2 hours at 37°C in the presence of 1.5M urea. The different dilutions are noted on the abscissa, NC – normal control, S – untreated substrate VWF, the measured M_{MW} is noted on each sample.

5.2.5 ADAMTS-13 degradation experiments

We have tested the sensitivity of M_{MW} by evaluating VWF degraded by ADAMTS13 (Fig. 13). The highest dilution of normal plasma caused measurable decrease in multimerization (ΔM_{MW}: -0.32, M_{MW} of substrate: 6.01), however the estimated limit of detection is about 4.9% ADAMTS13 activity under the described conditions. The degraded VWF contained similar sized oligomers as the healthy samples with the same amount of large oligomers. (The points of degraded VWF are scattered closely around the regression line or the extension of the regression line of normal samples in Fig. 12)

5.2.6 Correlation of M_{MW} with VWF:CB and VWF:RCo

Results of the functional tests of VWF — collagen binding activity and ristocetin cofactor assay — were compared to M_{MW} on normal and VWD type 2 samples (Fig. 14). The functional assays to antigen ratios were at least partially determined by multimerization (r^2=0.42 and 0.43 for VWF:RCo and VWF:CB respectively). Four patient samples (16%) had normal M_{MW}

but abnormal functional assays, these cases are possibly VWD type 2M. On the other hand three (12%) VWD type 2 patients had normal VWF:RCo to antigen and five (20%) type 2 patients had normal VWF:CB to antigen ratios but abnormal M_{MW}. Some of these samples (1 in case of VWF:RCo and 3 in case of VWF:CB) had low antigen levels, where the reproducibility of the functional assays tends to diminish. Furthermore five (19%) of normal samples had abnormal VWF:RCo to VWF:Ag ratio, while none of these samples had abnormal M_{MW} or VWF:CB to VWF:Ag values.

5.3 GP Ibα microspheres

5.3.1 Analysis of the surface capacities of the beads

Polystyrene beads coated with 24B3 have acquired the ability to bind glycocalicin and monoclonal anti-GP Ibα antibodies. The number of bound glycocalicin molecules, was measured by the standard of the ADIAflo Platelet GP kit. BSA-coated beads served as a negative control. The geomean values of fluorescence intensity for bead standard peaks were plotted against their known binding capacities to generate a regression line. 24B3 beads were incubated with a fluorescently labelled anti-mouse IgG antibody or with glycocalicin and subsequently with a fluorescently labelled anti-GP Ibα antibody, the number of bound labelled antibodies was calculated using the calibration curve (Fig. 15). We have found that the number of coupled 24B3 (~64000) was only partially saturated with glycocalicin (number of bound glycocalicin molecules ~3140). The significantly lower number of detectable glycocalicin molecules indicates that not all of the immobilised 24B3 is in a binding conformation.

5.3.2 Botrocetin-induced binding of VWF to the beads

These experiments were performed to demonstrate that the glycocalicin captured by 24B3 onto the beads is in an active conformation. VWF was gently

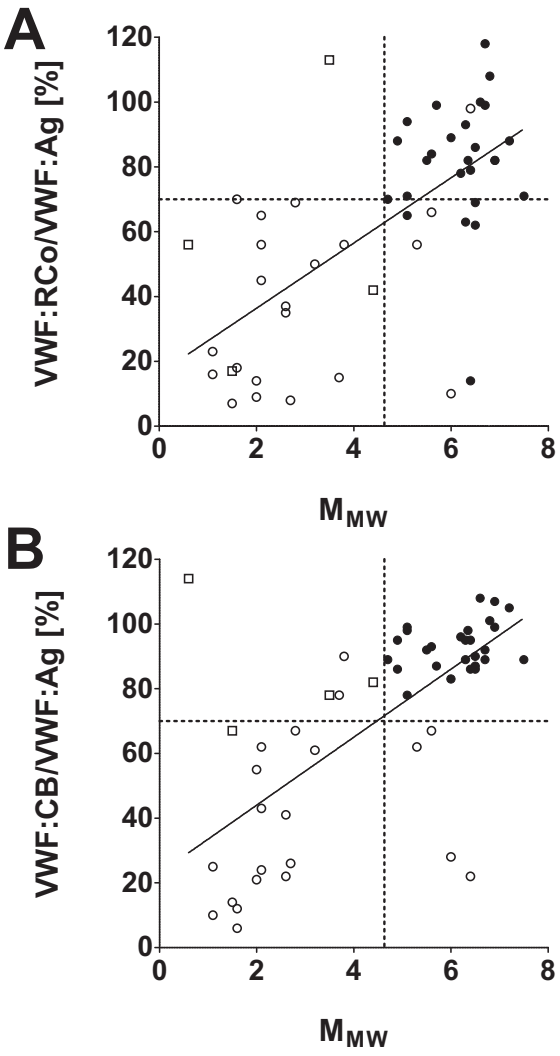

Figure 14: Correlation of VWF functional tests and M_{MW}. M_{MW} of normal (●) and VWD type 2 patients samples (○) was determined. Samples with antigen levels below 30% are marked with squares (□). Mean M_{MW}-2SD of the normal group and 70% activity-to-antigen ratio are marked with dotted lines. (A) VWF:RCo to VWF:Ag ratio versus M_{MW} (B) VWF:CB to VWF:Ag ratio versus M_{MW}.

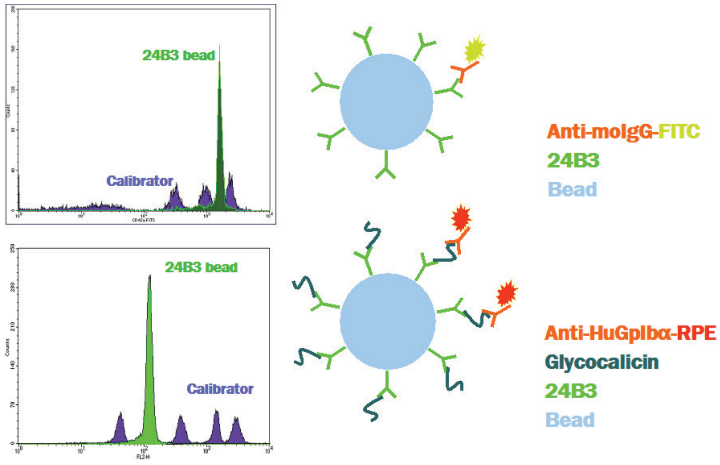

Figure 15: Validation of 24B3 beads. Upper part, the count of 24B3 molecules coupled to the carboxylate microspheres, lower part, count of glycocalicin bound to 24B3 beads. The number of the bound molecules, as calculated from the calibrator beads (blue) is 64334 and 3137 respectively

mixed and incubated with the 24B3 beads preincubated with glycocalicin and VWF was detected using a two-step labelling method. 1 U/mL VWF was mixed with the beads, but no VWF was detectable on the beads in the absence of a modulator. The addition of 40 µg/mL botrocetin (Fig. 16) however induced binding of VWF, which demonstrated that the glycocalicin captured by 24B3 is capable of binding to VWF. The specificity of the measurement was confirmed by omitting glycocalicin, which resulted in loss of VWF signal.

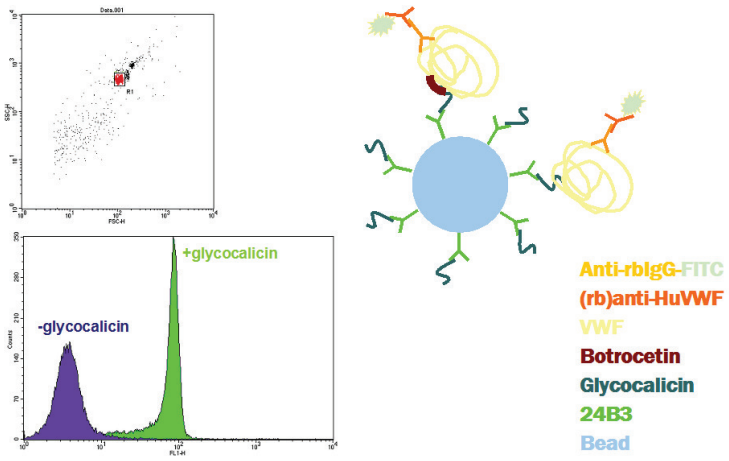

Figure 16: Demonstration of VWF binding to 24B3 beads. 24B3 beads were sequentially incubated with glycocalicin, VWF, polyclonal rabbit anti-VWF and anti rabbit IgG-FITC. Beads not incubated with glycocalicin served as negative control.

6 Discussion

The primary role of platelets can be summarised simply: "Platelets plug holes in blood vessels"[41]. More specifically, in the first step of this process platelets in the arterial side of circulation identify damaged vascular lining and stick to the areas of exposed subendothelium. Platelets in the capillaries move with an average velocity of 0.5 mm/s[98], this together with the fact that their diameter is approximately 2 µm means that they spend only approximately 4 ms above a given point of the vessel wall. This is a roughly the timeframe in which platelets have to identify injured vessel segments and adhere to it. The solution is similar to that of leukocytes[49,50] — at high shear rates, platelets also have a translocation phase between initial contact and firm adhesion, as seen in real-time intravital microscopic experiments[48]. In this process VWF acts as a bridge between the fast moving platelets and the stationary vessel wall[61]and enables their interaction. In order for this mechanism to work, VWF is present on activated endothelial cells[48], in the subendothelium and binds to subendothelial structures from the circulation itself. Interestingly VWF is present in the bloodstream together with platelets, but their interaction is only observed under very high shear conditions normally not present[63]. *In vitro*, binding of VWF to GP Ib can be induced by modulators such as ristocetin or botrocetin, although under these conditions binding is induced rather artificially. Even so it has been demonstrated that ristocetin dependent interactions quite closely correlate with the physiological sheardependent situation[63].

However *in vivo* binding is induced by the immobilisation of VWF and by exposure to shear. These observations suggest that the affinity toward GP Ib is regulated by conformational changes in VWF that are induced by shear and immobilisation and lead to exposure of functional sites. We have studied the possible role of interdomain interactions in this process by exploring the mechanism of action of the moAb 1C1E7[69]. This moAb interacts with the aa 764–1035 region in the N-terminal D'D3 domains in VWF but it is capable

of increasing the affinity of VWF towards GP Ib, although its binding site is distant from the GP Ib binding site[70]. This would suggest a modulator effect for the binding region of 1C1E7 in VWF on the GP Ib interaction, therefore we aimed to determine the functional role of the D'D3 region in binding of VWF to GP Ib. Deletion of the D'D3 region resulted in a higher affinity for GP Ib as demonstrated by the lower ristocetin threshold of the dimeric constructs ΔD'D3 (lacking the D'D3 region) compared to plusD'D3 (lacking the C-terminal region, but having intact D'D3 domains) in RIPA studies. Moreover, at lower platelet concentrations, ΔD'D3 was able to sustain spontaneous platelet agglutination in contrast to plusD'D3. All together, these data strongly suggest that the D'D3 region may act as an inhibitory region, limiting the accessibility of the A1 domain in VWF. Our data further confirm and extend previous studies that demonstrated the putative shielding of the GP Ib binding site in the A1 domain by the N-terminal flanking regions of the A1 domain (aa 1260–1271) and the C-terminal region of the D3 region (aa 1204–1259)[99–102]. It is known that immobilisation of VWF is a prerequisite for platelet adhesion at high shear stress, probably due to conformational changes. However, the exact nature of these conformational changes has not been elucidated yet. To further substantiate the idea that DD3 would interact with A1 in VWF in solution and no longer when immobilised / sheared, we looked to whether moAbs against the respective domains would block each others binding or not under those conditions when VWF was immobilised on a polystyrene surface, as it is known that this allows platelet recruitment. The anti-D'D3 moAb 418 cross-competed with the anti-A1 domain moAbs 701 and 724 when VWF was in solution, but not on immobilised VWF, indeed providing evidence for a changing distance between the domains upon immobilisation. Previous studies suggested a structural change in the D'D3 region upon immobilisation of VWF onto calf skin collagen, causing a reduced affinity for factor VIII[103]. The conformational change in the D'D3 region upon the immobilisation of VWF could also expose the GP Ib binding site. Finally, we also found sequence similarity between the primary sequence of the complementarity determining region 3 of the 1C1E7 heavy chain and the N-terminal flanking region of the VWF A1 domain (aa 1260–1271). This

N-terminal flanking region is shown to be important in modulating the binding of the A1 domain with GP Ib as modifications or deletions in this region increase the affinity of VWF for GP Ib[100,101]. In our view this might be a region within the A1 domain that interacts with the D'D3 region. It is possible that 1C1E7 interferes with the binding of the N-terminal flanking region to this site and disrupts their interaction. Based on these observations, the following hypothesis might be put forward. In native, resting conditions, the A1 domain and the D'D3 region are in close proximity, possibly through an interaction of the N-terminal flanking region of the A1 domain and the D3-domain. This interaction is limiting the accessibility of the GP Ib binding site. When VWF is immobilised, this interaction is disrupted through conformational changes in VWF — possibly in the DD3 — region which allows recruitment of platelets through their GP Ib receptors. This mode of regulation — ie internal inhibitory regions regulating the GP Ib A1 interaction — is not unique in case of VWF, as it has been shown, that the A2 domain is also capable of inhibiting the A1 domain under certain conditions[72,73].

VWF in solution has a coiled structure causing a large fraction of the GP Ib binding sites to be buried, this effect may largely be dependent on VWF multimer size. Large multimers have higher avidity because of the larger number of binding sites as well. In line with these observations there is a strong association between the presence of large multimers and the haemostatic function in case of VWF. The amount and presumably the multimerization of VWF oligomers released by the endothelial cells and the activity of the plasma enzyme ADAMTS-13 degrading the oligomers have a high inter-individual variability and known to change in pathological conditions[104]. Consequently, the size and the amount of the large oligomers, which are main determinants of the haemostatic activity of VWF, are expected to differ as well. Recently it has been demonstrated, that in the absence of ADAMTS13, multiple platelets form long string like structures anchored to the endothelial cells in flow experiments, which are degraded rapidly if ADMTS13 is added. As these structures are observable by light microscopy, it is clear that it is not a single ULVWF molecule that supports the platelets (not to mention the drag forces in flow). This suggests some kind of a self-

or lateral-association mechanism of VWF[18–20,78], by which the effective size of secreted VWF molecules may increase as well. The established method to quantify the amount of the large oligomers is to calculate the percentage of VWF protein larger than the icosamer[34] (10th band), though other approaches also exist[105]. However, the identification of VWF bands is not reliable with the commonly used Laemmli buffers as the separation of the small VWF oligomers is inadequate[34]. The transfer of large multimers is also inconsistent with the traditional blotting techniques. After evaluating several types of buffer systems we found that Tris-borate buffers combined with mercaptolysis-aided blotting[32] is better suited for this purpose. The characterisation of the degree of multimerization poses some problems. The size of the largest oligomer in the sample could be used as an obvious measure, however its quantity is so low that is not discernible from the background above VWF bands. Furthermore the size of this oligomer is in the range of 20 MDa, which is not resolved by agarose gels, so even if it was detected, the determination of its molecular weight would not be possible. These problems can be solved by detecting a proportion of the largest oligomers instead of just detecting the largest. On the other hand too large proportions may decrease selectivity. By comparing normal samples to either having less (VWD type 2) or having extra large (platelet lysate) multimers, we have found that at 25% the method is selective and the interference by the background is acceptable (the latter problem affects VWD type 2 samples more, as the VWF bands are further from the sample application wells). In studies only concentrating on large multimers using smaller proportions could increase the sensitivity. Further study of platelet lysate confirmed that the larger oligomers are detectable, even if the amount of large oligomers is the same as in plasma samples. When plasma VWF was further degraded by ADAMTS-13, both the amount and the size of large multimers decreased, but their proportions was close that is seen in normal plasma samples. To further evaluate M_{MW}, we investigated the relationship between M_{MW} and GP Ib binding (VWF:RCo) and collagen binding (VWF:CB) functions in healthy and VWD type 2 samples. There was moderately strong (r^2~0.4) relationship between M_{MW} and both of the functional assays, the higher sensitivity of collagen binding to the lack of

large multimers was not evident. It is worth noting, that the high variability of the functional test at low antigen concentrations may result in normal activity-to-antigen ratios in cases with abnormal electrophoresis results. These results demonstrate, that our techniques are accurate and reproducible enough to explore the relationships between the functional activities and the multimer distribution of VWF allowing further studies.

It is proposed that shear forces and/or immobilisation uncoils VWF, making the binding sites accessible[71,74,75]. However not all studies were able to confirm this hypothesis[76], suggesting that the binding of platelets to VWF, and the drag forces exerted on VWF by them in flow is also needed for uncoiling. Platelets under shear conditions become activated when binding to VWF or to the subendothelial structures. This renders the exploration of the above mentioned effect more difficult. We have planned to substitute platelets with similarly sized corpuscules, bearing functionally active GP Ibα to circumvent this problem. In previous attempts[94] glycocalicin (cleaved off extracellular part of GP Ib in plasma) was directly coupled to carboxylate beads, which required glycocalicin to be purified and did not guarantee the proper orientation and conformation. Instead, we have covalently coupled moAb 24B3 to 3 μm carboxylate polysterene beads, which is known to bind recombinant GP Ibα and glycocalicin in an active conformation[92]. This method has the advantage, that these beads can also capture glycocalicin from unpurified sources. We have demonstrated that 24B3 beads were capable of capturing glycocalicin from platelet lysate, and that the captured glycocalicin was capable of binding VWF if botrocetin was added. This confirms that these beads carry functionally active GP Ibα, and may turn into a valuable tool for further flow studies.

7 Summary of findings

- We have shown that the D'D3 domain inhibits the interaction of GPIbα and VWF-A1:
  - Cross-blocking studies demonstrated the proximity of D'D3 and A1 in solution, but not when immobilised
  - Ristocetin induced platelet agglutination studies demonstrated the inhibitory role of this region
  - The similarity of the peptide sequence of 1C1E7 and the A1 domain suggests, that they have a common bind site in D'D3. This would explain how 1C1E7 enhances the affinity of A1: 1C1E7 acts by disrupting the shielding of the A1 domain by D'D3.
- We have developed new electrophoresis and analysis techniques to quantitatively analyse the multimer distribution of VWF. We have demonstrated that these methods are accurate and reproducible:
  - We have assessed the sensitivity of this method to the presence of ultra large multimers and its utility on samples lacking large multimers.
  - We have compared the degree of multimerisation and the results of functional test in case of normal and VWD type 2 samples.
- We have developed a system to model the drag forces exerted by platelets on VWF. We have coated polysterene beads with glycocalicin, and we have demonstrated, that these beads are capable of binding VWF.

Bibliography

1. Piovella, F., Nalli, G., Malamani, G. D., Majolino, I., Frassoni, F., Sitar, G. M., Ruggeri, A., Dell'Orbo, C., and Ascari, E. (1978) The ultrastructural localization of factor VIII-antigen in human platelets, megakaryocytes and endothelial cells utilizing a ferritin-labelled antibody. *Br J Haematol 39*, 209–213.

2. Jahroudi, N., and Lynch, D. C. (1994) Endothelial-cell-specific regulation of von Willebrand factor gene expression. *Mol Cell Biol 14*, 999–1008.

3. Mancuso, D. J., Tuley, E. A., Westfield, L. A., Worrall, N. K., Shelton-Inloes, B. B., Sorace, J. M., Alevy, Y. G., and Sadler, J. E. (1989) Structure of the gene for human von Willebrand factor. *J Biol Chem 264*, 19514–19527.

4. Marti, T., Rösselet, S. J., Titani, K., and Walsh, K. A. (1987) Identification of disulfide-bridged substructures within human von Willebrand factor. *Biochemistry 26*, 8099–8109.

5. Dong, Z., Thoma, R. S., Crimmins, D. L., McCourt, D. W., Tuley, E. A., and Sadler, J. E. (1994) Disulfide bonds required to assemble functional von Willebrand factor multimers. *J Biol Chem 269*, 6753–6758.

6. Purvis, A. R., Gross, J., Dang, L. T., Huang, R.-H., Kapadia, M., Townsend, R. R., and Sadler, J. E. (2007) Two Cys residues essential for von Willebrand factor multimer assembly in the Golgi. *Proc Natl Acad Sci U S A 104*, 15647–15652.

7. Fowler, W. E., Fretto, L. J., Hamilton, K. K., Erickson, H. P., and McKee, P. A. (1985) Substructure of human von Willebrand factor. *J Clin Invest 76*, 1491–1500.

8. Titani, K., Kumar, S., Takio, K., Ericsson, L. H., Wade, R. D., Ashida, K., Walsh, K. A., Chopek, M. W., Sadler, J. E., and Fujikawa, K. (1986) Amino acid sequence of human von Willebrand factor. *Biochemistry 25*, 3171–3184.

9. Sadler, J. E. (2009) von Willebrand factor assembly and secretion. *J Thromb Haemost 7*, 24–27.

10. Mayadas, T., Wagner, D. D., and Simpson, P. J. (1989) von Willebrand factor biosynthesis and partitioning between constitutive and regulated pathways of secretion after thrombin stimulation. *Blood 73*, 706–711.

11. Orstavik, K. H., Magnus, P., Reisner, H., Berg, K., Graham, J. B., and Nance, W. (1985) Factor VIII and factor IX in a twin population. Evidence for a major effect of ABO locus on factor VIII level. *Am J Hum Genet 37*, 89–101.

12. Gill, J. C., Endres-Brooks, J., Bauer, P. J., Marks, W. J., and Montgomery, R. R. (1987) The effect of ABO blood group on the diagnosis of von Willebrand disease. *Blood 69*, 1691–1695.

13. Haberichter, S. L., Balistreri, M., Christopherson, P., Morateck, P., Gavazova, S., Bellissimo, D. B., Manco-Johnson, M. J., Gill, J. C., and Montgomery, R. R. (2006) Assay of the von Willebrand factor (VWF) propeptide to identify patients with type 1 von Willebrand disease with decreased VWF survival. *Blood 108*, 3344–3351.

14. Castaman, G., Tosetto, A., and Rodeghiero, F. (2009) Reduced von Willebrand factor survival in von Willebrand disease: pathophysiologic and clinical relevance. *J Thromb Haemost 7*, 71–74.

15. Moake, J. L., Turner, N. A., Stathopoulos, N. A., Nolasco, L. H., and Hellums, J. D. (1986) Involvement of large plasma von Willebrand factor (vWF) multimers and unusually large vWF forms derived from endothelial cells in shear stress-induced platelet aggregation. *J Clin Invest 78*, 1456–1461.

16. Arya, M., Anvari, B., Romo, G. M., Cruz, M. A., Dong, J.-F., McIntire, L. V., Moake, J. L., and López, J. A. (2002) Ultralarge multimers of von Willebrand factor form spontaneous high-strength bonds with the platelet glycoprotein Ib-IX complex: studies using optical tweezers. *Blood 99*, 3971–3977.

17. Sadler, J. E. (2005) von Willebrand factor: two sides of a coin. *J Thromb Haemost 3*, 1702–1709.

18. Li, Y., Choi, H., Zhou, Z., Nolasco, L., Pownall, H. J., Voorberg, J., Moake, J. L., and Dong, J.-F. (2008) Covalent regulation of ULVWF string formation and elongation on endothelial cells under flow conditions. *J Thromb Haemost 6*, 1135–1143.

19. Luken, B. M. (2008) Extracellular control of VWF multimer size and thiol-disulfide exchange. *J Thromb Haemost 6*, 1131–1134.

20. Hogg, P. J. (2009) Contribution of allosteric disulfide bonds to regulation of hemostasis. *J Thromb Haemost 7*, 13–16.

21. Tsai, H.-M. (2007) Thrombotic thrombocytopenic purpura: a thrombotic disorder caused by ADAMTS13 deficiency. *Hematol Oncol Clin North Am 21*, 609–32, v.

22. Sadler, J. E. (1994) A revised classification of von Willebrand disease. For the Subcommittee on von Willebrand Factor of the Scientific and Standardization Committee of the International Society on Thrombosis and Haemostasis. *Thromb Haemost 71*, 520–525.

23. Sadler, J. E. et al. (2006) Update on the pathophysiology and classification of von Willebrand disease: a report of the Subcommittee on von Willebrand Factor. *J Thromb Haemost 4*, 2103–2114.

24. Blann, A. D. (2006) Plasma von Willebrand factor, thrombosis, and the endothelium: the first 30 years. *Thromb Haemost 95*, 49–55.

25. Spiel, A. O., Gilbert, J. C., and Jilma, B. (2008) von Willebrand factor in cardiovascular disease: focus on acute coronary syndromes. *Circulation 117*, 1449–1459.

26. Favaloro, E. J., Thom, J., Patterson, D., Just, S., Dixon, T., Koutts, J., Baccala, M., Rowell, J., and Baker, R. (2009) Desmopressin therapy to assist the functional identification and characterisation of von Willebrand disease: differential utility from combining two (VWF:CB and VWF:RCo) von Willebrand factor activity assays? *Thromb Res 123*, 862–868.

27. Ruggeri, Z. M., and Zimmerman, T. S. (1981) The complex multimeric composition of factor VIII/von Willebrand factor. *Blood 57*, 1140–1143.

28. Raines, G., Aumann, H., Sykes, S., and Street, A. (1990) Multimeric analysis of von Willebrand factor by molecular sieving electrophoresis in sodium dodecyl sulphate agarose gel. *Thromb Res 60*, 201–212.

29. Krizek, D. R., and Rick, M. E. (2000) A rapid method to visualize von willebrand factor multimers by using agarose gel electrophoresis, immunolocalization and luminographic detection. *Thromb Res 97*, 457–462.

30. Studt, J. D., Budde, U., Schneppenheim, R., Eisert, R., von Depka Prondzinski, M., Ganser, A., and Barthels, M. (2001) Quantification and facilitated comparison of von Willebrand factor multimer patterns by densitometry. *Am J Clin Pathol 116*, 567–574.

31. Smejkal, G. B., Shainoff, J. R., and Kottke-Marchant, K. M. (2003) Rapid high-resolution electrophoresis of multimeric von Willebrand Factor using a thermopiloted gel apparatus. *Electrophoresis 24*, 582–587.

32. Bowen, D. J., and Bowley, S. J. (2007) Improved visualisation of high-molecular-weight von Willebrand factor multimers. *Thromb Haemost 97*, 1051–1052.

33. Weiss, D. R., Thiel, C., Strasser, E. F., Zimmermann, R., and Eckstein, R. (2008) An optimized electrophoresis method for high-resolution imaging of von-Willebrand multimers. *Thromb Haemost 100*, 949–951.

34. Budde, U. et al. (2008) Detailed von Willebrand factor multimer analysis in patients with von Willebrand disease in the European study, molecular and clinical markers for the diagnosis and management of type 1 von Willebrand disease (MCMDM-1VWD). *J Thromb Haemost 6*, 762–771.

35. Sporn, L. A., Marder, V. J., and Wagner, D. D. (1986) Inducible secretion of large, biologically potent von Willebrand factor multimers. *Cell 46*, 185–190.

36. Levy, G. G. et al. (2001) Mutations in a member of the ADAMTS gene family cause thrombotic thrombocytopenic purpura. *Nature 413*, 488–494.

37. fei Dong, J., Moake, J. L., Nolasco, L., Bernardo, A., Arceneaux, W., Shrimpton, C. N., Schade, A. J., McIntire, L. V., Fujikawa, K., and López, J. A. (2002) ADAMTS-13 rapidly cleaves newly secreted ultralarge von Willebrand factor multimers on the endothelial surface under flowing conditions. *Blood 100*, 4033–4039.

38. Moake, J. L., Rudy, C. K., Troll, J. H., Weinstein, M. J., Colannino, N. M., Azocar, J., Seder, R. H., Hong, S. L., and Deykin, D. (1982) Unusually large plasma factor VIII:von Willebrand factor multimers in chronic relapsing thrombotic thrombocytopenic purpura. *N Engl J Med 307*, 1432–1435.

39. Tsai, H. M. (1996) Physiologic cleavage of von Willebrand factor by a plasma protease is dependent on its conformation and requires calcium ion. *Blood 87*, 4235–4244.

40. Sadler, J. E. (2008) Von Willebrand factor, ADAMTS13, and thrombotic thrombocytopenic purpura. *Blood 112*, 11–18.

41. Roth, G. J. (1991) Developing relationships: arterial platelet adhesion, glycoprotein Ib, and leucine-rich glycoproteins. *Blood 77*, 5–19.

42. López, J. A., Andrews, R. K., Afshar-Kharghan, V., and Berndt, M. C. (1998) Bernard-Soulier syndrome. *Blood 91*, 4397–4418.

43. Berndt, M. C., Shen, Y., Dopheide, S. M., Gardiner, E. E., and Andrews, R. K. (2001) The vascular biology of the glycoprotein Ib-IX-V complex. *Thromb Haemost 86*, 178–188.

44. Andrews, R. K., Gardiner, E. E., Shen, Y., Whisstock, J. C., and Berndt, M. C. (2003) Glycoprotein Ib-IX-V. *Int J Biochem Cell Biol 35*, 1170–1174.

45. Huizinga, E. G., Tsuji, S., Romijn, R. A. P., Schiphorst, M. E., de Groot, P. G., Sixma, J. J., and Gros, P. (2002) Structures of glycoprotein Ibalpha and its complex with von Willebrand factor A1 domain. *Science 297*, 1176–1179.

46. Dumas, J. J., Kumar, R., McDonagh, T., Sullivan, F., Stahl, M. L., Somers, W. S., and Mosyak, L. (2004) Crystal structure of the wild-type von Willebrand factor A1-glycoprotein Ibalpha complex reveals conformation differences with a complex bearing von Willebrand disease mutations. *J Biol Chem 279*, 23327–23334.

47. Clemetson, K. J., McGregor, J. L., James, E., Dechavanne, M., and Lüscher, E. F. (1982) Characterization of the platelet membrane glycoprotein abnormalities in Bernard-Soulier syndrome and comparison with normal by surface-labeling techniques and high-resolution two-dimensional gel electrophoresis. *J Clin Invest 70*, 304–311.

48. André, P., Denis, C. V., Ware, J., Saffaripour, S., Hynes, R. O., Ruggeri, Z. M., and Wagner, D. D. (2000) Platelets adhere to and translocate on von Willebrand factor presented by endothelium in stimulated veins. *Blood 96*, 3322–3328.

49. McEver, R. P. (2001) Adhesive interactions of leukocytes, platelets, and the vessel wall during hemostasis and inflammation. *Thromb Haemost 86*, 746–756.

50. Yago, T., Lou, J., Wu, T., Yang, J., Miner, J. J., Coburn, L., López, J. A., Cruz, M. A., Dong, J.-F., McIntire, L. V., McEver, R. P., and Zhu, C. (2008) Platelet glycoprotein Ibalpha forms catch bonds with human WT vWF but not with type 2B von Willebrand disease vWF. *J Clin Invest 118*, 3195–3207.

51. Bernardo, A., Ball, C., Nolasco, L., Choi, H., Moake, J. L., and Dong, J. F. (2005) Platelets adhered to endothelial cell-bound ultra-large von Willebrand factor strings support leukocyte tethering and rolling under high shear stress. *J Thromb Haemost 3*, 562–570.

52. Cruz, M. A., Yuan, H., Lee, J. R., Wise, R. J., and Handin, R. I. (1995) Interaction of the von Willebrand factor (vWF) with collagen. Localization of the primary collagen-binding site by analysis of recombinant vWF a domain polypeptides. *J Biol Chem 270*, 10822–10827.

53. Lankhof, H., van Hoeij, M., Schiphorst, M. E., Bracke, M., Wu, Y. P., Ijsseldijk, M. J., Vink, T., de Groot, P. G., and Sixma, J. J. (1996) A3 domain is essential for interaction of von Willebrand factor with collagen type III. *Thromb Haemost 75*, 950–958.

54. Hoylaerts, M. F., Yamamoto, H., Nuyts, K., Vreys, I., Deckmyn, H., and Vermylen, J. (1997) von Willebrand factor binds to native collagen VI primarily via its A1 domain. *Biochem J 324 (Pt 1)*, 185–191.

55. Mazzucato, M., Spessotto, P., Masotti, A., Appollonia, L. D., Cozzi, M. R., Yoshioka, A., Perris, R., Colombatti, A., and Marco, L. D. (1999) Identification of domains responsible for von Willebrand factor type VI collagen interaction mediating platelet adhesion under high flow. *J Biol Chem 274*, 3033–3041.

56. Bonnefoy, A., Romijn, R. A., Vandervoort, P. A. H., Rompaey, I. V., Vermylen, J., and Hoylaerts, M. F. (2006) von Willebrand factor A1 domain can adequately substitute for A3 domain in recruitment of flowing platelets to collagen. *J Thromb Haemost 4*, 2151–2161.

57. Szanto, T., Vanhoorelbeke, K., Toth, G., Vandenbulcke, A., Toth, J., Noppe, W., Deckmyn, H., and Harsfalvi, J. (2009) Identification of a VWF peptide antagonist that blocks platelet adhesion under high shear conditions by selectively inhibiting the VWF-collagen interaction. *J Thromb Haemost.*

58. Doggett, T. A., Girdhar, G., Lawshé, A., Schmidtke, D. W., Laurenzi, I. J., Diamond, S. L., and Diacovo, T. G. (2002) Selectin-like kinetics and biomechanics promote rapid platelet adhesion in flow: the GPIb(alpha)-vWF tether bond. *Biophys J 83*, 194–205.

59. Andrews, R. K., and Berndt, M. C. (2008) Platelet adhesion: a game of catch and release. *J Clin Invest 118*, 3009–3011.

60. Marshall, B. T., Long, M., Piper, J. W., Yago, T., McEver, R. P., and Zhu, C. (2003) Direct observation of catch bonds involving cell-adhesion molecules. *Nature 423*, 190–193.

61. Savage, B., Saldívar, E., and Ruggeri, Z. M. (1996) Initiation of platelet adhesion by arrest onto fibrinogen or translocation on von Willebrand factor. *Cell 84*, 289–297.

62. Doggett, T. A., Girdhar, G., Lawshe, A., Miller, J. L., Laurenzi, I. J., Diamond, S. L., and Diacovo, T. G. (2003) Alterations in the intrinsic properties of the GPIbalpha-VWF tether bond define the kinetics of the platelet-type von Willebrand disease mutation, Gly233Val. *Blood 102*, 152–160.

63. Dong, J. F., Berndt, M. C., Schade, A., McIntire, L. V., Andrews, R. K., and López, J. A. (2001) Ristocetin-dependent, but not botrocetin-dependent, binding of von Willebrand factor to the platelet glycoprotein Ib-IX-V complex correlates with shear-dependent interactions. *Blood 97*, 162–168.

64. Chen, V. M., and Hogg, P. J. (2006) Allosteric disulfide bonds in thrombosis and thrombolysis. *J Thromb Haemost 4*, 2533–2541.

65. Lou, J., and Zhu, C. (2008) Flow induces loop-to-beta-hairpin transition on the beta-switch of platelet glycoprotein Ib alpha. *Proc Natl Acad Sci U S A 105*, 13847–13852.

66. Lillicrap, D. (2009) Genotype/phenotype association in von Willebrand disease: is the glass half full or empty? *J Thromb Haemost 7*, 65–70.

67. Andrews, R. K., Gorman, J. J., Booth, W. J., Corino, G. L., Castaldi, P. A., and Berndt, M. C. (1989) Cross-linking of a monomeric 39/34-kDa dispase fragment of von Willebrand factor (Leu-480/Val-481-Gly-718) to the N-terminal region of the alpha-chain of membrane glycoprotein Ib on intact platelets with bis(sulfosuccinimidyl) suberate. *Biochemistry 28*, 8326–8336.

68. Gralnick, H. R., Williams, S., McKeown, L., Kramer, W., Krutzsch, H., Gorecki, M., Pinet, A., and Garfinkel, L. I. (1992) A monomeric von Willebrand factor fragment, Leu-504–Lys-728, inhibits von Willebrand factor interaction with glycoprotein Ib-IX [corrected]. *Proc Natl Acad Sci U S A 89*, 7880–7884.

69. Tornai, I., Arnout, J., Deckmyn, H., Peerlinck, K., and Vermylen, J. (1993) A monoclonal antibody recognizes a von Willebrand factor domain within the amino-terminal portion of the subunit that modulates the function of the glycoprotein IB- and IIB/IIIA-binding domains. *J Clin Invest 91*, 273–282.

70. Ulrichts, H., Harsfalvi, J., Bene, L., Matko, J., Vermylen, J., Ajzenberg, N., Baruch, D., Deckmyn, H., and Tornai, I. (2004) A monoclonal antibody directed against human von Willebrand factor induces type 2B-like alterations. *J Thromb Haemost 2*, 1622–1628.

71. Singh, I., Themistou, E., Porcar, L., and Neelamegham, S. (2009) Fluid shear induces conformation change in human blood protein von Willebrand factor in solution. *Biophys J 96*, 2313–2320.

72. Martin, C., Morales, L. D., and Cruz, M. A. (2007) Purified A2 domain of von Willebrand factor binds to the active conformation of von Willebrand factor and blocks the interaction with platelet glycoprotein Ibalpha. *J Thromb Haemost 5*, 1363–1370.

73. Lenting, P. J., and Denis, C. V. (2007) von Willebrand factor A1 domain: stuck in the middle. *J Thromb Haemost 5*, 1361–1362.

74. Siedlecki, C. A., Lestini, B. J., Kottke-Marchant, K. K., Eppell, S. J., Wilson, D. L., and Marchant, R. E. (1996) Shear-dependent changes in the three-dimensional structure of human von Willebrand factor. *Blood 88*, 2939–2950.

75. Schneider, S. W., Nuschele, S., Wixforth, A., Gorzelanny, C., Alexander-Katz, A., Netz, R. R., and Schneider, M. F. (2007) Shear-induced unfolding triggers adhesion of von Willebrand factor fibers. *Proc Natl Acad Sci U S A 104*, 7899–7903.

76. Novák, L., Deckmyn, H., Damjanovich, S., and Hársfalvi, J. (2002) Shear-dependent morphology of von Willebrand factor bound to immobilized collagen. *Blood 99*, 2070–2076.

77. Dong, J.-F. (2005) Cleavage of ultra-large von Willebrand factor by ADAMTS-13 under flow conditions. *J Thromb Haemost 3*, 1710–1716.

78. Savage, B., Sixma, J. J., and Ruggeri, Z. M. (2002) Functional self-association of von Willebrand factor during platelet adhesion under flow. *Proc Natl Acad Sci U S A 99*, 425–430.

79. Scott, J. P., Montgomery, R. R., and Retzinger, G. S. (1991) Dimeric ristocetin flocculates proteins, binds to platelets, and mediates von Willebrand factor-dependent agglutination of platelets. *J Biol Chem 266*, 8149–8155.

80. Matsui, T., and Hamako, J. (2005) Structure and function of snake venom toxins interacting with human von Willebrand factor. *Toxicon 45*, 1075–1087.

81. Vanhoorelbeke, K., Depraetere, H., Romijn, R. A. P., Huizinga, E. G., Maeyer, M. D., and Deckmyn, H. (2003) A consensus tetrapeptide selected by phage display adopts the conformation of a dominant discontinuous epitope of a monoclonal anti-VWF antibody that inhibits the von Willebrand factor-collagen interaction. *J Biol Chem 278*, 37815–37821.

82. Depraetere, H., Ajzenberg, N., Girma, J. P., Lacombe, C., Meyer, D., Deckmyn, H., and Baruch, D. (1998) Platelet aggregation induced by a monoclonal antibody to the A1 domain of von Willebrand factor. *Blood 91*, 3792–3799.

83. Obert, B., Houllier, A., Meyer, D., and Girma, J. P. (1999) Conformational changes in the A3 domain of von Willebrand factor modulate the interaction of the A1 domain with platelet glycoprotein Ib. *Blood 93*, 1959–1968.

84. Piétu, G., Ribba, A. S., Meulien, P., and Meyer, D. (1989) Localization within the 106 N-terminal amino acids of von Willebrand factor (vWF) of the epitope corresponding to a monoclonal antibody which inhibits vWF binding to factor VIII. *Biochem Biophys Res Commun 163*, 618–626.

85. Subramani, S., Mulligan, R., and Berg, P. (1981) Expression of the mouse dihydrofolate reductase complementary deoxyribonucleic acid in simian virus 40 vectors. *Mol Cell Biol 1*, 854–864.

86. Lenting, P. J., Westein, E., Terraube, V., Ribba, A.-S., Huizinga, E. G., Meyer, D., de Groot, P. G., and Denis, C. V. (2004) An experimental model to study the in vivo survival of von Willebrand factor. Basic aspects and application to the R1205H mutation. *J Biol Chem 279*, 12102–12109.

87. Sblattero, D., and Bradbury, A. (1998) A definitive set of oligonucleotide primers for amplifying human V regions. *Immunotechnology 3*, 271–278.

88. Staelens, S., Desmet, J., Ngo, T. H., Vauterin, S., Pareyn, I., Barbeaux, P., Rompaey, I. V., Stassen, J.-M., Deckmyn, H., and Vanhoorelbeke, K. (2006) Humanization by variable domain resurfacing and grafting on a human IgG4, using a new approach for determination of non-human like surface accessible framework residues based on homology modelling of variable domains. *Mol Immunol 43*, 1243–1257.

89. Lilie, H., Schwarz, E., and Rudolph, R. (1998) Advances in refolding of proteins produced in E. coli. *Curr Opin Biotechnol 9*, 497–501.

90. Gerritsen, H. E., Turecek, P. L., Schwarz, H. P., Lämmle, B., and Furlan, M. (1999) Assay of von Willebrand factor (vWF)-cleaving protease based on decreased collagen binding affinity of degraded vWF: a tool for the diagnosis of thrombotic thrombocytopenic purpura (TTP). *Thromb Haemost 82*, 1386–1389.

91. Cejka, J. (1982) Enzyme immunoassay for factor VIII-related antigen. *Clin Chem 28*, 1356–1358.

92. Vanhoorelbeke, K., Pareyn, I., Schlammadinger, A., Vauterin, S., Hoylaerts, M. F., Arnout, J., and Deckmyn, H. (2005) Plasma glycocalicin as a source of GPIbalpha in the von Willebrand factor ristocetin cofactor ELISA. *Thromb Haemost 93*, 165–171.

93. Okumura, T., and Jamieson, G. A. (1976) Platelet glycocalicin: a single receptor for platelet aggregation induced by thrombin or ristocetin. *Thromb Res 8*, 701–706.

94. Li, F., Li, C. Q., Moake, J. L., López, J. A., and McIntire, L. V. (2004) Shear stress-induced binding of large and unusually large von Willebrand factor to human platelet glycoprotein Ibalpha. *Ann Biomed Eng 32*, 961–969.

95. Fischer, B. E., Kramer, G., Mitterer, A., Grillberger, L., Reiter, M., Mundt, W., Dorner, F., and Eibl, J. (1996) Effect of multimerization of human and recombinant von Willebrand factor on platelet aggregation, binding to collagen and binding of coagulation factor VIII. *Thromb Res 84*, 55–66.

96. Barington, K. A., and Kaersgaard, P. (1999) A very-high-purity von Willebrand factor preparation containing high-molecular-weight multimers. *Vox Sang 76*, 85–89.

97. Sugimoto, M., Ricca, G., Hrinda, M. E., Schreiber, A. B., Searfoss, G. H., Bottini, E., and Ruggeri, Z. M. (1991) Functional modulation of the isolated glycoprotein Ib binding domain of von Willebrand factor expressed in Escherichia coli. *Biochemistry 30*, 5202–5209.

98. Hackert, T., Pfeil, D., Hartwig, W., Fritz, S., Schneider, L., Gebhard, M.-M., Büchler, M. W., and Werner, J. (2007) Platelet function in acute experimental pancreatitis. *J Gastrointest Surg 11*, 439–444.

99. Sugimoto, M., Dent, J., McClintock, R., Ware, J., and Ruggeri, Z. M. (1993) Analysis of structure-function relationships in the platelet membrane glycoprotein Ib-binding domain of von Willebrand's factor by expression of deletion mutants. *J Biol Chem 268*, 12185–12192.

100. Matsushita, T., and Sadler, J. E. (1995) Identification of amino acid residues essential for von Willebrand factor binding to platelet glycoprotein Ib. Charged-to-alanine scanning mutagenesis of the A1 domain of human von Willebrand factor. *J Biol Chem 270*, 13406–13414.

101. Nakayama, T., Matsushita, T., Dong, Z., Sadler, J. E., Jorieux, S., Mazurier, C., Meyer, D., Kojima, T., and Saito, H. (2002) Identification of the regulatory elements of the human von Willebrand factor for binding to platelet GPIb. Importance of structural integrity of the regions flanked by the CYS1272-CYS1458 disulfide bond. *J Biol Chem 277*, 22063–22072.

102. am Esch, J. S., Robson, S. C., Knoefel, W. T., Eisenberger, C. F., Peiper, M., and Rogiers, X. (2005) Impact of O-linked glycosylation of the VWF-A1-domain flanking regions on platelet interaction. *Br J Haematol 128*, 82–90.

103. Bendetowicz, A. V., Wise, R. J., and Gilbert, G. E. (1999) Collagen-bound von Willebrand factor has reduced affinity for factor VIII. *J Biol Chem 274*, 12300–12307.

104. Claus, R. A., Bockmeyer, C. L., Budde, U., Kentouche, K., Sossdorf, M., Hilberg, T., Schneppenheim, R., Reinhart, K., Bauer, M., Brunkhorst, F. M., and Lösche, W. (2009) Variations in the ratio between von Willebrand factor and its cleaving protease during systemic inflammation and association with severity and prognosis of organ failure. *Thromb Haemost 101*, 239–247.

105. Lopes, A. A., Soares, R. P. S., and Maeda, N. Y. (2002) A mathematical framework for group analysis of von Willebrand factor multimeric composition following luminography. *Braz J Med Biol Res 35*, 1259–1263.

Original publications

Publications used in preparation of the thesis

1. **Udvardy, M. L.**, Szekeres-Csiki, K., and Hársfalvi, J. (2009) Novel evaluation method for densitometric curves of von Willebrand Factor multimers and a new parameter (M_{MW}) to describe the degree of multimerisation. *Thromb Haemost 102*, 412–417.
   Impact factor: 3.803 (2008)

2. Ulrichts, H.*, **Udvardy, M. L.***, Lenting, P. J., Pareyn, I., Vandeputte, N., Vanhoorelbeke, K., and Deckmyn, H. (2006) Shielding of the A1 domain by the D'D3 domains of von Willebrand factor modulates its interaction with platelet glycoprotein Ib-IX-V. *J Biol Chem 281*, 4699–4707.
   *Both authors contributed equall**y** to this work
   Impact factor: 5.808

Total impact factors of publications used in preparation of the thesis: 9.611

Publications related to the thesis

1. Szarvas, M., Oparaugo, P., **Udvardy, M. L.**, Toth J., Szanto T., Daroczi L., Vereb G., and Harsfalvi J. (2006) Differential platelet deposition onto collagen in cone-and-plate and parallel plate flow chambers. *Platelets 17*, 185-90.
   Impact factor: 1.679

2. Toth, J., Kappelmayer, J., **Udvardy, M. L.**, Szanto, T., Szarvas, M., Rejto, L., Soltesz, P., Udvardy, M., and Harsfalvi, J. (2009) Increased platelet glycoprotein Ib receptor number, enhanced platelet adhesion and severe cerebral ischaemia in a patient with polycythaemia vera. *Platelets 20*, 282–287.
   Impact factor: 2.271 (2008)

3. Molvarec, A., Rigó, J., Bőze, T., Derzsy, Z., Cervenak, L., Makó, V., Gombos, T., **Udvardy, M. L.**, Hársfalvi, J., and Prohászka, Z. (2009) Increased plasma von Willebrand factor antigen levels but normal von Willebrand factor cleaving protease (ADAMTS13) activity in preeclampsia. *Thromb Haemost 101*, 305–311.
Impact factor: 3.803 (2008)

Total impact factors of publications related to the thesis: 7.753

Other publications

1. Papp, M., Altorjay, I., Norman, G. L., Shums, Z., Palatka, K., Vitalis, Z., Foldi, I., Lakos, G., Tumpek, J., **Udvardy, M. L.**, Harsfalvi, J., Fischer, S., Lakatos, L., Kovacs, A., Bene, L., Molnar, T., Tulassay, Z., Miheller, P., Veres, G., Papp, J., Group, H. I. S. & Lakatos, P. L. (2007) Seroreactivity to microbial components in Crohn's disease is associated with ileal involvement, noninflammatory disease behavior and NOD2/CARD15 genotype, but not with risk for surgery in a Hungarian cohort of IBD patients. *Inflamm Bowel Dis 13*, 984-992.
Impact factor: 4,705

Keywords / tárgyszavak

Keywords:

- von Willebrand factor
- fluid shear
- conformational change
- shielding
- VWF multimer analysis
- scFv
- glycocalicin

Tárgyszavak

- von Willebrand faktor
- nyíró erő
- konformáció változás
- takarás (shielding)
- VWF multimer analízis
- scFv
- glycocalicin

Acknowledgements

First of all I am deeply grateful to my supervisor Jolán Hársfalvi, PhD for her guidance and for supporting me in the past years. I would like to thank her for introducing me to scientific research and for inspiring and encouraging me to continue.

I would like to express my sincere thanks to Professor László Muszbek, the head of the department, for his constructive comments and ideas and the opportunity to join the Clinical Research Center.

I would like to thank all of my colleagues and friends in the Clinical Research Center and at the Department of Clinical Biochemistry and Molecular Pathology for their continuous support and the great time we spent throughout the years.

I owe my deepest gratitude to Professor Hans Deckmyn for the inspiring discussions and ideas and for the opportunity to spend a great year with a group of talented sciences at the the Laboratory for Thrombosis Research, IRC, KULeuven. I would like to thank all of my colleagues and friends in Belgium, especially Hans Ulrichts for his help and assistance.

Most of all I would like to thank my family for their constant understanding, patience and encouragement.

Appendix

THE JOURNAL OF BIOLOGICAL CHEMISTRY VOL. 281, NO. 8, pp. 4699–4707, February 24, 2006

Shielding of the A1 Domain by the D′D3 Domains of von Willebrand Factor Modulates Its Interaction with Platelet Glycoprotein Ib-IX-V*

Received for publication, December 14, 2005, and in revised form, December 22, 2005 Published, JBC Papers in Press, December 22, 2005, DOI 10.1074/jbc.M513314200

Hans Ulrichts[‡1,2], **Miklós Udvardy**[‡§1], **Peter J. Lenting**[¶], **Inge Pareyn**[‡], **Nele Vandeputte**[‡], **Karen Vanhoorelbeke**[‡2], **and Hans Deckmyn**[‡3]

From the [‡]*Laboratory for Thrombosis Research, Interdisciplinary Research Center, Katholieke Universiteit Leuven Campus Kortrijk, B-8500 Kortrijk, Belgium,* [§]*Department of Clinical Biochemistry and Molecular Pathology, University Debrecen, Faculty of Medicine, H-4012 Debrecen, Hungary, and* [¶]*Laboratory for Thrombosis and Haemostasis, Department of Haematology, University Medical Center Utrecht, 3584 CX Utrecht, The Netherlands*

Soluble von Willebrand factor (VWF) has a low affinity for platelet glycoprotein (GP) Ibα and needs immobilization and/or high shear stress to enable binding of its A1 domain to the receptor. The previously described anti-VWF monoclonal antibody 1C1E7 enhances VWF/GPIbα binding and recognizes an epitope in the amino acids 764–1035 region in the N-terminal D′D3 domains. In this study we demonstrated that the D′D3 region negatively modulates the VWF/GPIb-IX-V interaction; (i) deletion of the D′D3 region in VWF augmented binding to GPIbα, suggesting an inhibitory role for this region, (ii) the isolated D′D3 region inhibited the GPIbα interaction of a VWF deletion mutant lacking this region, indicating that intramolecular interactions limit the accessibility of the A1 domain, (iii) using a panel of anti-VWF monoclonal antibodies, we next showed that the D′D3 region is in close proximity with the A1 domain in soluble VWF but not when VWF was immobilized; (iv) destroying the epitope of 1C1E7 resulted in a mutant VWF with an increased affinity for GPIbα. Our results support a model of domain translocation in VWF that allows interaction with GPIbα. The suggested shielding interaction of the A1 domain by the D′D3 region then becomes disrupted by VWF immobilization.

The plasma protein von Willebrand factor (VWF)[4] has a central role in normal primary hemostasis (1). The interaction of VWF with its platelet receptor glycoprotein (GP) Ibα in the GPIb-IX-V complex mediates platelet adhesion to extracellular matrices exposed at sites of vascular injury. This interaction is essential for thrombus formation at sites of high shear stress, as in microarterioles or in stenosed arteries.

Mature VWF comprises a series of multimers that are composed of homodimers interlinked through disulfide bridges. The mature VWF subunit consists of four distinct types of internal homology present in two to three copies in the following order from the N terminus: D′-D3-A1-A2-A3-D4-B1-B2-B3-C1-C2-CK.

Native VWF in solution has an extremely low affinity for GPIbα, suggesting the existence of specific regulatory mechanisms that maintain ligand and receptor in the same environment without adverse consequences. The affinity of VWF toward its primary receptor can be increased by artificial means, such as removal of sialic acid side chains (2) or the presence of modulators like the bacterial glycopeptide ristocetin (3) or the snake venom protein botrocetin (4). In pathophysiological conditions, however, binding is induced by immobilization of VWF or by elevated fluid shear stress, which is likely due to changes in interdomain interactions (5).

The VWF A1 domain (amino acids (aa) 1260–1479) contains the only known GPIbα binding site (6). A 39/34-kDa dispase fragment of human VWF (aa 1243/1244–1481) (7) and the recombinant VWF fragment VCL (aa 1267–1491) (8), both spanning the A1 domain, bind to platelet GPIb-IX-V in the absence of modulators, in contrast to full-length VWF. Therefore, it is not unlikely to suppose that the remainder of VWF, outside the A1 domain, serves as a masking environment, preventing binding to GPIb-IX-V. Conformational changes in VWF upon immobilization or upon exposure to shear might relieve this possible shielding effect of neighboring domains in VWF and might thereby reveal the functional binding site in the A1 domain. This mode of action is supported by kinetic and crystal studies, which demonstrated a higher binding affinity of the isolated A1 domain for GPIb-IX-V compared with full-length VWF (9–11). Moreover, these crystal studies confirm that conformational changes in both GPIbα and in the A1 domain are required for their mutual interaction.

The A1 domain contains a typical α/β-fold that is delimited by a single disulfide bridge (aa 1272–1456) (12). The N-terminal region in the A1 domain (aa 1260–1271), flanking the disulfide bridge, modulates the A1/GPIbα interaction; (i) crystal studies reveal a displacement of this flanking region upon binding to GPIbα (10, 11); (ii) naturally occurring mutations in this region have been reported to induce von Willebrand disease (VWD) type 2B phenotype, characterized by an increased affinity of VWF for GPIbα (13); (iii) Ala substitution mutants in this region show an increased affinity for GPIbα (14).

As mentioned before, it is suggested that neighboring domains in VWF might impede the accessibility of the GPIbα binding region. We have previously described a monoclonal antibody (moAb), 1C1E7, directed against the aa 764–1035 region in the N-terminal D′D3 domains of VWF (15). Although this moAb interacts with a region distinct from the VWF A1 domain, it induces von Willebrand disease-type 2B-like alterations (16). This would suggest that the binding region

* This work was supported in part by K.U. Leuven Grant GOA/2004/00, European Union-Research Training Network HPRN-CT-2002-00253, and a bilateral collaboration grant between Flanders and Hungary (BIL/04/35). The costs of publication of this article were defrayed in part by the payment of page charges. This article must therefore be hereby marked "*advertisement*" in accordance with 18 U.S.C. Section 1734 solely to indicate this fact.

[1] Both authors contributed equally to this work.

[2] Supported by postdoctoral fellowships of the Fonds voor Wetenschappelijk Onderzoek-Vlaanderen.

[3] To whom correspondence should be addressed: Laboratory for Thrombosis Research, KU Leuven, Campus Kortrijk, E. Sabbelaan 53, B-8500 Kortrijk, Belgium. Tel.: 32-56246422; Fax: 32-56246997; E-mail: Hans.Deckmyn@kuleuven-kortrijk.be.

[4] The abbreviations used are: VWF, von Willebrand factor; GP, glycoprotein; aa, amino acids; moAb, monoclonal antibody; RT, room temperature; scFv, single-chain variable fragment; PBS, phosphate-buffered saline; ON, overnight; TBS, Tris-buffered saline; r-recombinant; b-418, biotinylated moAb 418; WT, wild type.

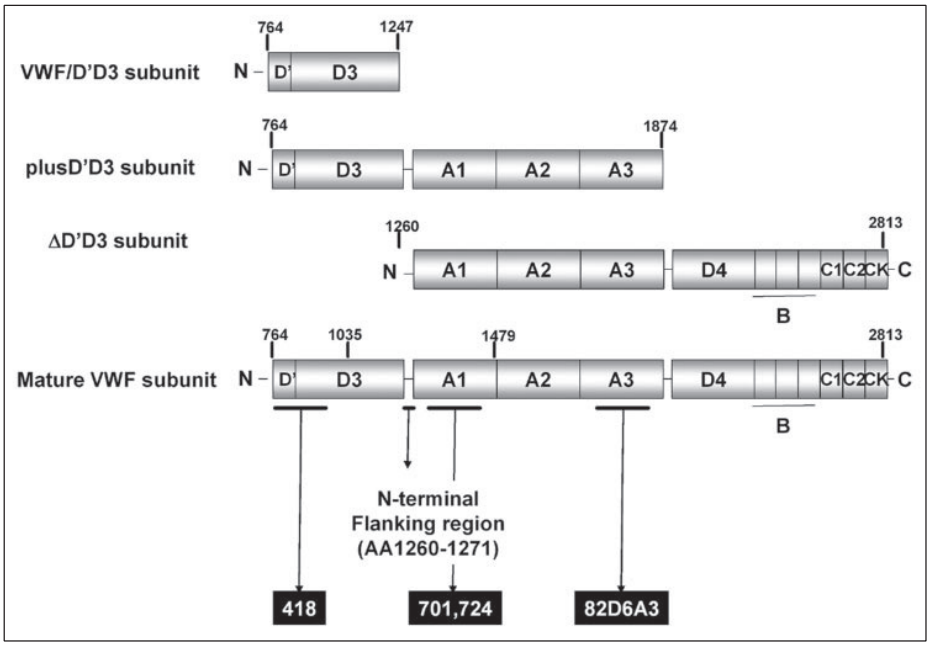

FIGURE 1. **Schematic representation of a mature VWF subunit and the VWF deletion mutants used in this study.** Binding regions of the anti-VWF moAbs are indicated.

of 1C1E7 in VWF might have a modulatory role for the VWF/GPIbα interaction and could be a shielding region for the GPIbα binding domain. The objectives of this study were to obtain evidence for the functionality of the D′D3 region in VWF for GPIbα binding using deletion mutants, constructed VWF chimeras, and recombinant 1C1E7 as tools.

EXPERIMENTAL PROCEDURES

Materials—Different moAbs against VWF were described previously. moAb 82D6A3 binds to the VWF A3 domain and inhibits VWF binding to collagen types I, III, and IV (17), and moAb 1C1E7 recognizes the N-terminal part of VWF (aa 764–1035) (15). moAbs 724, 701, and 418 were kind gifts of Dr. J. P. Girma (INSERM U143, le Kremlin-Bicêtre, Paris, France). moAbs 724 and 701 recognize the VWF A1 domain (18, 19), whereas moAb 418 interacts with the first 106 aa in mature VWF (20). VWF was purchased from the Red Cross (Brussels, Belgium). moAbs or VWF were biotinylated using EZ-link Sulfo-NHS-SS-Biotin (Perbio, Helsingberg, Sweden).

Pooled plasma was prepared from the plasma of 25 healthy volunteers (21). The vector pSV2-dhfr (22) was obtained from American Type Cell Culture (Manassas, VA). Restriction endonucleases were from MBI Fermentas (Vilnius, Lithuania).

Numbering of the aa sequence of VWF or the nucleotide sequence of the VWF gene starts with, respectively, the initiator methionine or the start codon as the +1 position. Recombinant VWF/D′A3 (aa 1–1874), VWF/D′D3 (aa 1–1247), and VWF/A1-CK (1260–2813) were expressed and purified as described before (23). For clarity, we renamed VWF/D′A3 and VWF/A1-CK as plusD′D3 and ΔD′D3, respectively. A representation of VWF, its fragments, and the binding sites of the moAbs is shown in Fig. 1.

Construction and Expression of 1C1E7 Single-chain Variable Fragment—Total cell RNA was extracted from 1C1E7-expressing hybridoma cells using the RNeasy mini kit (Qiagen, Venlo, The Netherlands) and was reverse-transcribed in the ThermoScript reverse transcription-PCR system (Invitrogen) using oligo(dT)$_{20}$ primers.

The N-terminal sequence of the heavy and light chain of 1C1E7 was determined by TopLab (Martinsried, Germany). Based on these data, degenerate sense primers were designed for the heavy and the light chain variable regions (V_H and V_L, respectively), and framework-specific antisense primers were used in the subsequent PCR reactions (24, 25). Amplification of V_H was performed using *Pfu* Turbo DNA polymerase (Stratagene, La Jolla, CA), and the resulting PCR product was ligated in the pCR®-Blunt vector (Invitrogen). V_L was amplified with Platinum® *Taq* DNA polymerase (Invitrogen), and the resulting PCR product was ligated in the pCR®2.1-TOPO® vector (Invitrogen). For the construction of the 1C1E7 single-chain variable fragment (scFv), both V_H and V_L were extended such that the following splice overlapping extension PCR resulted in a V_H-$(G_4S)_3$-V_L scFv coding sequence. This PCR product was ligated in the pSecTag/FRT/V5-His vector (Invitrogen).

The 1C1E7 scFv was expressed in *Escherichia coli* as a His-tag fusion protein. Briefly, NcoI and XhoI restriction sites were added to the 3′ and 5′ ends, respectively, by PCR using sequence-specific primers. The 1C1E7 scFv DNA was cloned in the pET26+ vector (Stratagene) using the NcoI and XhoI restriction sites. BL-21 *E. coli* were transformed with the construct and were induced for 2 h with 0.5 M isopropyl-β-D-galactoside. The bacteria were harvested (10,000 × *g* for 10 min), and cell proteins from the pellet were extracted with the BugBuster protein extraction reagent (Novagen, Merck). 1C1E7 scFv was expressed as inclusion bodies. To refold the scFv, inclusion bodies were dissolved in IB buffer (6 M guanidine-HCl, 1.5 M urea, 0.6 mM reduced glutathione, 0.3 mM oxidized glutathione in phosphate-buffered saline, PBS) (26). The solubilized proteins were subsequently dialyzed against a series of urea solutions (8, 6, 4, and 2 M overnight (ON) at 4 °C) and, finally against PBS.

Ristocetin- and Botrocetin-induced Binding of VWF, ΔD′D3, plusD′D3, or Recombinant VWF to a Recombinant GPIbα Fragment (aa 1–289)—The ristocetin- and botrocetin-induced binding of VWF, ΔD′D3, plusD′D3, or recombinant VWF (see later) to a GPIbα fragment was performed as previously described (21). Briefly, microtiter plates were coated ON at 4 °C with anti-GPIbα moAb 2D4 (5 μg/ml in PBS) and blocked with Tris-buffered Saline (TBS) containing 3% milk powder. A recombinant N-terminal, VWF binding GPIbα fragment (aa 1–289) (rGPIbα) was expressed in Chinese hamster ovary cells and

purified as described (27). Wells were incubated for 1.5 h at 37 °C with rGPIbα (1 μg/ml in TBS, 0.1% Tween 20) and incubated for 1.5 h at 37 °C with a dilution series of ristocetin (abp, New York, NY) or botrocetin purified from crude *Bothrops jararaca* venom (Sigma) (28) in the presence of a constant amount of purified VWF, ΔD′D3, plusD′D3, or recombinant VWF (0.5 μg/ml) and in the absence or presence of 12 μg/ml 1C1E7 IgG. Bound VWF, ΔD′D3, plusD′D3, or recombinant VWF was detected for 45 min at room temperature (RT) with a 1/3000 dilution of anti-VWF polyclonal antibodies labeled with horseradish peroxidase (anti-VWF-Ig-horseradish peroxidase, Dako, Glostrup, Denmark). Visualization was obtained with H_2O_2 and *ortho*-phenylenediamine (Sigma), and the coloring reaction was stopped with 4 M H_2SO_4, after which the absorbance was determined at 490 nm.

Platelet Agglutination—Agglutination studies were performed in an Elvi-840 dual channel aggregometer (Pabish, Brussels, Belgium) with constant stirring at 1000 rpm at 37 °C.

For the agglutination experiments using 1C1E7 scFv, blood was drawn from healthy volunteers on trisodium citrate, pH 7.5 (0.11 M, 10:1 v/v), and centrifuged at 180 × *g* for 10 min to obtain platelet-rich plasma. Platelet-rich plasma was incubated for 3 min with buffer and with 1C1E7 scFv or IgG, after which agglutination was induced by the addition of ristocetin.

For the agglutination experiments using the VWF fragments, blood was collected on acid citrate dextrose (0.085 M trisodium citrate, 0.065 M citric acid, 0.110 M glucose, pH 4.5) (10:1.5 v/v). Platelets were washed twice and resuspended in PBS containing 1 mg/ml glucose and 1 mg/ml bovine serum albumin. A final platelet concentration of 200,000 platelets/μl was used. ΔD′D3, plusD′D3, or VWF/D′D3 were added to a final concentration of 10 μg/ml, and the mixture was incubated for 3 min, after which agglutination was induced by the addition of ristocetin.

Construction of Expression Plasmid for Chimeric Porcine/Human Recombinant VWF—An expression plasmid for a chimeric porcine/human recombinant VWF in which the aa 786–960 region of the human sequence was exchanged by the corresponding porcine sequence was constructed. This recombinant VWF construct is further referred to as VWF(aa786–960)PIG.

Briefly, the expression vector pNUT-VWF cas (29) was digested with the restriction endonuclease BglII, and the resulting 4.7-kilobase fragment was ligated subsequently in the unique BglII site of the vector pSV2-dhfr to give the vector pSV2-pNUT.

RNA was isolated from a porcine umbilical cord using the mRNA isolation kit (Roche Molecular Biochemicals), and cDNA was prepared with the Thermoscript™ reverse transcription-PCR system (Invitrogen) using the sequence specific primer RP3 (5′-CGC AGG TTC CTC TCC TCG CAG TTC-3′, nucleotides 3384–3408). cDNA was amplified by PCR using the sense primer P5 (5′-CGC AGC AAG AGG AGT CTG AGC TGC CGG CCC CCC ATG-3′, nucleotides 2279–2314) and the antisense primer RP3. The PCR product was ligated in the vector PCR4 Blunt-TOPO vector (Invitrogen). A unique EagI restriction site at position 2875 was introduced by PCR using the sense primer P5 and the point-mutated antisense primer P6.2 (5′-GAT GAA CCG GCC GGA TTC CAC3′, nucleotide 2867–2887). The PCR product was cloned in the pBAD-TOPO TA vector (Invitrogen) to give the vector pBAD-PIG.

Subsequently, the XhoI-EagI fragment of the vector pBAD-PIG was ligated in XhoI-EagI-digested pSV2-pNUT to give the vector pSV2-pNUT-PIG. The vector pSV2-pNUT-PIG was digested with EcoRI and BglII. The resulting 4.7-kilobase fragment was exchanged by the corresponding sequence of pNUT-VWF cas to give the final expression vector pNUT-VWF PIG.

Construction of Expression Plasmids for VWF Point or Double Mutants—Expression plasmids for human VWF or for VWF(aa786–960)PIG containing K968S, K991Q or S1009G,N1011S mutations were constructed starting from the plasmid pSV2-pNUT or pSV2-pNUT-PIG, respectively. Using the QuikChange XL site-directed mutagenesis kit (Stratagene) and specific primers, the desired mutations were introduced. The resulting vectors were digested with EcoRI and BglII, and the resulting 4.7-kilobase fragment was exchanged by the corresponding sequence of pNUT-VWF cas or pNUT-VWF PIG as described above to obtain expression plasmids for full-length VWF.

Expression of Recombinant VWF—VWF was transiently expressed in COS-7 cells (30) or stably expressed in baby hamster kidney cells overexpressing furin (BHK-fur) as described before (6). The VWF:Ag level was determined in a sandwich immunoassay as previously described (21).

Binding of VWF to moAb 1C1E7—96-Well microtiter plates (Greiner, Frickenhausen, Germany) were coated ON at 4 °C with moAb 1C1E7 (10 μg/ml in PBS), blocked for 2 h at RT with TBS containing 3% milk powder, and incubated for 2 h at 37 °C with a dilution series of VWF expression medium in TBS containing 0.3% milk powder. Bound VWF was detected as described above.

Binding of VWF to Human Collagen Type III—96-Well microtiter plates were coated ON at 4 °C with 25 μg/ml human collagen type III (Sigma) in PBS. Wells were blocked with PBS containing 3% milk powder and incubated with a dilution series of purified recombinant VWF in PBS containing 0.3% milk powder. Bound VWF was detected as described above (24).

Multimeric Analysis—The multimeric pattern of VWF was determined essentially as described (31). Briefly, 0.08 μg of VWF was separated on SDS 0.65% Seakem HGT, agarose gel (Cambrex, Bio Science Rockland, Inc., ME). Gels were fixed on Gelbond (Cambrex), and VWF was immunodetected using anti-VWF-Ig labeled with alkaline phosphatase (32) and further revelation with the AP conjugate substrate kit (Bio-Rad).

Cross-blocking Analysis for Antibody Binding to Immobilized VWF—96-Well microtiter plates were coated ON at 4 °C with VWF (10 μg/ml in PBS) and blocked for 2 h at RT with TBS containing 3% milk powder. Wells were incubated for 1 h at 37 °C with biotinylated moAb 418 (b-418) at its half-maximal binding concentration (0.15 μg/ml) in the presence of the competing moAbs 701, 724, 418, or 82D6A3 (15 μg/ml) using TBS containing 0.3% milk powder as buffer. Residual bound b-418 was detected for 45 min at RT with peroxidase-labeled streptavidin (1/10000 in TBS containing 0.3% milk powder). Visualization was performed as described above.

Cross-blocking Analysis for Antibody Binding to "Soluble" VWF—96-Well microtiter plates were coated with moAb 418 (2 μg/ml in PBS) and blocked for 2 h at RT with TBS containing 3% milk powder. Biotinylated VWF (b-VWF, 6 μg/ml) was preincubated with one of the anti-VWF moAbs (0.5–60 μg/ml) for 1 h at 37 °C after which this solution was transferred to the coated wells. After a further incubation of 30 min at 37 °C, residual bound b-VWF was detected with peroxidase-labeled streptavidin as described above.

Statistics—In this study means and S.E. are shown. Statistical significance of differences between means was evaluated using Student's *t* test.

RESULTS

Functionality of VWF Lacking the D′D3 Region—It has been suggested that the remainder of VWF outside the A1 domain might shield the GPIbα binding region. However, the exact mechanism of this

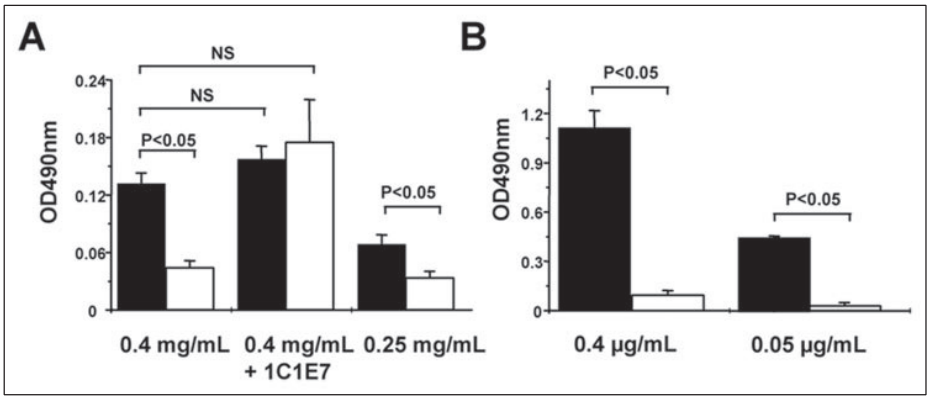

FIGURE 2. **Ristocetin- and botrocetin-induced binding of VWF(−fragments) to rGPIbα.** Microtiter plates were coated with anti-GPIbα moAb 2D4 and incubated with rGPIbα. Wells were incubated with a constant amount of ΔD′D3 (*filled bars*) or plusD′D3 (*open bars*) in the presence or absence of 1C1E7 IgG (12 μg/ml) and in the presence of ristocetin (*A*) or botrocetin (*B*) at the indicated amounts. Bound VWF was detected (mean ± S.E., $n = 3$). *NS*, not significant.

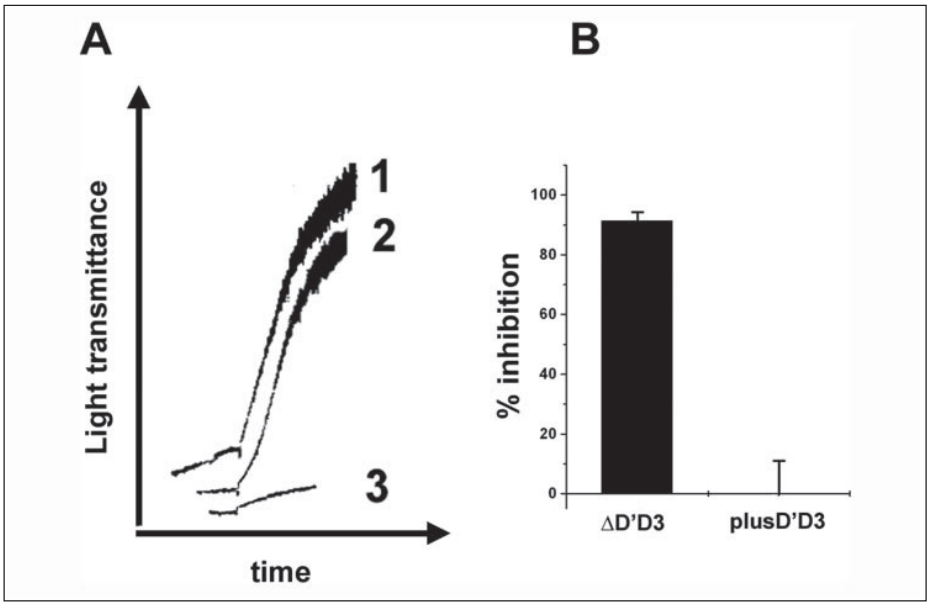

FIGURE 3. **Ristocetin-induced platelet agglutination.** *A*, washed platelets (200,000 platelets/μl) were incubated with 10 μg/ml ΔD′D3 (1) or plusD′D3 (*2* and*3*) after which agglutination was induced by the addition of 0.1 mg/ml ristocetin (*1* and *3*) or 0.2 mg/ml ristocetin (*2*). Results are representative of three independent experiments. *B*, washed platelets (200,000 platelets/μl) were incubated with 10 μg/ml ΔD′D3 or plusD′D3 in the presence of 10 μg/ml VWF/D′D3, after which agglutination was induced by the addition of a threshold dose of ristocetin (0.1 and 0.2 mg/ml, respectively). The percentage inhibition is shown (mean ± S.E., $n = 3$). As the 100% value, agglutination in the absence of VWF/D′D3 was chosen.

shielding has not been elucidated yet. The anti-VWF moAb 1C1E7 interacts with the aa 764–1035 region in the N-terminal D′D3 domains and modulates the binding of VWF to GPIbα. This would suggest a functional role of the D′D3 region in the binding of the A1 domain to its receptor. Therefore, we decided to study this putative modulatory role using VWF constructs lacking the D′D3 region.

Recombinant ΔD′D3 (aa 1260–1874) is a dimer composed of two VWF monomers lacking the D′D3 region but still contains the N-terminal flanking region of the VWF A1 domain. We verified the ristocetin- and botrocetin-induced binding of this construct to a recombinant GPIbα fragment and compared its affinity to that of recombinant plusD′D3 (aa 1–1874). This construct is a dimer as well but lacks the C-terminal D4-B1-B2-B3-C1-C2-CK regions.

In the presence of ristocetin as a modulator, ΔD′D3 interacted stronger with rGPIbα compared with plusD′D3 (Fig. 2*A*). Similar results were obtained with botrocetin (Fig. 2*B*). These results suggest that the D′D3 region has an inhibitory effect on the interaction of the A1 domain with GPIbα. The addition of 1C1E7 to plusD′D3 increased ristocetin-induced binding to rGPIbα to the level of ΔD′D3 while not affecting the GPIbα interaction of ΔD′D3 (Fig. 2*A*). This suggests that the observed effects are likely not due to a different affinity of the deletion mutants for the modulators used in the assay.

We further identified the inhibitory role exhibited by the D′D3 region in VWF/GPIbα interaction in platelet agglutination experiments. Dimeric constructs were used because previous studies demonstrated the necessity of the use of at least dimeric molecules for sustaining platelet aggregation (33). The threshold dose needed for ristocetin-induced agglutination of washed platelets was lower for ΔD′D3 than for plusD′D3 (Fig. 3*A*), also demonstrating the inhibitory effect of the D′D3 region on the interaction of VWF with GPIbα.

In line with this, VWF/D′D3 inhibited the ristocetin-induced agglutination supported by ΔD′D3 while having no effect on the agglutination supported by plusD′D3 (Fig. 3*B*). These results show that the lack of inhibition by deletion of the D′D3 region in ΔD′D3 could be reverted by external addition of these isolated D′D3 domains.

These experiments demonstrate the functionality of the D′D3 region in the interaction of VWF with GPIbα, strongly suggesting that this region shields the GPIbα binding site in VWF, restricting its accessibility and preventing spontaneous VWF binding to platelets.

Epitope Mapping of moAb 1C1E7—To discover residues in the D′D3 region that would be responsible for its inhibitory effect, we identified the binding region of 1C1E7 in VWF. Previous studies demonstrated that 1C1E7 interacted with a tryptic fragment comprising the aa 764–1035 sequence in VWF, which is located in the D′D3 region (15). The location of the epitope was further corroborated by the fact that 1C1E7 failed to interact with ΔD′D3 but recognized the isolated D′D3 region (data not shown). Because 1C1E7 does interact with VWF in Western blot, this moAb probably recognizes a linear epitope. Therefore, the

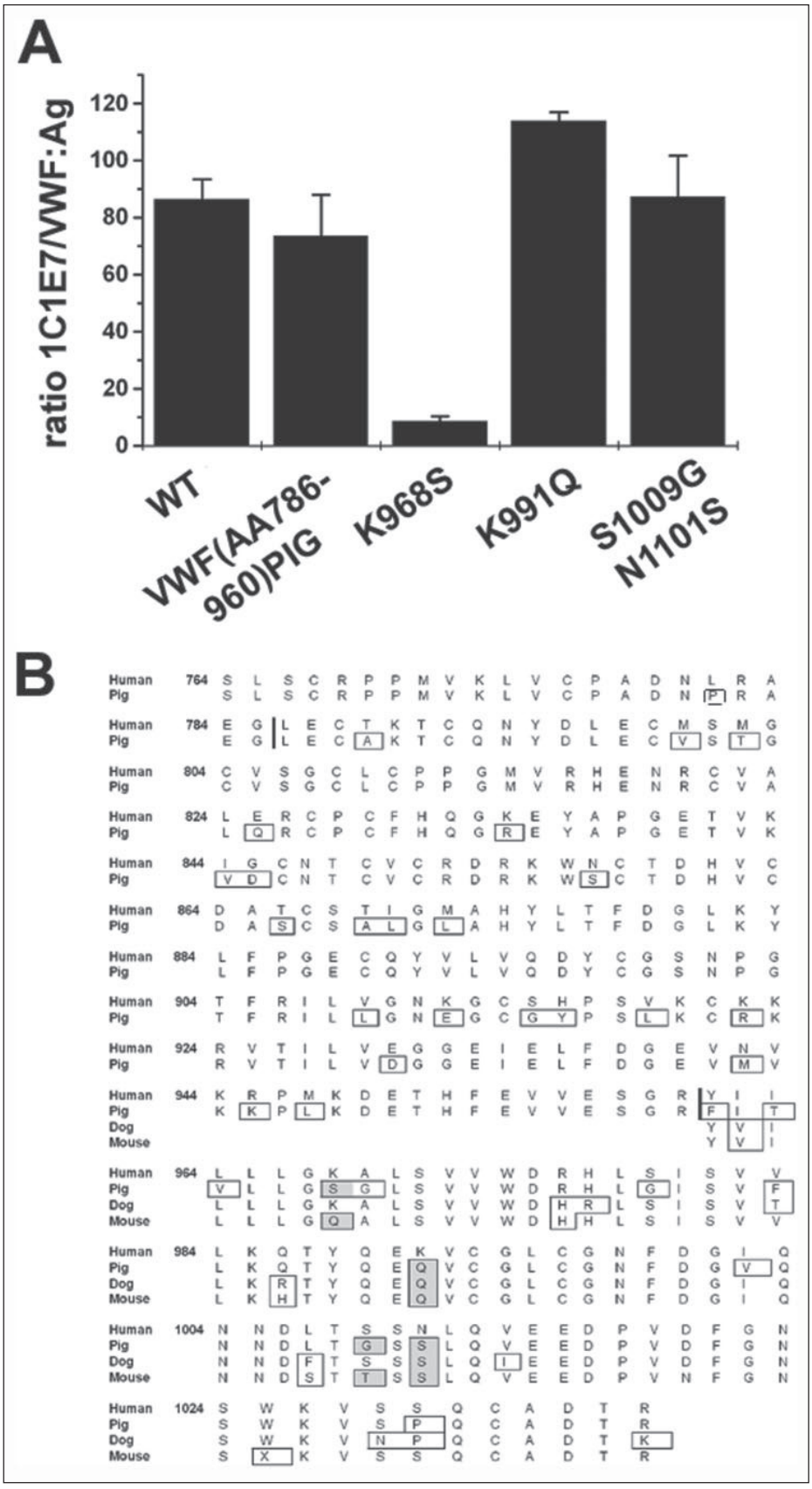

FIGURE 4. **Epitope mapping of 1C1E7.** *A*, binding of recombinant WT and mutant VWF to 1C1E7. Microtiter plates were coated with 1C1E7 or anti-VWF-Ig and incubated with expression medium of recombinant VWF. Bound VWF was detected with anti-VWF-Ig-horseradish peroxidase. The ratio of the A_{490} nm values for the 1C1E7 binding on the values for the anti-VWF-Ig are shown in percentages (mean ± S.E., $n = 3$). *B*, alignment of the primary sequence of human, canine, porcine, and murine VWF in the aa 764–1035 region. Sequence alignment of human (Medline submission number NP_000543), canine (Q28295), porcine (Q28833), and murine (NM_017708) VWF. The aa 786–961 fragment, which was exchanged in the chimeric construct, is delineated. Residues between aa 961–1035 that are different between human and porcine, canine, or murine VWF are *marked* with *boxes*. The residues that are different between human and both porcine and murine VWF but are similar between human and canine VWF are *shaded* in *gray*.

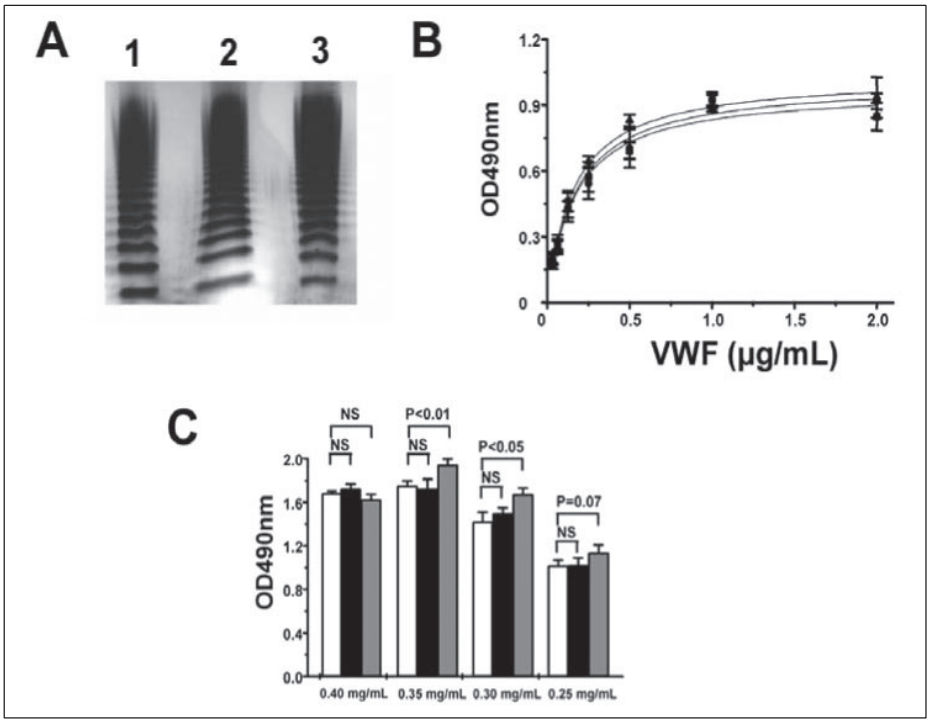

FIGURE 5. **Functionality of chimeric constructs.** *A*, VWF multimer analysis. Samples of WT VWF (*1*), VWF(aa786–960)PIG (*2*), and VWF(aa786–960)PIG-K968S (*3*) were analyzed by SDS-0.65% agarose gel electrophoresis and detected with anti-VWF-Ig labeled with alkaline phosphatase. *B*, collagen binding assay. Microtiter plates were coated with human collagen type III and incubated with a dilution series of WT VWF (■), VWF(aa786–960)PIG (●), and VWF(aa786–960)PIG-K968S (▲), after which bound VWF was detected (mean ± S.E., $n = 3$). *C*, ristocetin-induced binding of VWF to rGPIbα. Microtiter plates were coated with anti-GPIbα moAb 2D4 and incubated with rGPIbα. Wells were incubated with WT VWF (*open bars*), VWF(aa786–960)PIG (*filled bars*), and VWF(aa786–960)PIG-K968S (*gray bars*) (0.5 μg/ml) in the presence of ristocetin at the indicated amounts. Bound VWF was detected (mean ± S.E., $n = 3$). *NS*, not significant.

cross-reactivity of 1C1E7 with VWF of different species was verified to determine if differences in the primary structure of VWF have an effect on the binding of 1C1E7.

1C1E7 failed to recognize porcine plasma VWF but was still able to interact with canine VWF (data not shown). This suggests that some of the 35 residues in the aa 764–1035 region of human VWF that are not shared with the porcine VWF sequence might maintain the epitope of 1C1E7. To identify these residues, a chimeric recombinant VWF (VWF(aa786–960)PIG) in which the aa 786–960 region of the human sequence was exchanged by the corresponding porcine sequence was constructed. For cloning reasons, only this part of the N-terminal aa 764–1035 region in human VWF was exchanged. This construct, containing 23 residues differing from the human sequence, was transiently expressed in COS-7 cells, and the interaction with 1C1E7 was determined. 1C1E7 still interacted with VWF(aa786–960)PIG (Fig. 4*A*), suggesting that the aa 961–1035 region in VWF probably maintains the epitope of this moAb. Further comparison of the primary sequence of human VWF in this region with sequences of porcine, canine, and murine VWF highlighted residues Lys-968, Lys-991, Ser-1009, and Asn-1011 as possible candidates for maintaining the epitope of 1C1E7 (Fig. 4*B*). These residues are different between human and both porcine and murine VWF but are similar between the human and canine protein. VWF mutants in which these residues were exchanged for the porcine analogues were constructed and transiently expressed in COS-7 cells. 1C1E7 bound as strongly with the K991Q and S1009G, N1011S mutant as to WT VWF, suggesting that these residues are not important for maintaining the epitope. However, binding was completely abolished for the K968S point mutant, identifying this residue as critical for the interaction of 1C1E7 (Fig. 4*A*).

Functionality of Chimeric Recombinant VWF—In a next step the ristocetin-induced binding of the recombinant full-length WT VWF and chimeric constructs to GPIbα was measured to verify if altering the structure in the D′D3 region might influence this interaction. Recombinant WT VWF, VWF(aa786–960)PIG, and VWF(aa786–960)PIG, in which a K968S point mutation was inserted (VWF(aa786–960)PIG-K968S), were expressed in BHK-fur (baby hamster kidney cells overexpressing furin) cells. The multimeric pattern of both mutants was similar to WT VWF with at least 16 detectable multimer bands (Fig. 5*A*). Binding characteristics of the mutants to anti-VWF moAbs 418, 82D6A3, 701, and 724 was similar to WT VWF (data not shown), suggesting a similar overall structural fold.

Next, the functional effects of the exchange of several residues in the D′D3 region was verified. The interaction with fibrillar collagen was not statistically different for mutant VWF as compared with the WT, resulting in a VWF:collagen binding assay of 1.09 ± 0.06 and 1.10 ± 0.07 units/ml for VWF(aa786–960)PIG ($p = 0.28$, $n = 3$) and VWF(aa786–960)PIG-K968S ($p = 0.25$, $n = 3$), respectively, using WT VWF as a reference (Fig. 5*B*).

VWF(aa786–960)PIG and VWF(aa786–960)PIG-K968S bound comparably to rGPIbα in the presence of 0.4 mg/ml ristocetin (Fig. 5*C*). However, at submaximal doses of ristocetin, VWF(aa786–960)PIG-K968S showed a small but significant increase in binding compared with VWF(aa786–960)PIG and WT. These results suggest that altering residues in the D′D3 region and, more specifically the binding region of 1C1E7, influences the binding affinity of VWF for GPIbα.

Cross-blocking Studies—Next, the structural proximity of the D′D3 region with the A1 domain in immobilized VWF and in soluble VWF was verified by analyzing whether binding of moAb 418 (interacting with the D′D3 region) could be blocked by moAbs 701 and 724 (both interacting with the A1 domain). This would give us the opportunity to gather information on the structural changes in VWF upon immobilization. As a negative control, moAb 82D6A3 (interacting with the A3 domain) was used. Two different enzyme-linked immunosorbent assay set-ups were developed, (i) cross-blocking of binding of b-418 to immobilized VWF by unlabeled moAbs and (ii) the inhibition of the capture of b-VWF to immobilized moAb 418 by the unlabeled moAbs. Previous data demonstrated that biotinylation of VWF had no effect on the interaction with fibrillar collagen or GPIbα, which would suggest that the

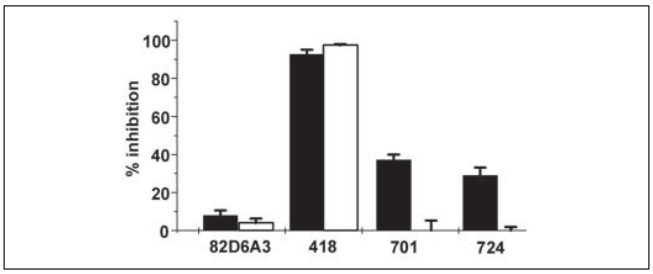

FIGURE 6. **Cross-blocking studies; inhibition of the binding of b-418 to immobilized VWF or b-VWF to immobilized moAb 418 by anti-VWF moAbs.** Microtiter plates were coated with VWF (*open bars*) or with moAb 418 (*filled bars*) and incubated with b-418 or b-VWF, respectively, in the presence of the anti-VWF moAbs 82D6A3, 418, 701, or 724. Residual bound b-418 or b-VWF was detected. Percentage inhibition is shown (mean ± S.E., $n = 3$). As a 100% reference, the binding of b-418 to immobilized VWF or the binding of b-VWF to immobilized 418 was chosen.

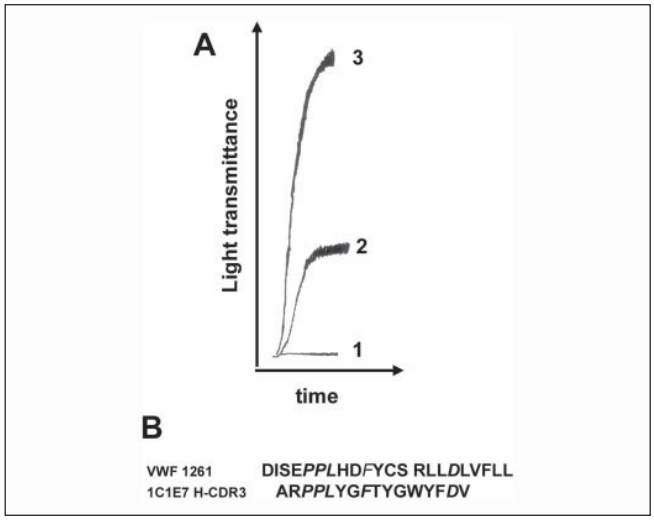

FIGURE 7. **Functionality of 1C1E7 scFv.** *A*, stimulating effect of 1C1E7 scFv on platelet aggregation in platelet-rich plasma. Platelet-rich plasma was incubated with PBS buffer (*1*), 1C1E7 scFv refolded from inclusion bodies (~20 μg/ml) (*2*), or 25 μg/ml 1C1E7 IgG (3), after which a subthreshold dose of ristocetin (0.2 mg/ml) was added. Results are representative of three independent experiments. *B*, alignment of the primary sequence of the N-terminal flanking region of the human A1 domain and the complimentarity determining region 3 of the 1C1E7 heavy chain.

conformation of VWF is not altered upon biotinylation (34). When VWF was immobilized, no measurable inhibition of the binding of b-418 was observed by any of the moAbs except with unlabeled 418 as the positive control (Fig. 6, *open bars*), although all moAbs were able to interact with immobilized VWF (data not shown). In contrast, moAbs 701 and 724 did compete with moAb 418 for the binding to soluble b-VWF, whereas moAb 82D6A3 had again no effect (Fig. 6, *filled bars*).

This would suggest that in solution the A1 domain and the D′D3 region are in close proximity since moAbs interacting with these regions cross-block each other. However, when VWF was immobilized, moAbs interacting with the A1 domain failed to block binding of moAb 418 interacting with the D′D3 region, suggesting that these regions are now more distant from each other.

Construction and Expression of 1C1E7 scFv—To further characterize the VWF-activating potency of the moAb 1C1E7, the scFv was expressed as a His-tagged fusion protein in *E. coli*. 1C1E7 scFv increased ristocetin-induced platelet aggregation, similarly to 1C1E7 IgG (Fig. 7*A*), providing evidence that the construction was correct. Moreover, 1C1E7 scFv inhibited binding of the IgG to VWF, suggesting a same interaction site in VWF (data not shown). Comparison of the primary sequence of the complimentarity determining region 3 of the 1C1E7 heavy chain revealed a strong similarity with the N-terminal flanking region of the VWF A1 domain (Fig. 7*B*). As mentioned before, there is good evidence that this N-terminal flanking region modulates the binding of VWF to GPIbα. Based on our observation, we hypothesized that 1C1E7 might be able to mimic this region of the A1 domain. Because 1C1E7 does bind to the D′D3 region in VWF, the N-terminal flanking region of the A1 domain might have similar binding characteristics. This putative interaction of the A1 domain with the D′D3 region could modulate the VWF binding to GPIbα.

DISCUSSION

Human VWF in solution does not interact with its platelet receptor GPIb-IX-V under normal conditions. Binding, however, is induced by immobilization of VWF or by exposure to shear. These observations suggest that the affinity toward GPIb-IX-V is regulated by conformational changes in VWF that are induced by shear and/or immobilization and lead to exposure of functional sites.

In vitro, binding of VWF to GPIb-IX-V can be provided by modulators such as ristocetin or botrocetin. Although in these conditions binding is induced rather artificially, it has been demonstrated that ristocetin-dependent interactions quite closely correlate with the physiological shear-dependent situation (35).

We have previously identified the moAb 1C1E7 (15) which interacts with the aa 764–1035 region in the N-terminal D′D3 domains in VWF, increases the affinity of VWF for GPIbα, and hence, induces von Willebrand disease type 2B alterations, although it does not bind near the GPIb-IX-V binding site (16). This would suggest a modulatory effect for the binding region of 1C1E7 in VWF on the GPIbα interaction. Therefore, the goal of this study was to determine the functional role of the D′D3 region in binding of VWF to GPIb-IX-V.

Deletion of the D′D3 region in VWF resulted in a higher affinity for GPIbα as demonstrated in an enzyme-linked immunosorbent assay system; the dimeric deletion mutant ΔD′D3, lacking the D′D3 region, showed an increased ristocetin- and botrocetin-induced interaction with a recombinant GPIbα fragment compared with the dimeric deletion mutant plusD′D3, which lacks the C-terminal region in VWF. The addition of 1C1E7 IgG to plusD′D3 increased the ristocetin-induced binding to rGPIbα, now equaling the binding of ΔD′D3. This confirms again the modulatory effect of 1C1E7 on the VWF/GPIbα interaction but in addition proves that the observed difference in affinity of both deletion mutants for GPIbα is not due to a different affinity for ristocetin. These results were confirmed in a platelet agglutination assay; the threshold dose of ristocetin needed to induce agglutination of washed platelets was lower in the presence of ΔD′D3 as compared with plusD′D3. Moreover, at lower platelet concentrations, ΔD′D3 was able to sustain spontaneous platelet agglutination in contrast to plusD′D3 (data not shown). All together, these data strongly suggest that the D′D3 region may act as an inhibitory region, shielding the A1 domain in VWF.

Our data further confirm and extend previous studies that demonstrated the putative shielding of the GPIb binding site in the A1 domain by the N-terminal flanking regions of the A1 domain (aa 1260–1271) and the C-terminal region of the D3 region (aa 1204–1259). (i) Peptides derived from these regions inhibited ristocetin-induced binding of purified VWF to human platelets (36), (ii) stepwise N-terminal deletions in the aa 1204–1271 region of a recombinant VWF fragment comprising the A1 domain (aa 1204–1496) resulted in stepwise increased ristocetin-induced binding to human platelets (37); (iii) Ala mutations in the N-terminal flanking region of the A1 domain (aa 1260–1271) in full-length VWF resulted in an increased ristocetin-induced binding to human platelets (14); (iv) deletions in the aa 1222–1271 region in full-

length VWF in which an additional R1308A mutation was added resulted in an increased ristocetin-induced or even spontaneous binding to human platelets when compared with the R1308A VWF point mutant (38); (v) specific *O*-linked glycosylation in the aa 1248–1256 region negatively modulated the binding to human platelets as demonstrated using glycosylphosphatidylinositol COS-7 cell-anchored FLAG-tagged VWF A1 domains (39).

To further identify the exact residues within VWF important for the binding region of 1C1E7, we took advantage of the observation that 1C1E7 does not interact with porcine VWF. To confirm the putative role of the deviating residues in human *versus* pig VWF in maintaining the epitope of 1C1E7, a chimeric porcine/human VWF was constructed in which the aa 786–960 region of human VWF was exchanged by the corresponding porcine sequence. In the resulting recombinant protein, VWF(aa786–960)PIG, 22 of the possibly important residues were mutated. Compared with the published sequence, an extra mutation was inserted (P812L); however, in line with previous studies (40), this is probably a result of strain specificity, because sequencing of different cDNA clones resulted in the identification of the identical substitution. VWF(aa786–960)PIG, however, bound as good to 1C1E7 as did WT VWF, suggesting that the remaining aa 961–1035 region in VWF probably maintains the epitope of this moAb. Further mutagenesis of the rest of the differing residues identified Lys-968, located in the VWF D3 domain, as essential for the binding of moAb 1C1E7. As yet, this residue has not been linked with a functional deficiency of VWF. The ristocetin-induced interaction with rGPIbα of VWF(aa786–960)PIG containing an additional K968S mutation was slightly but significantly increased at submaximal doses of this modulator compared with WT VWF. Similar results were obtained in platelet agglutination studies (data not shown); in the presence of VWF(aa786–960)PIG and VWF(aa786–960)PIG-K968S, lower doses of ristocetin were needed to induce agglutination compared with WT VWF. These results would suggest that this residue and/or the surrounding region might be important for modulating the interaction of VWF with GPIbα. However, additional mutagenesis studies are needed to further confirm this.

VWF/D′D3 blocks both spontaneous and ristocetin-induced platelet agglutination in the presence of ΔD′D3. Similarly, VWF/D′D3 inhibited the spontaneous agglutination supported by ΔD′D3 (data not shown). This is in line with our hypothesis that in solution the D′D3 region interacts with structures in ΔD′D3 and that these intramolecular interactions in VWF shield the A1 domain from interacting with GPIbα.

It is known that immobilization of VWF is a prerequisite for platelet adhesion at high shear stress, probably due to conformational changes (41). However, the exact nature of these conformational changes has not been elucidated yet (42).

To further substantiate the idea that D′D3 would interact with A1 in VWF in solution and no longer when immobilized/sheared, we looked to whether moAbs against the respective domains would block each other's binding or not under those conditions when VWF was immobilized on a polystyrene surface, as it is known that this allows platelet recruitment (34). The anti-D′D3 moAb 418 cross-competed with the anti-A1 domain moAbs 701 and 724 when VWF was in solution, but not on immobilized VWF, indeed providing evidence for a changing distance between the domains upon immobilization. Previous studies suggested a structural change in the D′D3 region upon immobilization of VWF onto calf skin collagen, causing a reduced affinity for factor VIII (43). It could be that similar conformational changes in the D′D3 region are induced by immobilization of VWF on a polystyrene surface, leading to disruption of the structural proximity of this region with the A1 domain, thereby exposing the GPIbα binding site.

Finally, we also found a striking sequence similarity between the primary sequence of the complimentarity determining region 3 of the 1C1E7 heavy chain and the N-terminal flanking region of the VWF A1 domain (aa 1260–1271). This N-terminal flanking region is important in modulating the binding of the A1 domain with GPIbα as modifications or deletions in this region increase the affinity of VWF for GPIbα (14, 38), and in our view this might be the region within the A1 domain that interacts with the D′D3 region. 1C1E7 then would compete with this N-terminal flanking region disrupting this interaction. Because 1C1E7 interacts with K968 in the D3 domain, it is possible that the N-terminal flanking region interacts with this residue as well.

In conclusion, our results demonstrate an inhibitory role for the aa 764–1035 region in VWF for the GPIbα interaction. Based on these observations, the following hypothesis might be put forward. In native, resting conditions, the A1 domain and the D′D3 region are in close proximity, possibly through an interaction of the N-terminal flanking region of the A1 domain with the D3-domain, more precisely with the region of residue Lys-968. This interaction would limit the accessibility of the GPIbα binding site. When VWF is immobilized, this interaction is disrupted through conformational changes in VWF, possibly in the D′D3 region which allows recruitment of platelets through their GPIb-IX-V complex. Further studies are required to confirm this hypothesis.

Acknowledgments—We thank Stephan Vauterin and Dr. J. P. Girma, respectively, for performing the multimer analysis and providing us with the anti-VWF moAbs.

REFERENCES

1. Ruggeri, Z. M. (2002) *Nat. Med.* **8,** 1227–1234
2. Vermylen, J., Donati, M. B., De Gaetano, G., and Verstraete, M. (1973) *Nature* **244,** 167–168
3. Vicente, V., Houghten, R. A., and Ruggeri, Z. M. (1990) *J. Biol. Chem.* **265,** 274–280
4. Read, M. S., Smith, S. V., Lamb, M. A., and Brinkhous, K. M. (1989) *Blood* **74,** 1031–1035
5. Siedlecki, C. A., Lestini, B. J., Kottke-Marchant, K. K., Eppell, S. J., Wilson, D. L., and Marchant, R. E. (1996) *Blood* **88,** 2939–2950
6. Lankhof, H., Wu, Y. P., Vink, T., Schiphorst, M. E., Zerwes, H. G., de Groot, P. G., and Sixma, J. J. (1995) *Blood* **86,** 1035–1042
7. Andrews, R. K., Gorman, J. J., Booth, W. J., Corino, G. L., Castaldi, P. A., and Berndt, M. C. (1989) *Biochemistry* **28,** 8326–8336
8. Gralnick, H. R., Williams, S., McKeown, L., Kramer, W., Krutzsch, H., Gorecki, M., Pinet, A., and Garfinkel, L. I. (1992) *Proc. Natl. Acad. Sci. U. S. A.* **89,** 7880–7884
9. Miura, S., Li, C. Q., Cao, Z., Wang, H., Wardell, M. R., and Sadler, J. E. (2000) *J. Biol. Chem.* **275,** 7539–7546
10. Huizinga, E. G., Tsuji, S., Romijn, R. A., Schiphorst, M. E., de Groot, P. G., Sixma, J. J., and Gros, P. (2002) *Science* **297,** 1176–1179
11. Dumas, J. J., Kumar, R., McDonagh, T., Sullivan, F., Stahl, M. L., Somers, W. S., and Mosyak, L. (2004) *J. Biol. Chem.* **279,** 23327–23334
12. Emsley, J., Cruz, M., Handin, R., and Liddington, R. (1998) *J. Biol. Chem.* **273,** 10396–10401
13. Meyer, D., Fressinaud, E., Hilbert, L., Ribba, A. S., Lavergne, J. M., and Mazurier, C. (2001) *Best. Pract. Res. Clin. Haematol.* **14,** 349–364
14. Matsushita, T., and Sadler, J. E. (1995) *J. Biol. Chem.* **270,** 13406–13414
15. Tornai, I., Arnout, J., Deckmyn, H., Peerlinck, K., and Vermylen, J. (1993) *J. Clin. Investig.* **91,** 273–282
16. Ulrichts, H., Harsfalvi, J., Bene, L., Matko, J., Vermylen, J., Ajzenberg, N., Baruch, D., Deckmyn, H., and Tornai, I. (2004) *J. Thromb. Haemost.* **2,** 1622–1628
17. Vanhoorelbeke, K., Depraetere, H., Romijn, R. A. P., Huizinga, E. G., De Maeyer, M., and Deckmyn, H. (2003) *J. Biol. Chem.* **278,** 37815–37821
18. Depraetere, H., Ajzenberg, N., Girma, J. P., Lacombe, C., Meyer, D., Deckmyn, H., and Baruch, D. (1998) *Blood* **91,** 3792–3799
19. Obert, B., Houllier, A., Meyer, D., and Girma, J. P. (1999) *Blood* **93,** 1959–1968
20. Pietu, G., Ribba, A. S., Meulien, P., and Meyer, D. (1989) *Biochem. Biophys. Res. Commun.* **163,** 618–626
21. Vanhoorelbeke, K., Cauwenberghs, N., Vauterin, S., Schlammadinger, A., Mazurier, C., and Deckmyn, H. (2000) *Thromb. Haemostasis* **83,** 107–113
22. Subramani, S., Mulligan, R., and Berg, P. (1981) *Mol. Cell. Biol.* **1,** 854–864
23. Lenting, P. J., Westein, E., Terraube, V., Ribba, A. S., Huizinga, E. G., Meyer, D., de

Groot, P. G., and Denis, C. V. (2004) *J. Biol. Chem.* **279,** 12102–12109
24. Staelens, S., Desmet, J., Ngo, T. H., Vauterin, S., Pareyn, I., Barbeaux, P., Van, R., I, Stassen, J. M., Deckmyn, H., and Vanhoorelbeke, K. (2005) *Mol. Immunol.,* in press
25. Sblattero, D., and Bradbury, A. (1998) *Immunotechnology* **3,** 271–278
26. Lilie, H., Schwarz, E., and Rudolph, R. (1998) *Curr. Opin. Biotechnol.* **9,** 497–501
27. Ulrichts, H., Vanhoorelbeke, K., Cauwenberghs, S., Vauterin, S., Kroll, H., Santoso, S., and Deckmyn, H. (2003) *Arterioscler. Thromb. Vasc. Biol.* **23,** 1302–1307
28. Fujimura, Y., Titani, K., Usami, Y., Suzuki, M., Oyama, R., Matsui, T., Fukui, H., Sugimoto, M., and Ruggeri, Z. M. (1991) *Biochemistry* **30,** 1957–1964
29. van der Plas, R. M., Gomes, L., Marquart, J. A., Vink, T., Meijers, J. C., de Groot, P. G., Sixma, J. J., and Huizinga, E. G. (2000) *Thromb. Haemostasis* **84,** 1005–1011
30. Sixma, J. J., Schiphorst, M. E., Verweij, C. L., and Pannekoek, H. (1991) *Eur. J. Biochem.* **196,** 369–375
31. Ruggeri, Z. M., and Zimmerman, T. S. (1981) *Blood* **57,** 1140–1143
32. Goudemand, J., Mazurier, C., Parquet-Gernez, A., and Goudemand, M. (1977) *Pathol. Biol.* (*Paris*) **25,** 241–243
33. Sugimoto, M., Ricca, G., Hrinda, M. E., Schreiber, A. B., Searfoss, G. H., Bottini, E., and Ruggeri, Z. M. (1991) *Biochemistry* **30,** 5202–5209
34. Ulrichts, H., Vanhoorelbeke, K., Girma, J. P., Lenting, P. J., Vauterin, S., and Deckmyn, H. (2005) *J. Thromb. Haemost.* **3,** 552–561
35. Dong, J. F., Berndt, M. C., Schade, A., McIntire, L. V., Andrews, R. K., and Lopez, J. A. (2001) *Blood* **97,** 162–168
36. Mohri, H., Fujimura, Y., Shima, M., Yoshioka, A., Houghten, R. A., Ruggeri, Z. M., and Zimmerman, T. S. (1988) *J. Biol. Chem.* **263,** 17901–17904
37. Sugimoto, M., Dent, J., McClintock, R., Ware, J., and Ruggeri, Z. M. (1993) *J. Biol. Chem.* **268,** 12185–12192
38. Nakayama, T., Matsushita, T., Dong, Z., Sadler, J. E., Jorieux, S., Mazurier, C., Meyer, D., Kojima, T., and Saito, H. (2002) *J. Biol. Chem.* **277,** 22063–22072
39. Schulte am Esch, J., Robson, S. C., Knoefel, W. T., Eisenberger, C. F., Peiper, M., and Rogiers, X. (2005) *Br. J. Haematol.* **128,** 82–90
40. Schulte am Esch, J., Cruz, M. A., Siegel, J. B., Anrather, J., and Robson, S. C. (1997) *Blood* **90,** 4425–4437
41. Savage, B., Almus-Jacobs, F., and Ruggeri, Z. M. (1998) *Cell* **94,** 657–666
42. Novak, L., Deckmyn, H., Damjanovich, S., and Harsfalvi, J. (2002) *Blood* **99,** 2070–2076
43. Bendetowicz, A. V., Wise, R. J., and Gilbert, G. E. (1999) *J. Biol. Chem.* **274,** 12300–12307

Novel evaluation method for densitometric curves of von Willebrand Factor multimers and a new parameter (M_{MW}) to describe the degree of multimersation

Miklós L. Udvardy[1,2]; Katalin Szekeres-Csiki[1]; Jolán Hársfalvi[1]

[1]Clinical Research Center, University of Debrecen, Debrecen, Hungary; [2]Thrombosis, Haemostasis and Vascular Biology Research Group of the Hungarian Academy of Sciences, University of Debrecen, Debrecen, Hungary

Summary

Von Willebrand factor (VWF) is built up from a varying number of subunits, of which the larger molecules have higher haemostatic activity. Von Willebrand disease (VWD) and thrombotic thrombocytopenic purpura are the best known disorders with pathognomonic changes of the highly multimerised VWF forms. There is an established method to calculate the relative amount of large oligomers. Our aim is to quantify the degree of VWF multimerisation as well, to complete the densitometric analysis of VWF electrophoresis. After optimisation, we have defined this new parameter (M_{MW}) as the molecular weight corresponding to the lower boundary of the largest 25% of VWF protein. M_{MW} was significantly different ($p<.0001$) in platelet lysate, normal samples and VWD type 2 samples (10.4, 6.3, 2.1, respectively). There was strong correlation between the M_{MW} and the amount of large multimers in normal samples ($r^2=0.98$) and in platelet lysate. However M_{MW} was higher in platelet lysate, in which VWF is not cleaved by ADAMTS-13, than in healthy samples with the same amount of large multimers. Comparison of the new parameter and the collagen binding and ristocetin cofactor activity of VWF, showed that the functional tests are at least partially determined by the multimerisation; however, about 15% of VWD samples had normal activity to antigen ratios. The quantification of multimerisation aids the classification in these cases, especially at low antigen concentrations, and also might help in the detection of thrombotic conditions.

Keywords

VWF multimer analysis, von Willebrand disease

Thromb Haemost 2009; 102: 412–417

Introduction

Von Willebrand factor (VWF) is one of the largest glycoporteins in circulation and it is built up from a variable number of dimeric units, ranging from the dimer (0.5 MDa) up to the tetracontamer (40-mer, 20 MDa). One of its main functions is to aid the temporary re-establishment of the continuity of the vessel wall immediately following injury. VWF in this process slows down and tethers the circulating platelets when subendothelial molecules, primarily collagens are exposed (1, 2) thus allows platelets to adhere at sites of high shear flow. The structure of VWF seems to be well-suited to this function as the repeating VWF subunits provide a high local density of binding sites for platelets. Correspondingly, it is accepted that the largest multimers have the highest haemostatic activity. The momentary multimer distribution of VWF is determined by the collective effect of oppositely acting processes: assembly on one hand, and clearance or degradation by ADAMTS-13 on the other (3). Recent publications suggest additional ways, which could influence the size of VWF oligomers through thiol-disulfide exchange as well (4). The deficiency of large multimers is usually seen either because of the faster clearance (von Willebrand disease [VWD] 2B, platelet type VWD) or because of the disorders of synthesis (VWD type 2A) (5–7). Substantial increase in the amount of large multimers is only rarely observed. It is described in VWD type Vicenza and in the recovery phase or remission of thrombotic thrombocytopenic purpura (TTP), because of the deficiency of VWF's proteolytic enzyme ADAMTS-13 in the latter. In otherwise healthy individuals it is currently unclear whether the increase in the total amount of VWF or in the large multimers alone is an indepen-

Correspondence to:
Jolán Hársfalvi
Clinical Research Center
Medical and Health Science Center, University of Debrecen
98 Nagyerdei krt., Debrecen, H-4012, Hungary
Tel.: +36 52 431 956, Fax: + 36 52 340 011
E-mail: harsfalv@med.unideb.hu

Financial support:
This work was supported by Grants OTKA K62317, OTKA-NKTH NI 69238 (Hungarian Scientific Research Fund) and MTA 2006TKI227 (Hungarian Academy of Sciences).

Received: January 14, 2009
Accepted after major revision: May 21, 2009

Prepublished online: July 3, 2009
doi:10.1160/TH09-01-0032

dent risk factor for thrombosis (8, 9). There is even less information available on how the size of the largest multimers influences haemostasis.

Presently, antigen (VWF:Ag) and activity assays, such as the ristocetin cofactor assay (VWF:RCo) and the collagen binding activity (VWF:CB) are available for the evaluation of VWF. The disproportionate decrease of activity assays and the antigen level is usually treated as a sign of type 2 VWD, and according to some opinions the selective decrease of VWF:CB indicates the lack of large multimers (10). However, direct information about the amount and the degree of multimerization of VWF is only available through non-reducing SDS agarose gel electrophoresis.

Routinely these gels are qualitatively evaluated, which is a potential source of variability in the interpretation of the results. Inter-laboratory variation is further increased by the large number of running conditions for the VWF SDS agarose electrophoresis (11–17) In addition the most commonly used Laemmli buffers do not to resolve small multimers in low resolution gels (18).

There is a published approach for qualitative analyses that assesses the amount of large multimers by calculating the percentage of VWF protein in bands 11 and above. However, the size of these multimers is not measured even though it is assumed to have a strong impact on VWF's haemostatic function. In this paper we aim to develop the methods needed to quantitatively describe the degree of multimerisation of VWF, including the electrophoresis conditions and the data analysis techniques.

Materials and methods

Samples

Blood samples were collected by venipuncture from the antecubital vein into tubes containing 3.2% sodium citrate (9:1, vol/vol). Platelet-poor plasma was prepared by centrifuging the samples twice at 2,000×g for 15 minutes (min) at room temperature, after which 500 µl aliquots of the supernatants were stored at –70°C until use. Normal control plasma was purchased from Dade-Behring (Marburg, Germany). Platelet lysate was prepared from healthy subjects' (n=20) EDTA anticoagulated whole blood. First platelet-rich plasma was prepared by centrifuging the samples for 10 min at 150×g. Then the platelets were pelleted at 3,000×g, and washed once with HEPES buffer supplemented with 0.05 M EDTA pH=7.4. 2×10^7 platelets were pelleted again, and suspended in 100 µl of sample buffer.

Normal samples were provided by 35 healthy volunteers. Twenty-five VWD type 2 patients diagnosed at the University hospital were included in the study. Written informed consent was obtained from all subjects in accordance with the Declaration of Helsinki and our Institutional Review Board approved the study.

SDS agarose gelelectrophoresis

VWF molecules were separated either by using the modified Laemmli buffers as described by Ruggeri and Zimmerman (12) or by a Tris-Borate discontinuous buffer system according to the agarose manufacturer's recommendation (Seakem HGT, Lonza, Basel, Switzerland). Briefly, low resolution (0.8%) agarose running gels (12.5 cm×10 cm×1.2 mm) were cast on glass plates. Not more than 2 hours (h) before the runs the first 2.5 cm strip was replaced with stacking gel. The samples were mixed with sample buffer (10 mM Tris, 1 mM EDTA, 8 M urea, 2% SDS, 0.05% bromophenolblue, pH=8.0) so that the final VWF concentration was 0.05 $U\times mL^{-1}$ and then were denatured for 20 min at 60°C. Electrophoresis was performed at constant current for either 6 h at 20 mA/gel, or overnight at 6 mA/gel on a plate cooled to 18°C. The modified Laemmli system consists of an SDS Tris-Glycine electrophoresis buffer (0.05 M Tris, 0.384 M glycine, 0.1% SDS), SDS Tris-HCl stacking gel buffer (0.125 M Tris, 0.1% SDS, pH=6.8 at 18°C) and SDS Tris-Glycine running gel buffer (0.375 M Tris, pH=8.0 at 18°C). The Tris-Borate discontinuous buffer system includes an SDS Tris-boric acid electrophoresis buffer (0.09 M Tris, 0.09 M boric acid, 0.1% SDS), a Tris-HCl stacking gel buffer (0.125 M Tris, pH=8.0 at 18°C) and Tris-boric acid running gel buffer supplemented with urea (0.5 M Tris, 0.16 M boric acid, 1 M urea).

Immunoblotting

The proteins were transferred to PVDF membranes (Immobilon-P, Millipore Corp, Bedford, MA, USA) using the tank electro-blotting method. To enhance the transfer of the largest VWF molecules, VWF multimers were degraded by treating the gels for 10 min with 1 mM β-mercaptoethanol (mercaptolysis) before blotting as reported recently by Bowen and Bowley (15). VWF was visualised by immunostaining using HRP labelled polyclonal rabbit anti-human VWF antibody (DakoCytomation, Glostrup, Denmark) and DAB substrate. Some membranes were stained for IgM in a second step, using goat anti-human IgM and HRP labelled anti goat antibodies. In these cases an image was captured before and after the IgM immunostaining.

Quantitative multimer analysis

Digital images of the membranes were obtained by a GS-800 calibrated densitometer and processed by its QuantityOne software (Bio-Rad Laboratories, Richmond, CA, USA). First the background density of the image was subtracted coarsely, the background level was assessed as an average value from a representative, protein-free area. The resulting reflective density (RD) against relative mobility (RF) data was used for subsequent calculations. The background was further reduced in each lane based on the average RD not containing VWF. The resulting RD versus RF curves were smoothed by the moving average method, and the VWF peaks were identified.

The quantitative analysis was performed using two methods (Fig. 1). For the first method the relative amount of large multimers (M_{10}) was calculated. Large multimers were defined as oligomers larger than the icosamer (band 10) including the area where VWF did not resolve into bands.

For the second method we assessed the degree of multimerisation. The degree of multimerisation was characterised by the molecular weight corresponding to the lower boundary of the largest 25% of VWF protein. First, a cumulative RD against RF curve was constructed, and the the RF value where the curve has reached 25% was determined. The molecular weight corresponding to this RF (M_{MW}) was estimated based on the correlation of the VWF peaks mobility and their molecular weight (estimated as 0.5 MDa for a homodimer unit) in each lane and was

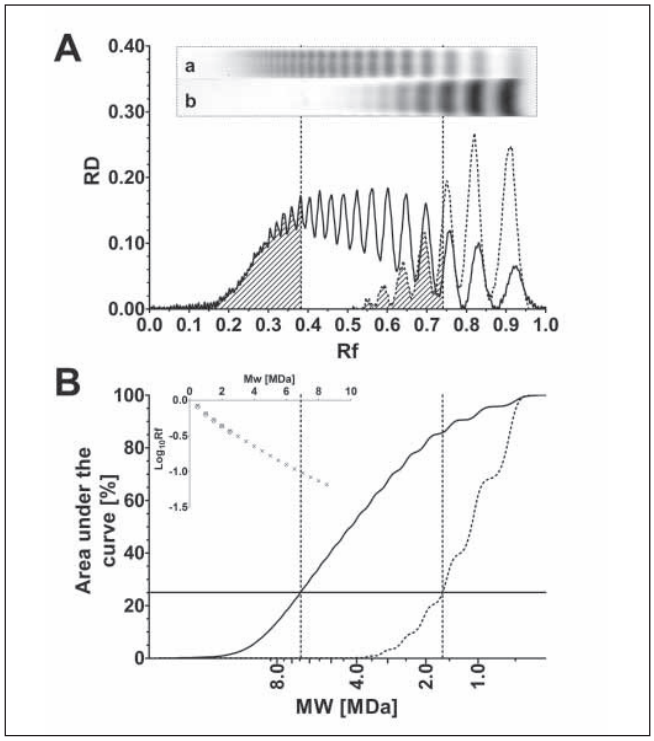

Figure 1: Calculation of the M_{MW} parameter. A) reflective density (RD) versus relative front (RF) curves from the normal (continuous line) and the VWD type 2 (dashed line) sample. The filled area represents the upper 25% of the total area under the curve. A picture of the normal (a) and the VWD type 2 sample (b) is shown in the inset. B) Cumulative curve of the samples. The abscissa represents the MW calculated from the correlation between the logarithm of the VWF RF values and their corresponding MW (correlation is shown in the inset, normal samples ×, VWD type 2 samples o). The ordinate shows the area under the curve between the origin and the given MW, expressed as percentage of the total area under the curve. The 25% threshold is marked with a horizontal line on the graph.

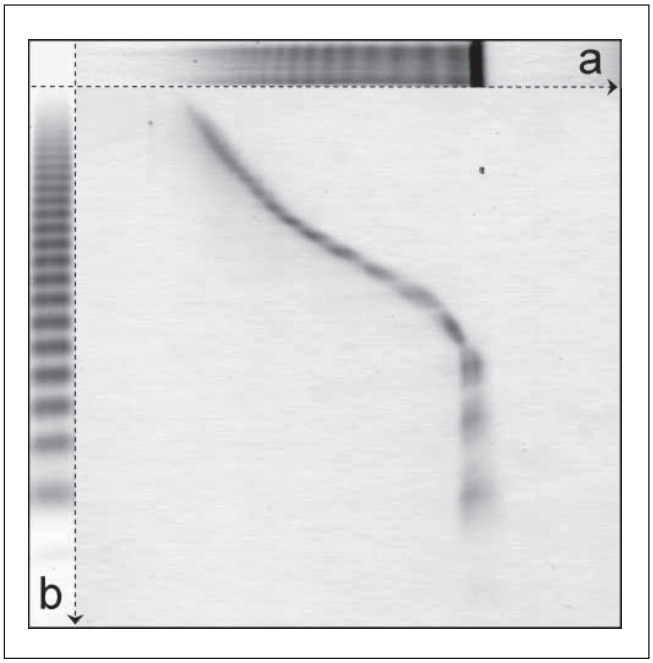

Figure 2: Comparison of VWF multimer separation in Laemmli and Tris-Borate buffers. Denatured normal plasma sample was separated by two dimensional electrophpresis, Laemmli buffers in the first dimension (a), Tris-borate gel in the second (b). For reference a representative lane from the Laemmli gel (a) and from a Tris-Borate gel is shown (b).

calculated using the coefficients of regression of the log RF versus estimated Mw data. The 25% boundary was chosen after comparing the M_{MW} of groups of samples lacking large multimers, normal samples and samples containing unusually large multimers using different boundaries.

The processing of densitometric data in case of both the M_{MW} and the M_{10} calculation was computerised, no manual steps were involved. For statistical analysis, Graphpad Prism software (version 5.00 for Windows, GraphPad Software, San Diego, CA, USA) was used.

VWF cleavage by ADAMTS-13

VWF digestion experiments were performed according to Gerritsen et al. (19), briefly substrate plasma was prepared by dialysing the plasma of a healthy individual against 4.5% polyethylene glycol 5 mM Tris, pH 8.0. Before use, the substrate was mixed with 8 M urea in 5 mM Tris pH=8.0 so that the final concentration of urea was 1.5 M. A series of plasma dilutions between 1/5 – 1/320 in 1.5 M urea, 5 mM Tris were prepared and aliquots of 50 µl were preincubated with 5 µl 93 mM $BaCl_2$ for 30 min at 37°C. One hundred µl of substrate was added to the aliquots (the concentration of $BaCl_2$ was 3 mM in the reaction mixture) and further incubated for 2 h at 37°C. The digestion was stopped by adding 10 µl of 0.825 M Na_2SO_4, and samples were analysed by gel electrophoresis.

VWF antigen, collagen binding activity and ristocetin cofactor assay

VWF:Ag was measured by ELISA (20). VWF:CB was measured as Ag, but Type III collagen (Sigma, St Louis, MO, USA) was used for coating. Optical density reading was carried out using Infiniti 200M (Tecan Trading AG, Männedorf, Switzerland), and the Magellan software of the instrument was used for calculations, applying four-parameter Marquardt curve fitting. VWF:RCo was measured by Ristocetin Reagent Helena BioSciences (Sunderland Enterprise Park, Sunderland, UK) and Chrono-Log 810-CA lumiaggregometer (Chronolog, Havertown, PA, USA). WHO Standard was used for calibration in all of these methods.

Results

Comparison of buffers

We detected 18 to 22 discrete bands in normal samples when using the Tris-borate buffers. Fewer bands were resolved with the Laemmli buffers, where also a distorted band near the running front was commonly visible. To compare the resolving power of the gels, and to elucidate the contents of the distorted band, a sample was separated in a two-dimensional electrophoresis with a Laemmli gel in the first dimension and a Tris-Borate gel in the

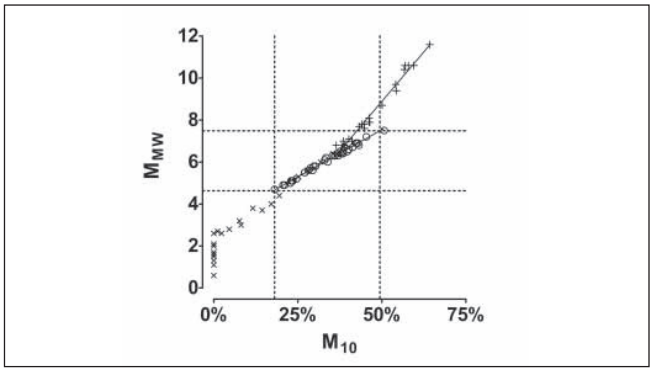

Figure 3: Correlation between M_{MW} and M_{10}. M_{MW} and M_{10} was calculated for VWD type 2 (×), healthy (o) and platelet lysate samples (+), mean ± 2 SD is shown for the normal group (dotted lines). In cases of normal samples there is a good agreement between methods (r^2=0.98), in the case of platelet lysate the M_{MW} seems to increase more than M_{10}. For most VWD type 2 samples only M_{MW} was able to provide results other than 0.

second (Fig. 2). The separation of large multimers was superior in the direction of Tris-Borate buffers, and also the distorted band in the Laemmli gel resolved into multiple bands. We excluded the possibility that the extra bands in the Tris-Borate buffers are VWF degradation products by comparing their relative mobilities to IgM (MW: ~0.8 MDa). We have found that only one VWF band – presumably the VWF dimer (MW: ~0.5 MDa) – had a smaller molecular weight than IgM.

Optimisation of M_{MW} calculation

After optimisation, M_{MW} was defined as the molecular weight of the lower boundary of the largest 25% of VWF protein. The 25% limit was established by evaluating a subset of data (7 platelet lysate, 11 normal and 8 VWD 2B samples) using a range of limits between 1–80%. The method's ability to distinguish between the groups of samples (platelet lysate, normal and VWD type 2) was evaluated by the Student's t-test. At smaller thresholds the discrimination between the platelet lysate and normal groups increased, whereas the best discrimination between the normal and VWD 2B groups was observed when calculating with larger thresholds (see Supplementary Figure available online at www.thrombosis-online.com). The 25% threshold is equally spaced from the threshold where platelet lysate (10%) and where VWD type 2 samples (40%) are separated better from normal samples. At this threshold the statistical difference between groups is highly significant (mean ± SD 10.42 ± 0.78, 6.27 ± 0.68, 2.13 ± 1.12 MDa for platelet lysate, normal, VWD type 2 group respectively, p<<0.01)

Method characteristics

Reproducibility, expressed as the coefficient of variation of M_{MW} and M_{10} measurements of the same normal control sample on different days (n=20) was 7.8% and 15.9%, respectively. The M_{MW} and M_{10} of 35 healthy individuals was 6.1 ± 0.72 and 33.5 ± 7.9 (mean ± SD). The methods' tolerance towards the variations in the intensity of immunostaining was studied by evaluating a series of dilutions of one sample between 0.25 to 2.5

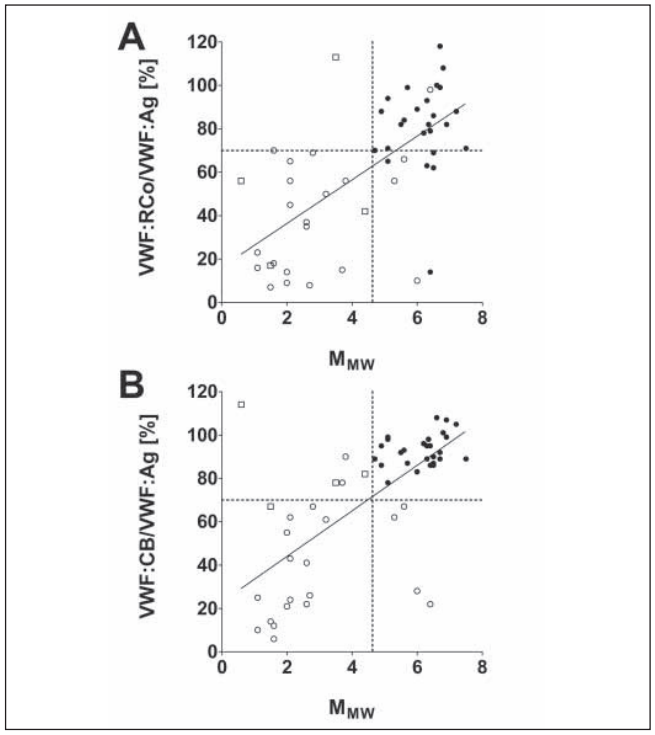

Figure 4: Correlation of VWF functional tests and M_{MW}. M_{MW} of normal (●) and VWD type 2 patients samples (o) was determined. Samples with antigen levels below 30% are marked with **squares**. Mean M_{MW}-2SD of the normal group and 70% activity-to-antigen ratio are marked with dotted lines. A) VWF:RCo to VWF:Ag ratio versus M_{MW}. B) VWF:CB to VWF:Ag ratio versus M_{MW}.

times the standard dilution. The different dilutions yielded an average RD between 0.061 and 0.319 for the VWF containing part of the lanes, M_{MW} or M_{10} results were not affected in this range. The coefficient of variation (CV) of the different dilutions was 4.4% and 7.7% for M_{MW} and M_{10}, respectively.

Correlation of M_{MW} and M_{10}

We evaluated M_{MW} and M_{10} of platelet lysate, control samples, VWF degraded by ADAMTS-13 and samples from VWD type 2 patients. The VWF in platelet lysate is protected from plasma proteases and consequently it contains larger multimers, whereas VWD type 2 patients typically have less or no large multimers. We found good correlation between the degree of multimerisation and the amount of large multimers in normal samples (r^2=0.98) and platelet lysate; however, the slope of the regression lines were different (p<0.001). Characteristically VWF in platelet lysate contained larger multimers than healthy samples with the same amount of large multimers. The M_{10} was 0 in about 50% of VWD type 2 samples (Fig. 3) as these patients do not have icosamers or larger oligomers. The rest of the VWD type 2 samples tend to have smaller multimers (lower M_{MW}) than ADAMTS-13 degraded VWF with the same amount of large multimers (M_{10}).

ADAMTS-13 degradation experiments

We have tested the sensitivity of M_{MW} by evaluating VWF degraded by ADAMTS-13. The highest dilution of normal plasma

caused measurable decrease in multimerization (ΔM_{MW}: -0.32, M_{MW} of substarte: 6.01); however, the estimated limit of detection is about 4.9% ADAMTS-13 activity under the described conditions. The degraded VWF contained similar sized oligomers as the healthy samples with the same amount of large oligomers. (The points of degraded VWF are scattered closely around the regression line or the extension of the regression line of normal samples in Figure 3).

Correlation of M_{MW} with collagen binding activity and ristocetin cofactor assay

Results of the functional tests of VWF – collagen binding activity and ristocetin cofactor assay – were compared to M_{MW} on normal and VWD type 2 samples (Fig. 4). The functional assays to antigen ratios were at least partially determined by multimerisation (r^2=0.42 and 0.43 for VWF:RCo and VWF:CB, respectively). Four patient samples (16%) had normal M_{MW} but abnormal functional assays, these cases are reclassified as type 2M. On the other hand, three (12%) VWD type 2 patients had normal VWF:RCo to antigen and five (20%) type 2 patients had normal VWF:CB to antigen ratios but abnormal M_{MW}. Some of these samples (1 in case of VWF:RCo and 3 in case of VWF:CB) had low antigen levels, where the reproducibility of the functional assays tends to diminish. Furthermore, five (19%) of normal samples had abnormal VWF:RCo to VWF:Ag ratio, while none of these samples had abnormal M_{MW} or VWF:CB to VWF:Ag values.

What is known about this topic?

- Only the large von Willebrand factor (VWF) oligomers are capable of providing adequate haemostatic function. VWF gelelectrophoresis is used to assess the distribution of the different sized oligomers, and it is a part of the von Willebrand disease classification process, if inital test are positive
- VWF gelelectrophoresis results are only qualitatively analysed, if quantitative analysis is used, it is restricted to the determination of the amount of oligomers larger than the 10mer, the size of the oligomers is not evaluated.

What does this paper add?

- We have developed a novel, computerised approach to multimer analysis to measure the degree of multimerisation of the VWF oligomers.
- We have assessed the sensitivity of this method to the presence of ultra large multimers and its utility on VWD type 2 samples lacking large multimers.
- We have compared the degree of multimerisation and the results of functional test (VWF:CB and VWF:RCo) in case of normal and VWD type 2 samples.

Discussion

The amount and presumably the multimerization of VWF oligomers released by the endothelial cells and the activity of the plasma enzyme ADAMTS-13 degrading the oligomers have a high inter-individual variability and known to change in pathologic conditions (21). Consequently, the size and the amount of the large oligomers, which are main determinants of the haemostatic activity of VWF, are expected to differ as well.

The established method to quantify the amount of the large oligomers is to calculate the percentage of VWF protein larger than the icosamer (10^{th} band, [18]), though other approaches also exist (22). However, the identification of VWF bands is not reliable with the commonly used Laemmli buffers as the separation of the small VWF oligomers is inadequate (18). The transfer of large multimers is also inconsistent with the traditional blotting techniques. After evaluating several types of buffer systems (11–17, 23), we found that Tris-borate buffers combined with mercaptolysis-aided blotting (15) is better suited for this purpose.

The characterisation of the degree of multimerisation poses some problems. The size of the largest oligomer in the sample could be used as an obvious measure; however, its quantity is so low that is not discernible from the background above VWF bands. Furthermore the size of this oligomer is in the range of 20 MDa, which is not resolved by agarose gels, so even if it was detected, the determination of its molecular weight would not be possible. These problems can be solved by detecting a proportion of the largest oligomers instead of just detecting the largest. On the other hand too large proportions may decrease selectivity. By comparing normal samples to either having less (VWD type 2) or having extra large (platelet lysate) multimers, we have found that at 25% the method is selective and the interference by the background is acceptable (the latter problem affects VWD type 2 samples more, as the VWF bands are further from the sample application wells). In studies only concentrating on large multimers using smaller proportions could increase the sensitivity. Further study of platelet lysate confirmed that the larger oligomers are detectable, even if the amount of large oligomers is the same as in plasma samples. When plasma VWF was further degraded by ADAMTS-13, both the amount and the size of large multimers decreased, but their proportions was close that is seen in normal plasma samples.

There is a strong association between the presence of large multimers and the haemostatic function in case of VWF. To further evaluate M_{MW}, we investigated the relationship between M_{MW} and GPIb binding (VWF:RCo) and collagen binding (VWF:CB) functions in healthy and VWD type 2 samples. There was moderately strong (r^2~0.4) relationship between M_{MW} and both of the functional assays, the higher sensitivity of collagen binding to the lack of large multimers was not evident. It is worth noting, that the high variability of the functional test at low antigen concentrations may result in normal activity-to-antigen ratios in cases with abnormal electrophoresis results.

The quantification of multimerisation may aid the classification in these cases, and also might be a useful tool for the investigation of the connection between VWF and thrombotic conditions.

Acknowledgements

We thank Ms. Andrea Bezi and Ms. Szabo Zsuzsanna for their assistance and Prof Hans Deckmyn and Ms. Nomsa Maphango for careful reading of the text. We also thank Dr. Agota Schlammadinger for providing patient samples.

References

1. Ruggeri ZM. Von Willebrand factor. Curr Opin Hematol 2003; 10: 142–149.

2. Marx I, Christophe OD, Lenting PJ, et al. Altered thrombus formation in von Willebrand factor-deficient mice expressing von Willebrand factor variants with defective binding to collagen or GPIIbIIIa. Blood 2008; 112: 603–609.

3. Sadler JE. von Willebrand factor: two sides of a coin. J Thromb Haemost 2005; 3: 1702–1709.

4. Luken BM. Extracellular control of VWF multimer size and thiol-disulfide exchange. J Thromb Haemost 2008; 6: 1131–1134.

5. Tsai HM. Thrombotic thrombocytopenic purpura: a thrombotic disorder caused by ADAMTS13 deficiency. Hematol Oncol Clin North Am 2007; 21: 609–632.

6. Sadler JE. A revised classification of von Willebrand disease. For the Subcommittee on von Willebrand Factor of the Scientific and Standardization Committee of the International Society on Thrombosis and Haemostasis. Thromb Haemost 1994; 71: 520–525.

7. Sadler JE, Budde U, Eikenboom JC, et al. Update on the pathophysiology and classification of von Willebrand disease: a report of the Subcommittee on von Willebrand Factor. J Thromb Haemost 2006; 4: 2103–2114.

8. Spiel AO, Gilbert JC, Jilma B. von Willebrand factor in cardiovascular disease: focus on acute coronary syndromes. Circulation 2008; 117: 1449–1459.

9. Blann AD. Plasma von Willebrand factor, thrombosis, and the endothelium: the first 30 years. Thromb Haemost 2006; 95: 49–55.

10. Favaloro EJ, Thom J, Patterson D, et al. Desmopressin therapy to assist the functional identification and characterisation of von Willebrand disease: Differential utility from combining two (VWF:CB and VWF:RCo) von Willebrand factor activity assays? Thromb Res 2009; 123: 862-868.

11. Raines G, Aumann H, Sykes S, et al. Multimeric analysis of von Willebrand factor by molecular sieving electrophoresis in sodium dodecyl sulphate agarose gel. Thromb Res 1990; 60: 201–212.

12. Ruggeri ZM, Zimmerman TS. The complex multimeric composition of factor VIII/von Willebrand factor. Blood 1981; 57: 1140–1143.

13. Smejkal GB, Shainoff JR, Kottke-Marchant KM. Rapid high-resolution electrophoresis of multimeric von Willebrand Factor using a thermopiloted gel apparatus. Electrophoresis 2003; 24: 582–587.

14. Studt JD, Budde U, Schneppenheim R, et al. Quantification and facilitated comparison of von Willebrand factor multimer patterns by densitometry. Am J Clin Pathol 2001; 116: 567–574.

15. Bowen JD, Bowley SJ. Improved visualisation of high-molecular-weight von Willebrand factor multimers. Thromb Haemost 2007; 97: 1051–1052.

16. Krizek DR, Rick ME. A rapid method to visualize von willebrand factor multimers by using agarose gel electrophoresis, immunolocalization and luminographic detection. Thromb Res 2000; 97: 457–462.

17. Weiss DR, Thiel C, Strasser EF, et al. An optimized electrophoresis method for high-resolution imaging of von-Willebrand multimers. Thromb Haemost 2008; 100: 949–951.

18. Budde U, Schneppenheim R, Eikenboom J, et al. Detailed von Willebrand factor multimer analysis in patients with von Willebrand disease in the European study, molecular and clinical markers for the diagnosis and management of type 1 von Willebrand disease (MCMDM-1VWD). J Thromb Haemost 2008; 6: 762–771.

19. Gerritsen HE, Turecek PL, Schwarz HP, et al. Assay of von Willebrand factor (vWF)-cleaving protease based on decreased collagen binding affinity of degraded vWF: a tool for the diagnosis of thrombotic thrombocytopenic purpura (TTP). Thromb Haemost 1999; 82: 1386–1389.

20. Cejka J. Enzyme immunoassay for factor VIII-related antigen. Clin Chem 1982; 28: 1356–1358.

21. Claus RA, Bockmeyer CL, Budde U, et al. Variations in the ratio between von Willebrand factor and its cleaving protease during systemic inflammation and association with severity and prognosis of organ failure. Thromb Haemost 2009; 101: 239–247.

22. Lopes AA, Soares RP, Maeda NY. A mathematical framework for group analysis of von Willebrand factor multimeric composition following luminography. Braz J.Med Biol Res 2002; 35: 1259–1263.

23. Mazurier C, Dieval J, Jorieux S, et al. A new von Willebrand factor (vWF) defect in a patient with factor VIII (FVIII) deficiency but with normal levels and multimeric patterns of both plasma and platelet vWF. Characterization of abnormal vWF/FVIII interaction. Blood 1990; 75: 20–26.